



## **Sustainable Weed Management in Agriculture with Laser-Based Autonomous Tools**

### **D5.3 – Equipment integration, testing, evaluation, and impact on crops and soil**



Funded by the Horizon 2020 programme of  
the European Union

[This page was intentionally left blank]



### Acknowledgement

WeLASER is a project funded by the Horizon 2020 Research and Innovation Programme of the European Union under the call “Food security, sustainable agriculture and forestry, marine and maritime and inland water research and the bio-economy” and the topic “Integrated health approaches and alternatives to pesticide use.”

(H2020-SFS-04-2019-2020)

Grant agreement N. 101000256

### Disclaimer

The views and opinions expressed in this document are solely those of the project, not the European Commission.

Deliverable number	D5.3
Work-package Task	WP5
Work-package leader	CSIC
Deliverable type *	Report
Dissemination level**	Public
Status –Version	V1
Contractual delivery date	M34
Actual delivery date	M39
Start date/end date of the project	October 1, 2020 / December 31, 2023
Author(s)/contributor(s)	P. Gonzalez-de-Santos, L. Emmi (CISC); K. Scholle (FUT); H. Sandmann, M. Wollweber (LZH); G. Vitali, M. Francia (UNIBO) and C. Andreasen (UCPH).
Approved by	General Assembly
	* Report; Prototype; Demonstrator; Other.
	**Public; Restricted to other programme participants (including the Commission Services); Restricted to a group specified by the consortium (including the Commission Services); Confidential, only for members of the consortium (including the Commission Services).

[This page was intentionally left blank]





## EXECUTIVE SUMMARY

This deliverable deals with the integration of the whole system, which consists of (i) the autonomous vehicle, (ii) the AI perception system, and (iii) the weeding system (agricultural tool). The autonomous vehicle comprises the mobile platform, the Smart Navigation System, the IoT sensor networks and communication with the cloud. Its integration and validation were reported in “D4.1 – Autonomous vehicle (Platform, smart central controller, IoT and cloud computing): Design, integration and TRL assessment”. The AI-perception system was described and evaluated in “D3.1- Weed-meristem perception system: Design, integration and TRL assessment”. The weeding system consists of a high-power laser source and a laser scanner. These components were described, integrated and validated in the deliverable “D2.1-Laser-based weeding system: Design, integration and TRL assessment”.

Having the system integrated (Section 2), the next step is to assess and validate the system’s weeding efficiency (Section 3). These activities are completed by reporting the system’s impact on crops and soil (Section 4).

[This page was intentionally left blank]



## TABLE OF CONTENTS

Executive Summary .....	5
Table of Contents.....	7
List of acronyms and abbreviations .....	9
1. Introduction .....	11
2. Final system integration .....	11
2.1. Integrating the Autonomous Vehicle with the Weeding Tool .....	11
2.1.1. <i>Mechanical and Electrical Integration</i> .....	11
2.1.2. <i>Cabinet bases</i> .....	17
2.1.3. <i>Interfaces Between Subsystems</i> .....	17
2.1.3.1. Smart Navigation Manager (M4) / Perception System (M1) interface....	17
2.1.3.2. Smart Navigation Manager (M4) / Weeding system (M3) interface .....	17
2.1.3.3. Autonomous Vehicle (M2) / Weeding System (M3) interface.....	18
2.1.3.4. Perception System (M1) / Weeding System (M3) .....	18
2.2. Integrating the IoT devices .....	18
3. System assessment .....	23
3.1. Experimental fields and testing periods .....	23
3.1.1. <i>CSIC, Arganda del Rey, Spain</i> .....	23
3.1.2. <i>UCPH, Taastrup, Denmark</i> .....	24
3.1.3. <i>VDBP, Reusel, The Netherlands</i> .....	25
3.2. Tests and experiments .....	25
3.2.1. <i>Percentage of detected weeds</i> .....	26
3.2.1.1. Measurement procedure: .....	26
3.2.1.2. Results .....	26
3.2.2. <i>Percentage of detected meristems</i> .....	30
3.2.2.1. Measurement procedure: .....	30
3.2.2.2. Results .....	30
3.2.3. <i>Percentage of targeted meristems (KPI only, not SO)</i> .....	33
3.2.3.1. Measurement procedure (LZH test field only): .....	33
3.2.3.2. Results .....	33
3.2.4. <i>Percentage of killed plants</i> .....	35
3.2.4.1. Measurement procedure, LZH test field only: .....	36
3.2.4.1. Results .....	36
3.2.5. <i>Testing the IoT devices</i> .....	41
3.3. Performances of the final equipment .....	42
3.3.1. <i>Safety system</i> .....	42
3.3.2. <i>Crop detection and row-follow tests</i> .....	47
3.3.2.1. Row follower for maize12 .....	52

3.3.2.1. Row follower for maize	57
3.3.2.1. Row follower for sugarbeet	61
3.3.3. Planner	64
3.3.4. Supervisor	66
3.3.5. Motion controller	73
3.3.5.1. LineFollowing results	74
3.3.5.1. GoToGoal results	76
3.3.6. Laser source	78
3.3.7. AI-perception system	81
3.3.8. Targeting system	83
3.3.9. IoT sensor network	85
3.3.10. Cloud computing	87
3.4. Stakeholder's Evaluation	88
4. System impact on crops and soil	90
4.1. System impact on crops	91
4.1.1. Effect of Autonomous vehicles	91
4.1.2. Effect of Laser	91
4.1.3. Combined effect	92
4.2. System impact on soil	92
4.2.1. Effect of the Autonomous Robot	92
4.2.2. Effect of laser	93
4.2.3. Combined effect	94
4.3. Conclusions	95
5. Annex 1 Status of the final system integration	96
6. Annex 2. Questionnaire forms and results	99

## LIST OF ACRONYMS AND ABBREVIATIONS

AGC:	AGREENCULTURE
AI:	Artificial Intelligence
AMARE:	<i>Amaranthus retroflexus</i>
BBCH:	( <i>Biologische Bundesanstalt, Bundessortenamt und CHemische Industrie</i> ) Scale to identify the phenological development stages of plants
CANbus:	Controller Area Network bus
CF:	Chlorophyll Fluorescence
COAG:	Spanish coordinator of farmers and livestock breeders
CSIC:	Spanish National Research Council
CSS:	Cascading Style Sheets
DMP:	Data Management Plan
DoA:	Description of the Action (Annex I of the Grant Agreement)
DSN:	Device Sensor Network
FOC:	Field of View
FIWARE:	A curated framework of open-source platform components to accelerate the development of Smart Solutions
FTP:	File Transfer Protocol
FUT:	FUTONICS
GPS:	Global Positioning System
GUI:	Graphical User Interface
HTTP:	Hypertext Transfer Protocol
IETU:	Institute for the Ecology of Industrial Areas
IMU:	Inertial Measurement Unit
IoT:	Internet of Things
IoU:	Intersection over Union
IP:	Ingress protection
JS:	Java Script
KPI:	Key Performance Indicators
LabView:	Laboratory Virtual Instrument Engineering Workbench
LD:	Lethal Dose
LIDAR:	Laser Imaging Detection and Ranging
LoRa:	Long-Range connectivity
LZH:	Laser Zentrum Hannover
mAP:	Mean Average Precision
MQTT:	Message Queuing Telemetry Transport
OTA:	“Over-The-Air” is a technology that updates and changes data in SIM cards
PIR:	Passive Infra-Red
PostGRES:	Open source object-oriented relational database management system
PV:	FotoVoltaic
PVC:	Polyvinyl Chloride
RF:	Radio Frequency
RGB:	Red-Green-Blue colour system
ROS:	Robot Operating System
ROSSERIAL:	Protocol for wrapping standard ROS serialized messages and multiplexing multiple topics and services over a character device such as a serial port or network socket
RTK:	Real-time kinematics
SIM:	Subscriber Identification Module used in Mobiles
SNM:	Smart Navigation Manager
SSL:	Secure Sockets Layer
Svelte:	Free and open-source front-end component framework and language
TCP/IP:	Transmission Control Protocol/Internet Protocol
ToF:	Time-of-Flight camera
TRL:	Technology Readiness Level

---

UCPH:	University of Copenhagen
UGENT:	Gent University
UNIBO:	University of Bologna
USB:	Universal Serial Bus
VDBP:	Van der Borne Projecten
WiFi:	Wireless network protocols
WLAN:	Wireless Local Area Network





## 1. INTRODUCTION

Once every WeLASER subsystem has been validated at its developer's facilities and delivered at the coordinator facilities, the final integration is carried out according to the indications in deliverable "D5.1 - System breakdown and integration procedures" (Subtask 5.2.3 – Final integration). The system integration-related activities are reported in Section 2 of this deliverable.

With the system integrated, the next step is to conduct the evaluation and assessment of the whole system (TASK 5.3 - Equipment evaluation and TRL assessments), which is carried out in the following steps (Section 3):

- Conducting the final tests and experiments;
- Evaluating the performances of the final equipment, according to the indications in Table 1.7 of the DOA and
- Determining if the TRL-7 is achieved.

A project objective is also to analyse the impact of the overall system on the crops and soil and the possible advantages of the proposed weeding solution.

This deliverable was approved by the General Assembly on January 10, 2024, after being circulated among the consortium.

## 2. FINAL SYSTEM INTEGRATION

This Section presents the integration of (i) the autonomous vehicle, (ii) the AI perception system and (iii) the weeding system (agricultural tool). Integrating these systems demands a precise definition of the subsystem's attachments to the mobile platform (Mechanical Integration), power supply requirements (Electrical Integration), and a detailed description of the interfaces between subsystems. First, the mechanical/electrical integration is described, and then the interfaces between these subsystems are detailed.

### 2.1. Integrating the Autonomous Vehicle with the Weeding Tool

#### 2.1.1. Mechanical and Electrical Integration

Deliverable "D5.1 - System breakdown and integration procedures", submitted on month 3, reported a preliminary estimation of masses and dimensions for the subsystems to be placed onboard the mobile platform and their electrical requirements. These characteristics were refined in "D5.2 - Preliminary Integration" and submitted in month 19. The implement was attached to the mobile platform through a motionless three-point hitch. Table 2.1 summarises the dimensions and weight of the different subsystems onboard the mobile platform for the current system version (two-row solution). Table 2.2 contains the estimations for the four-row solution. In both solutions, the different

components are placed as indicated to balance the weight on both sides of the mobile platform.

Figure 2.1 illustrates the top view of the location of the engine, the electronic cabinets, the Smart Navigation Manager (SNM), and the weeding tool. The dimensions are specified in meters (m) or height units U (1 U = 0.04445 m tall).

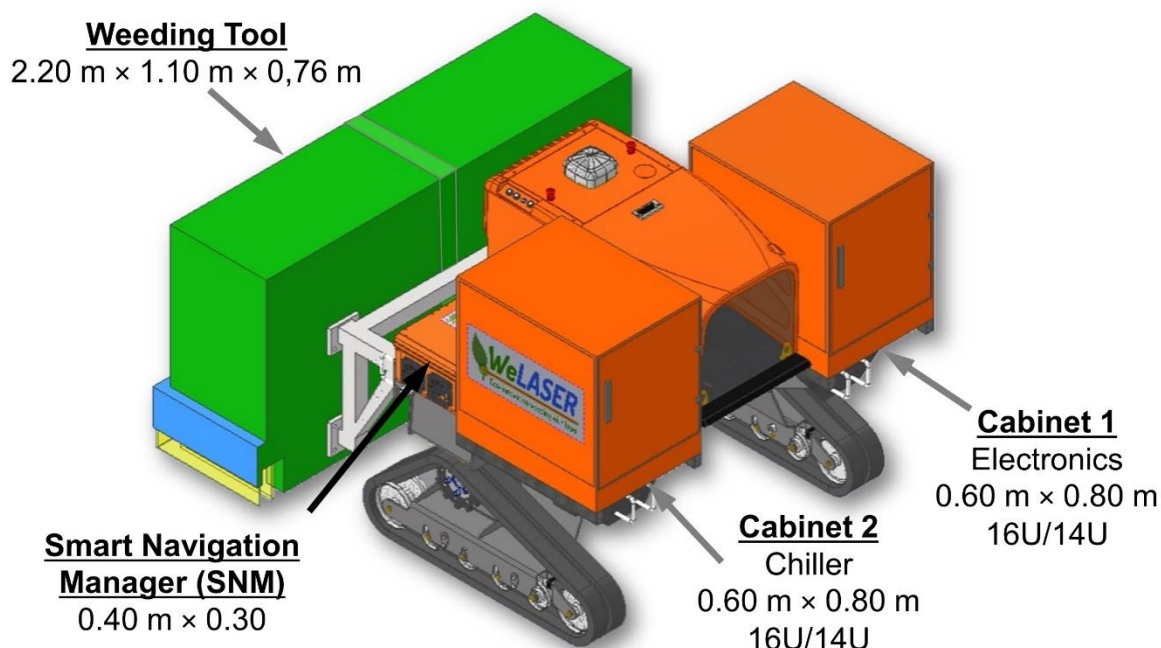


**Fig. 2.1. Distribution of the WeLASER components onboard the vehicle for the 2-row configuration (top view).**

**Table 2.1. Summary of the weight dimensions of the system components (2 rows).**

ELECTRONIC CABINET 1				ELECTRONIC CABINET 2			
Electronic equipment	Height	Weight (kg)	Volume (mm <sup>3</sup> ) (W×H×D)	Electronic equipment	Height	Weight (kg)	Volume (mm <sup>3</sup> ) (W×H×D)
Laser system (unit)	10 U	60	482.6×444.5×703	Chiller (Unit 1)	5U	26	482.6×221.45×480
Image recognition computer	2 U	20	482.6×88.9×688	Chiller (Unit 2)	5U	26	482.6×221.45×480
Targeting (scanner) controller	2 U	10	482.6×88.9×500	Safety controller	2 U	5	482.6×88.9×688
<b>Subtotal</b>	14 U	90	482.6×622,3×703	<b>Subtotal</b>	12 U	57	482.6×53.4×688
19' rack cabinet (IP55)	14 U	30	600×650×800	19' rack cabinet (IP55)	14 U	30	600×650×800
<b>Total</b>		<b>120</b>	<b>Custom-made cabinet</b>	<b>Total</b>		<b>87</b>	<b>Custom-made cabinet</b>

Smart Navigation Manager (SNM) BOX			
Smart navigation manager (front of left side)	Height	Weight (kg)	Volume (mm <sup>3</sup> ) (W×H×D)
Central Controller	110.5	5	240×110.5×225
Others (regulators, switch, router, etc.)	133.35	3	240×133.35×300
Box (IP55)	300	8	400×300×300
Total		16	Custom-made box

Others	Height	Weight (kg)	Volume (mm <sup>3</sup> ) (W×H×D)
Cables		10	
Front camera		0.33	
Total		10.33	

3-point hitch	Height	Weight (kg)	Volume (mm <sup>3</sup> ) (W×H×D)
3-point hitch		30	
Total		30	

Cabinet bases	Height	Weight (kg)	Volume (mm <sup>3</sup> ) (W×H×D)
Left-cabinet base		30	
Right-cabinet base		30	
Total		60	

Weeding implement (center-back)	Weight (kg)	Volume (mm <sup>3</sup> ) (W×H×D)
Weeding implement and other components inside	236	2200×1100×760
Total one box	236	2200×1100×760

<b>TOTAL PAYLOAD: 559.33 KG</b>
---------------------------------

The electronic cabinets (Fig. 2.2) can be moved forward/backwards to balance the front-rear weight. Figure 2.3 illustrates the components' static mass balance (momentum) and final positions.

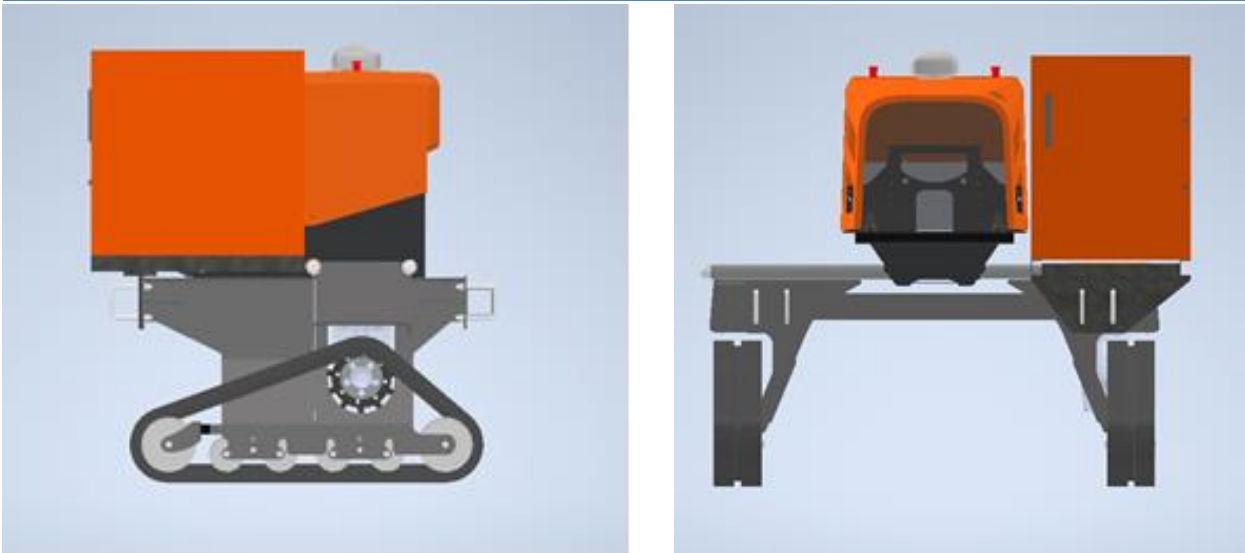


**Fig. 2.2. Electronic boxes (14 U).**

This static stability study was performed at the due time but included in this deliverable as a part of the system integration. However, it was requested in the review report.

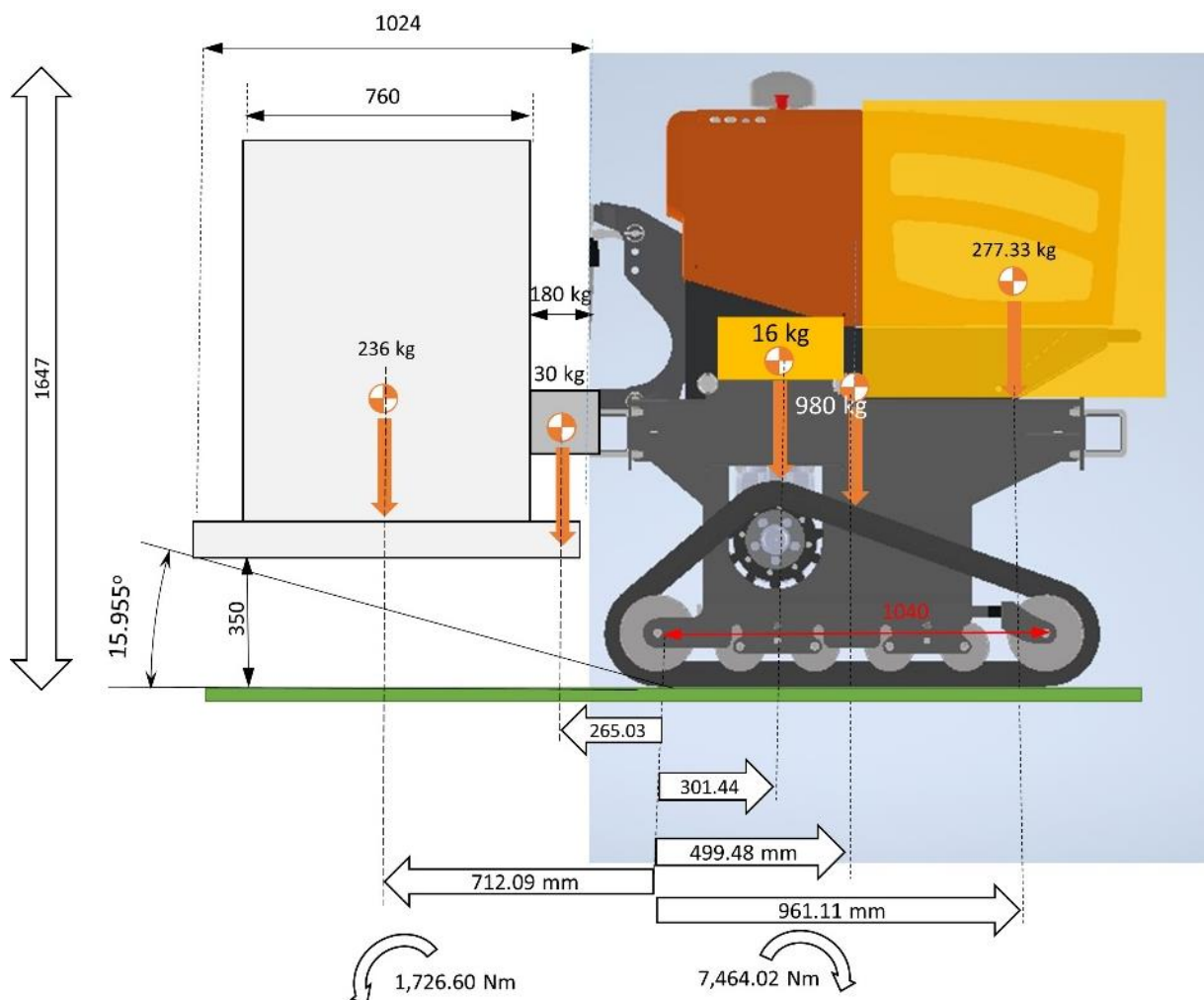


**Fig. 2.3. Mobile platform scheme - top view (2-row).**

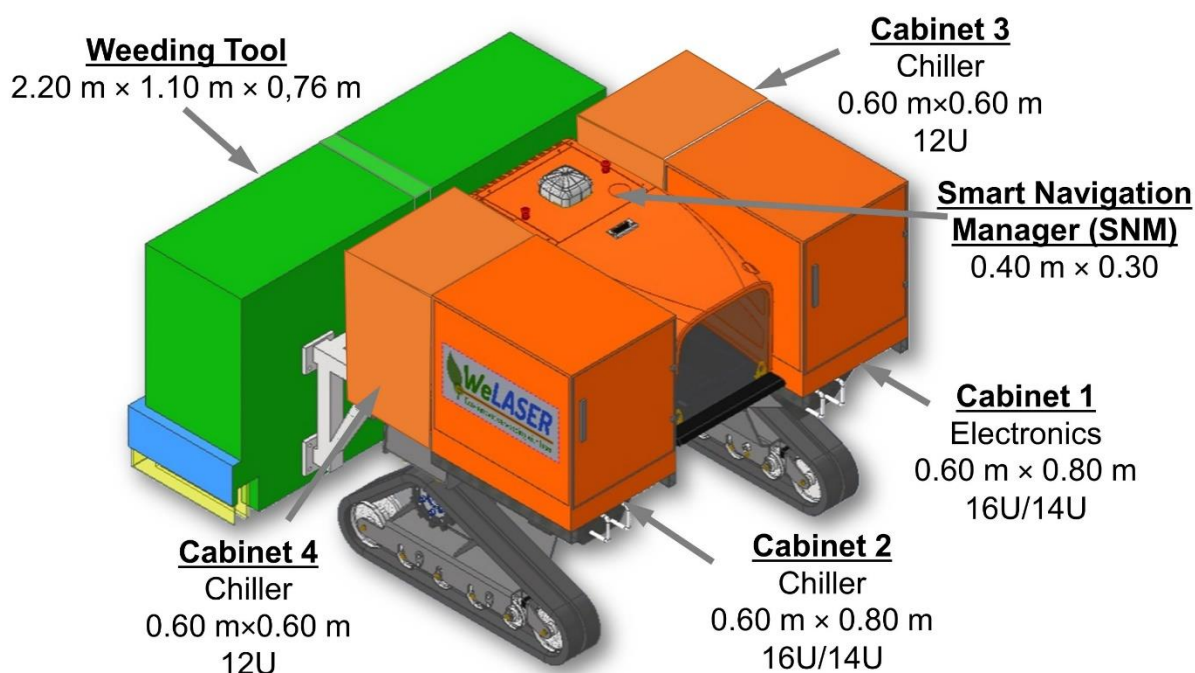


Fig. 2.4 Distribution of the WeLASER components onboard the vehicle for the 4-row configuration (top view).

Table 2.2. Summary of the weight dimensions of the system components (4 rows)

ELECTRONIC CABINET 1				ELECTRONIC CABINET 2			
Electronic equipment	Height	Weight (kg)	Volume (mm <sup>3</sup> ) (W×H×D)	Electronic equipment	Height	Weight (kg)	Volume (mm <sup>3</sup> ) (W×H×D)
Laser system (unit)	10U	60	482.6×444.5×703	Laser system (unit)	10U	60	482.6×444.5×703
Image recognition computer	2 U	20	482.6×88.9×688	Image recognition computer	2 U	20	482.6×88.9×688
Safety controller	2 U	5	482.6×88.9×688	Safety controller	2 U	5	482.6×88.9×688
Targeting (scanner) controller	2 U	10	482.6×88.9×500	Targeting (scanner) controller	2 U	10	482.6×88.9×500
<b>Subtotal</b>	<b>16 U</b>	<b>95</b>	<b>482.6×711.2×703</b>	<b>Subtotal</b>	<b>16 U</b>	<b>95</b>	<b>482.6×711.2×703</b>
19' rack cabinet (IP55)	18 U	35	600×950×800	19' rack cabinet (IP55)	18 U	35	600×950×800
<b>Total</b>		<b>130</b>	<b>Custom-made cabinet</b>	<b>Total</b>		<b>130</b>	<b>Custom-made cabinet</b>

ELECTRONIC CABINET 3				ELECTRONIC CABINET 4			
Electronic equipment	Height	Weight (kg)	Volume (mm <sup>3</sup> ) (W×H×D)	Electronic equipment	Height	Weight (kg)	Volume (mm <sup>3</sup> ) (W×H×D)
Chiller (Unit 1)	5U	26	482.6x221.45x480	Chiller (Unit 1)	5U	26	482.6x221.45x480
Chiller (Unit 2)	5U	26	482.6x221.45x480	Chiller (Unit 2)	5U	26	482.6x221.45x480
19' rack cabinet (IP55)	14 U	30	600x950x800	19' rack cabinet (IP55)	14 U	30	600x950x800
Total		82	Custom-made cabinet	Total		82	Custom-made cabinet

SNM BOX			
Smart navigation manager (Front of left side)	Height	Weight (kg)	Volume (mm <sup>3</sup> ) (W×H×D)
Central Controller	110.5	5	240x110.5x225
Others (regulators, switches, router, etc.)	133.35	3	240x133.35x300
Box (IP55)	300	8	400x300x300
Total		16	Custom-made box

Others	Height	Weight (kg)	Volume (mm <sup>3</sup> ) (W×H×D)
Cables		10	
Front camera		0.33	
Total		10.33	

Others	Height	Weight (kg)	Volume (mm <sup>3</sup> ) (W×H×D)
Cables		10	
Front camera		0.33	
Total		10.33	

3-point hitch	Height	Weight (kg)	Volume (mm <sup>3</sup> ) (W×H×D)
3-point hitch		30	
Total		30	

Cabinet bases	Height	Weight (kg)	Volume (mm <sup>3</sup> ) (W×H×D)
Left-cabinet base		30	
Right-cabinet base		30	
Total		60	

Weeding implement (centre-back)	Weight (kg)	Volume (mm <sup>3</sup> ) (W×H×D)
Weeding implement and other components inside	300	2200x1100x600
Total (4 rows)	300	2200x1100x760

TOTAL PAYLOAD: 850.66
-----------------------



### 2.1.2. Cabinet bases

The bases described in Fig. 2.5 were designed and manufactured to attach the electronic cabinets to the mobile platform. Their weights are indicated in Table 2.2.

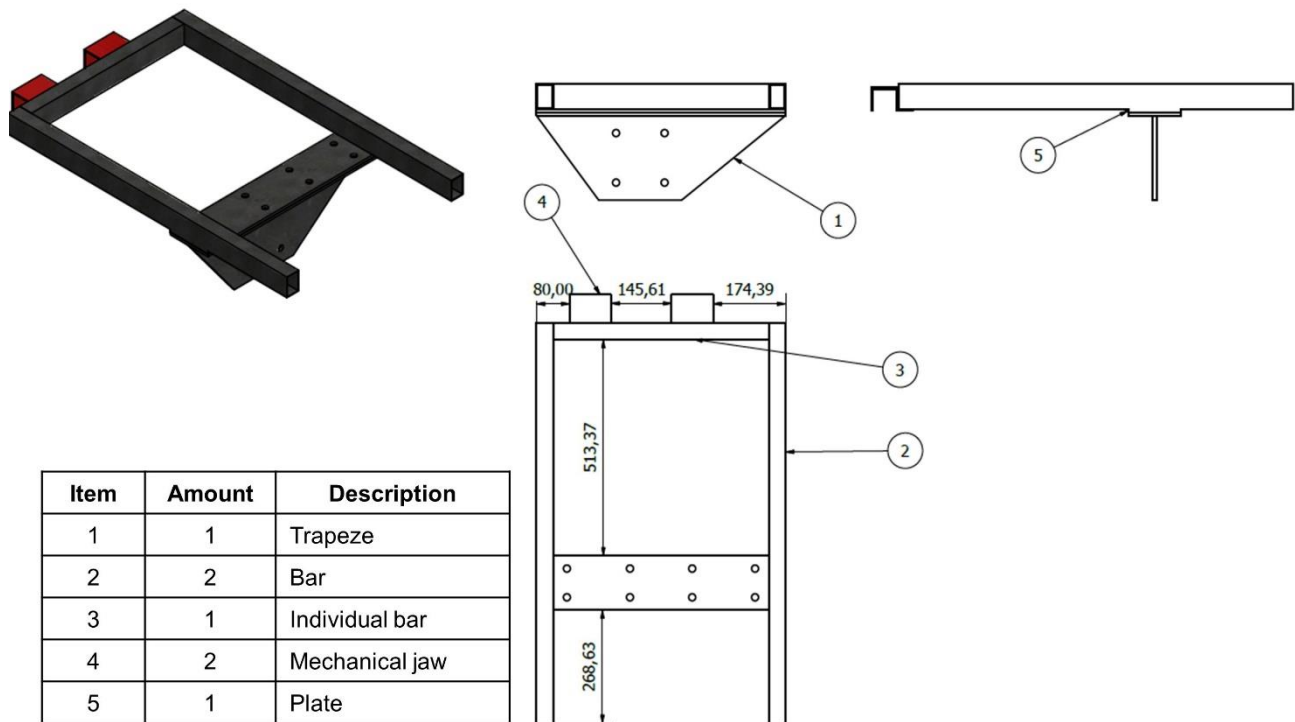


**Fig. 2.5. Cabinet bases.**

### 2.1.3. Interfaces Between Subsystems

The system considers four main interfaces between systems and modules (These interfaces are also described in “D4.1-Autonomous vehicle”.):

#### 2.1.3.1. Smart Navigation Manager (M4) / Perception System (M1) interface

To receive the basic information from the perception system (sensors, cameras, etc.), the Central Manager uses direct connections via Transmission Control Protocol/Internet Protocol (TCP/IP) for sensors and Universal Serial Bus (USB) for RGB and ToF cameras. All IoT devices use the available wireless communication technologies (WiFi and LoRa) to access the Internet and the cloud.

The Obstacle Detection System obtains data from the Guiding Vision System (RGB and ToF cameras) through the ethernet that communicates the Central Manager with the Perception System to guide the robot. This communication uses the ROS Manager and the Perception-ROS bridge of the [Robot Operating System](#).

#### 2.1.3.2. Smart Navigation Manager (M4) / Weeding system (M3) interface

These systems can communicate through ROS messaging protocols, where the publisher-subscriber pattern is preferred. This interface exchanges simple test messages to verify the communication interface.

It is worth mentioning that the Perception System and the Agricultural Tool are connected directly in the WeLASER system. This solution decreases the latency of data communication but demands moving a portion of the decision algorithms from the Smart Navigation Manager to the tool controller; therefore, the tool exhibits computational features.

### 2.1.3.3. Autonomous Vehicle (M2) / Weeding System (M3) interface

Usually, the Smart Navigation Manager coordinates the actions between the vehicle and the tool. However, as autonomous vehicles and agricultural tools usually have independent safety controllers, there is wired communication between the two safety controllers. In such a case, the autonomous vehicle safety controller works as a master and commands the tool safety controller to stop the tool if a dangerous situation appears.

### 2.1.3.4. Perception System (M1) / Weeding System (M3)

This communication is required to inform the Agricultural Tool about the crop status. In weeding applications, the information is related to the positions of the weeds. In this specific application, the Perception System (Weed Meristem Detection Module) sends the weed meristem positions to the Laser Scanner module of the Agricultural Tool. This communication is carried out using a conventional Ethernet connection. The metadata generated via the detection system is made available in the existing ROS network and sent to the Smart Navigation Manager.

## 2.2. Integrating the IoT devices

The IoT devices developed in WeLASER make a Device Sensor Network (DSN) supervised and controlled from the same cloud used to control the robot - they populate the WeLASER technoecosystem using the same set of communication protocols of the robot (WIFI, MQTT, FIWARE), enriching the Smart Data Model with the entity structure reported in Table 2.3. Table 2.4 lists the main devices with their specific attributes.

**Table 2.3. FIWARE entity descriptors.**

attribute	context	Mandatory	value
type	Creation	y	"Device"   "Camera"
name	Creation	n	"dev-name" See Table 2.4
id	Creation, Update	y	"urn:ngsi-Id:Device:dev-name"
areaServed	Creation	y	"urn:ngsi-Id:<xxx>"
Location	Creation	y	{"coordinates": [-3.48043486, 40.3130826], "type": "Point"}
dateCreated	Creation	y	Unix epoch (ms) e.g. 1671469959535
dateInstalled	Creation	n	Unix epoch (ms) e.g. 1671469959535
timestamp	Update	y	Unix epoch (ms) e.g. 1671469959535
controlledProperty	Update	Device	[ .. , .. , .. ] See Table 2.4
value	Update	Device	[ .. , .. , .. ] See Table 2.4
unit	Update	n	[ .. , .. , .. ] See Table 2.4
imageName	Update	Camera	URL

**Table 2.4. List of FIWARE devices and related attributes (and unit)\*.**

#	Device name	type	attribute	value
1	RobotCamera_1.4	camera	imageName	URL string
2	FieldCamera_1:8	camera	imageName	URL string
3	FieldBridge	device	attributes	["RobotPresent", "PeriodicShot"]
			unit	[y n, y n]
4	WeatherStation_n	device	attributes	["TempAir", "RH", "SunRad", "Prec", "WindVel", "WindDir"]
			unit	["degC", "%", "W/m2", "mm", "m/s", "degNcw"]
5	ETRometer_n	device	attributes	["CO2", "TempAir", "RH" ]
			unit	["ppm", "degC", "%"]

(\*\*) The table reports a simplified version of entity structures, which also support a hierarchical structure

The devices have been integrated into the system and the WeLASER contexts in the following manner:

### RobotCamera

This class of devices is not provided with an autonomous power supply as they are connected directly to the robot power system. They may receive signals from the robot to take snapshots upon request. To the scope, a camera (Master, front left) has been connected to the robot to be plugged into the robot power supply (12V) and a serial cable to communicate with its controller (by ROSSERIAL interface). The master then communicates with the other 3 slave cameras (Front right, Rear right, Rear left). Every camera autonomously sends its images via WiFi (Robot AP) to the Robot server FTP, where a service (daemon) is also running to send the images to the main server (cloud). The robot cameras have been applied to the robot so it can be easily removed (Fig 2.6).


**Fig. 2.6. Robot cameras (left) and their application bar (right).**



### FieldCameras

This class of devices is provided with an autonomous power supply harvesting energy from a (circa 100 cm<sup>2</sup>) external photo voltaic (PV) cell. To host the PV panel, an 8 square section profile pole (200×5×5 cm) has been prepared (at CSIC facilities). In the experimental field (at CSIC), 8 boreholes have been made to host 8 PVC pipes (40×8 cm external diameter) whose internal diameter was well fitting the squares poles, allowing them to set in place easily, remove and rotate the poles. The poles were also provided with support for the camera nodes (see Fig. 2.7).



**Fig. 2.7. Field cameras and their application.**

### FieldBridge

One of the poles (bottom right in Fig. 2.7) was also equipped with the fittings required to host the bridge. Though the cameras are independent mesh-connected devices that need a WLAN success

point to send and receive messages and images over the Internet to the cloud, all of these functionalities have been integrated into the bridge. The bridge is a node enabled to receive FieldCamera and RobotCamera alarms, awake the FieldCamera network, or take time-lapse snapshots. The bridge hosts a long-time battery and is fed by a larger PV cell as it has been designed to stay alive all the time. The bridge also hosts a portable access point equipped with a SIM to cover areas without an available WLAN.

### Weather Station

A low-cost, low-power, low-maintenance weather station has been designed to provide the techno-ecosystem with a collector of information detailing weather data for more precise decision-making. The Weather Station harness the same base technology of other nodes and, to address the characteristic mentioned above, includes recent approaches for wind and precipitation measurement (see Fig. 2.8).



**Fig. 2.8. Weather Station (left) beside the Standard one used for calibration (right).**

### ETRometer

A portable and easily configurable device for the measurement of atmospheric concentration of CO<sub>2</sub>, Relative Humidity and Temperature, capable of observing till 6 points, has been designed accounting for the growing address to evaluate fluxes of CO<sub>2</sub> and Water from cropped surfaces see Fig. 2.9).





**Fig. 2.9. ETRometer box (left) and its 3-sensor configuration (right).**

To complete the integration, during the project, further devices have been developed, including:

- Remote command to simulate the activities of the bridge.
- Weather Station Standard, including Standard Sensors (non low-cost, non low-maintenance.)

For these extra devices, an *ad hoc* board has been developed for debugging and calibration, involving the development of proper firmware supporting the same connection protocols of WeLASER.

For each of the devices, 3 supplementary dashboards have been realised to verify communication and easiness of data access using LabView for Cameras debugging: (i) PostGRES to store MQTT messages and access their contents, (ii) HTML-CSS-JS to make information interfaced to Web-Apps, 3DJS and (iii) Svelte libraries to display data graphs.

Related SSL, MQTTS, FTP, HTTPS, and PostGRES services have been further raised and maintained on UNIBO servers. Information treatment strategies and rules are detailed in the Data Management Plan (DMP).



### 3. SYSTEM ASSESSMENT

The WeLASER system was tested in three scenarios and was evaluated during various periods, and some of which concluded on a WeLASER Field Day. The final status of the system integration is summarised in Annex 1.

#### 3.1. Experimental fields and testing periods

##### 3.1.1. CSIC, Arganda del Rey, Spain

An experimental field in Arganda del Rey, Madrid, Spain (40°18'45.2"N -3°28'51.1"W) was built by CSIC to test the final system. It consisted of three areas of 60 × 20 m<sup>2</sup>, each divided into three sections of 20 × 20 m<sup>2</sup>. The sections in one area were seeded in consecutive weeks, allowing us to conduct experiments in three-week windows. In our tests, the three areas grew wheat (*Triticum aestivum* L.), maize (*Zea mays* L.) and sugar beet (*Beta vulgaris*). The crop rows were at a distance of 0.10 m for wheat and 0.50 m for maize and sugar beet. Figure 3.1 shows the experimental field and the distribution of the areas and sections.

The testing periods and the participants in this experimental field are indicated in Table 3.1.

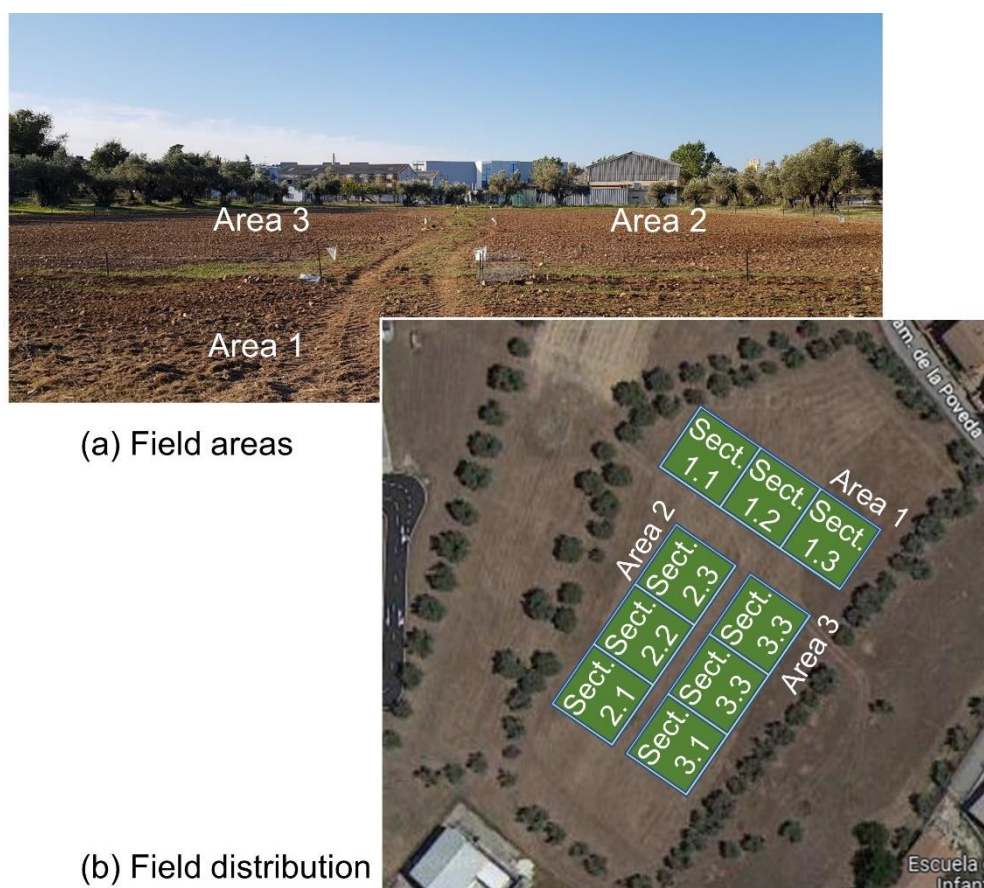


**Fig 3.1. Experimental field in Arganda del Rey, Spain.**

**Table 3.1. Integration and testing period in Arganda del Rey, Spain.**

Activity	Period	Partners involved
Final system integration and testing	5-8/06/2023	CSIC, UNIBO, FUT, LZH
Final system integration and testing	18-25/07/2023	CSIC, UNIBO, FUT, LZH
Reintegration and tests, Field Day 1.	24-26/07/2023	CSIC, FUT, LZH, UNIBO, IETU, UGENT, VDBP
Reintegration and tests, Field Day 4.	23-26/09/2023	CSIC, FUT, LZH, UCPH, UNIBO, IETU, UGENT

### 3.1.2. UCPH, Taastrup, Denmark

The second reintegration and testing period of the WeLASER system was conducted at the research facility Højbakkegaard, Taastrup (12°17'59.624"N, 55°40'11.389"W), belonging to the University of Copenhagen.

The field consisted of two areas of about 20×50 m with maize (1 to 2 leaves) and sugar beet (2

**Fig 3.2. Experimental field in Taastrup, Denmark.**

cotyledons). The activities began on August 15, 2023, and ended on August 18, 2023, with the WeLASER Field Day 2.

Figure 3.2 shows the experimental field and the distribution of the areas and sections.

### 3.1.3. VDBP, Reusel, The Netherlands

VDBP provided a large booth and a 37×15-m<sup>2</sup> field with maize () and sugar beet () plants to test the WeLASER weeding system in Reusel, The Netherlands (5°10'32.241"N, 51°19'12.298"W). From August 22 to 26, 2023, the developers of the WeLASER consortium worked together to tune the system (training the perception and targeting systems) and conducted tests and experiments for system validation and assessment. Figure 3.3 shows the experimental field and the distribution of the areas and sections.



**Fig 3.3. Experimental field in Reusel, The Netherlands.**

### 3.2. Tests and experiments

As planned, the majority of the tests and trials for the KPIs of the weeding implement were carried out at the LZH field in Hannover. Here, the LZH team was able to choose the right time and setting according to plant growth to check the KPIs and carry out the post-treatment evaluation. Besides, the KPIs preassigned for the WeLASER weeding device cover the weeding process step by step. This perspective is advantageous for determination of the bottlenecks of the automated weeding process. However, for most of these step-related KPIs, there is no valid measurement procedure, in particular, if the measurement is to be done on-field. So, LZH developed and defined measurement procedures for each of these step-wise KPIs for subsystem assessment under relevant but better defined and controlled conditions (see following subsections) and then reevaluated the performance qualitatively during the field-trials of the fully integrated system.



Accordingly, the tests and experiments proposed for Madrid (CSIC), Spain, Copenhagen (UCPH), Denmark, and Reusel (VDBP), the Netherlands, were primarily for TRL evaluation and to provide supporting data for KPI evaluation of laser treatment at other sites.

The following tests and measurements were performed:

### 3.2.1. Percentage of detected weeds

This study primarily centered on assessing the AI vision system's capacity for accurately identifying weeds in agricultural fields, with a specific focus on sugar beet and maize fields. Wheat fields were excluded from the study due to limited available images and the specific challenge of distinguishing wheat, a type of grass crop, from grass weeds. Evaluating the system's performance is crucial, especially in terms of false negatives (weed detection misses) and false positives (misidentification of non-weed elements as weeds). False positives are problematic as they can result in the unintended treatment of crop plants. While reducing false negatives is important, their impact is generally less significant than that of false positives. The study aims to improve the precision of weed detection to enhance the efficiency of weeding operations and minimise potential damage to crops due to misidentifications.

#### 3.2.1.1. *Measurement procedure:*

Thus, the measurement procedure for weed detection aims at assessing how frequent different weed and crop classes are confused by the AI. It consisted in the following steps:

- Take images of the test areas.
- Run AI crop-weed discriminator.
- Count plants manually / by AI on the images of the test areas.
- Measure accuracy between bounding boxes drawn by AI versus those drawn by a human operator.

#### 3.2.1.2. *Results*

The image dataset was divided into three parts: training, validation and test. The network was trained using the training and validation data. The test dataset, which was completely unknown to the trained network, was used for evaluation.

The confusion matrix, represented in Figure 3.4, is a critical element in this analysis. It categorizes the AI's performance in distinguishing various plant types, including "beets", "maize", "grass", "plants", and "background". This matrix is a tabular representation showing how well the classification algorithm has performed, visualizing the percentage of correct and incorrect predictions of the model, categorizing them in relation to the actual classes. It is key to evaluating the AI's differentiation capabilities, which are central to its precision in weed detection.



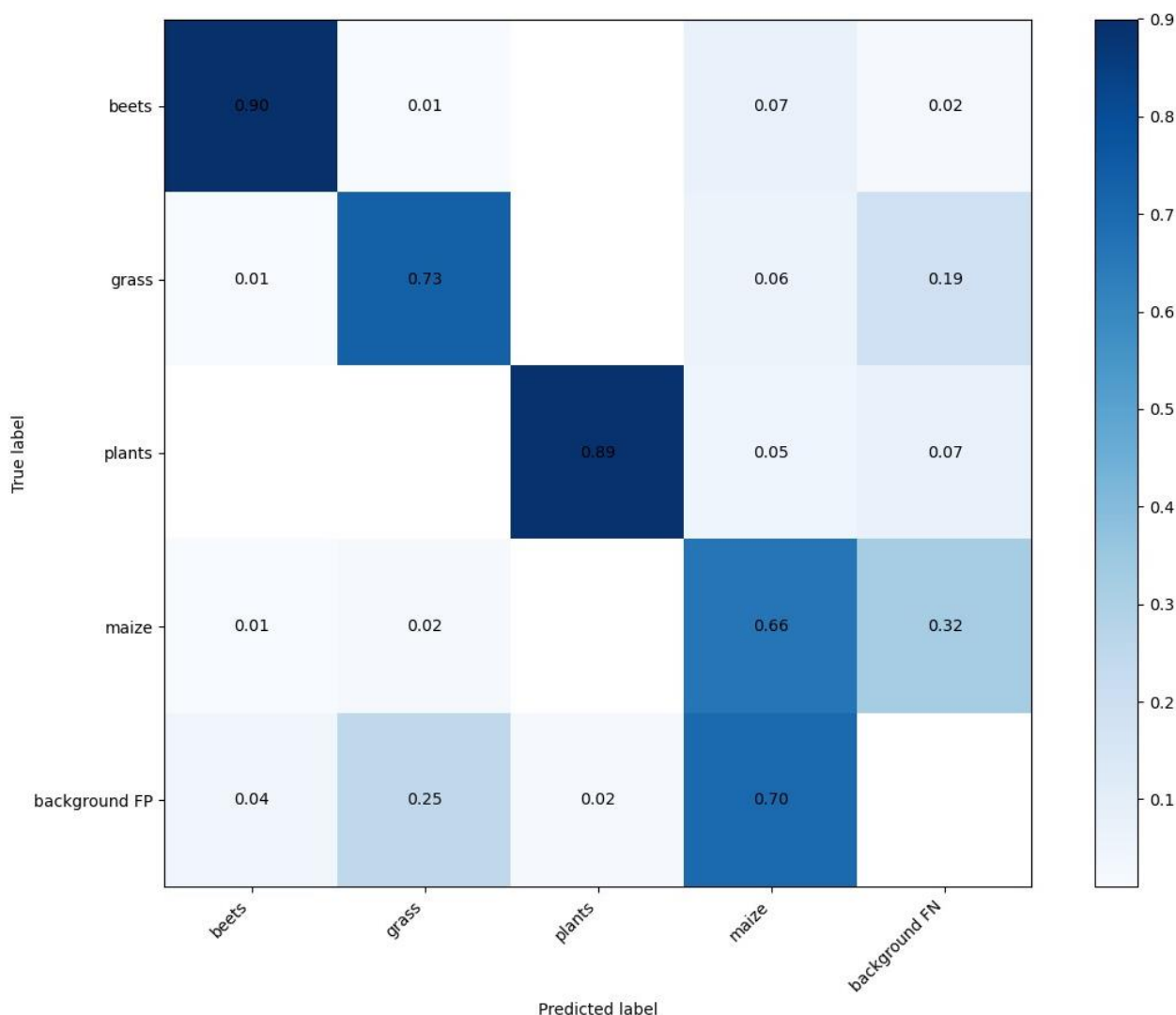


**Fig. 3.4. Confusion Matrix: Crop-weed classification accuracy for beets, maize, grass weeds, other plants, and background.**

The precision-recall curve, shown in Fig. 3.5, provides deeper insights into the AI's balance between precision and recall. This curve is a vital metric for gauging the overall effectiveness of the system, indicating how well the AI identifies weeds while minimizing false positives. Precision measures the proportion of correct positive predictions relative to the total number of positive predictions made by the model, while recall measures the proportion of correct positive predictions relative to the total number of actual positive cases. The precision-recall curve is a graphical tool that shows the relationship between precision and recall for a classification model at different threshold levels.

The real-world applicability of the AI system is further demonstrated through a series of sample images from different test fields across Europe, including images from German (top row) and Spanish fields under various environmental conditions (see Fig. 3.6). These images showcase the AI's weed detection capabilities under varied field conditions, highlighting its adaptability and versatility in diverse environments.

Specifically, the images display the AI's proficiency in detecting weeds in sugar beet fields. Challenges encountered include identifying very young or small weeds, differentiating weeds from stones, and recognizing various weed species, including many-leaved, possibly perennial weeds. The AI's ability to adapt to the different weed spectra and the varying appearances of the same crop under different growth conditions is evident.

It is important to note that in the classification, 'plants' refer to dicotyledonous weeds, while 'grass' signifies monocotyledonous weeds.

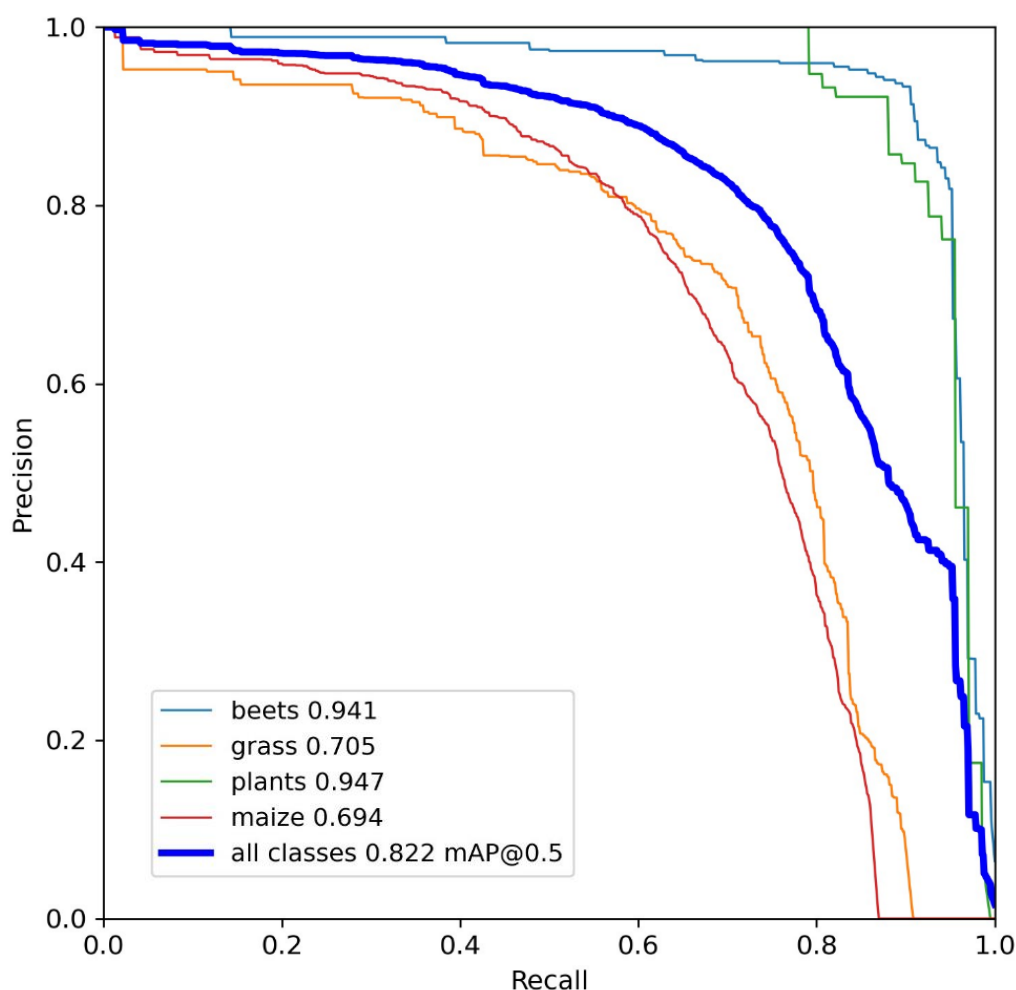


**Fig. 3.5. Precision-recall curve: Illustrating the AI's balance between accuracy and detection rate.**



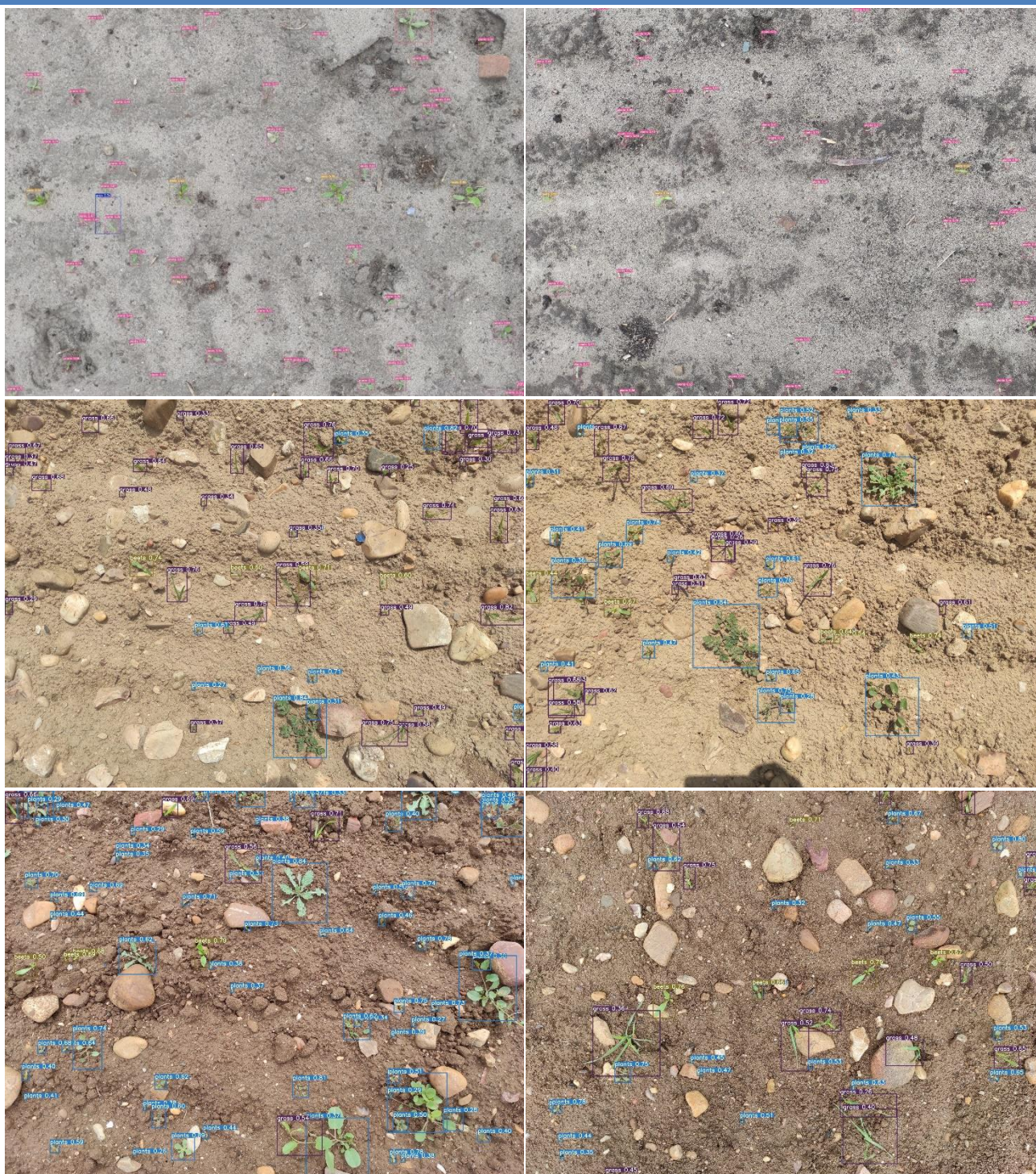


**Fig. 3.6. Sample images: Demonstrating the AI's weed detection in different test field conditions. Top row: sugar beet field in Germany with sandy soil and fairly optimal growth stage of the weeds for laser weeding. Crop plants are marked in mustard yellow, dicot weeds in pink, and monocot weeds in blue. Mid and bottom row: sugar beet field in Spain with many stones and weeds in a wider range of growth stages including perennial weeds. The sugar beet crop is again mustard-coloured, dicotyledon weeds in blue and monocotyledon weeds in purple.**



**KPI check for subsystem - Statement in Grant Agreement:**

*Identification of at least 80% of the weeds [with a] detection accuracy of  $\pm 3$  mm (Measurements based on picture analysis).*

The localization of whole weeds is not relevant for the process, but only the localization of the impact point (see Section 3.2.2 and following), so this is not assessed here. As shown in the confusion matrix (Fig. 3.4), the classification accuracy for dicot weed plants ('plants') is 89% and 73% for monocot weed plants ('grass'). Generally, it can be assumed that dicot weeds outnumber monocot weeds on the field. So, this KPI is accomplished.

### 3.2.2. Percentage of detected meristems

After the weed plants have been detected, their position needs to be determined for laser targeting. The laser is not to treat the whole plant but ideally only to hit certain 'impact points' where the laser application most strongly affects the survival rate. These impact points are the apical meristem or the stem base depending on the type of weed. For this KPI, the percentage of detected meristems in the group of identified weeds was determined.

#### 3.2.2.1. Measurement procedure:

For correct target localization, the AI needs to find the apical meristem (or other impact point) of the weed plants and to localize them in space in order to provide targeting coordinates for the laser application in the next step. The measurement procedure for performance of the meristem detection is as follows:

- Take images of the test areas.
- Run AI crop-weed discriminator and meristem localizer.
- Count the number of meristems detected by AI in the group of weed plants detected by AI on the images of the test areas.
- Measure accuracy: Meristem position as determined by AI versus positions that are manually found (on the images of the test areas).

In the GA, the performance of meristem detection was also associated with the accuracy of meristem localization. However, in fact, the precision of the localization is quite a separate point in the assessment of the process. It could have been tested on 2D images as proposed in the Grant Agreement. However, as the targeting process is not a 2D but a 3D process, we propose to test and assess the meristem localization in 3D together with the targeting accuracy in the following section 3.2.3.

#### 3.2.2.2. Results

The confusion matrix in Fig. 3.7 once again plays a pivotal role, this time showcasing how effectively the AI distinguishes meristems among other plant parts. The accuracy of this categorization is crucial for understanding the AI's performance in this task.



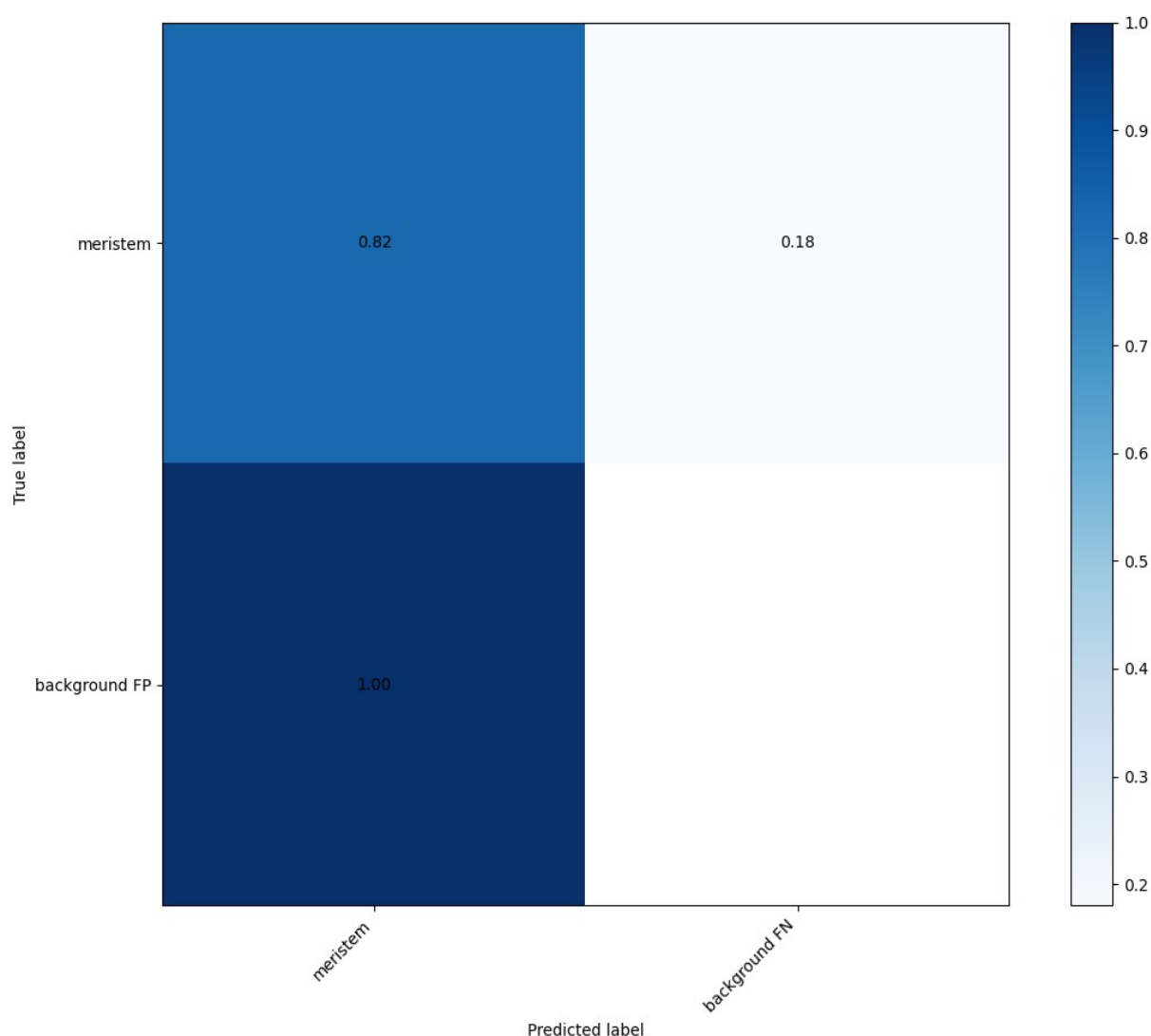


**Fig. 3.7. Confusion Matrix: Display of AI's classification accuracy in identifying meristems among other plant structures.**

Following this, Fig. 3.8 demonstrates the balance the AI maintains between precision and recall in the context of meristem detection. This curve is particularly insightful for understanding how the AI performs in accurately identifying meristems while minimizing false identifications.

Lastly, Figure 3.9 provide a visual representation of the AI's performance in real-world scenarios. The top 14 images originate from a German field, the bottom 14 from a Spanish field. These images depict the AI's capability in identifying meristems in various test fields, thus illustrating the practical application and adaptability of the AI system. Both monocotyledonous and dicotyledonous plants are shown in these images. Importantly, the plants are at the desired growth stage for the laser process, specifically between BBCH stages 10 and 12. This is ideal for effective weed control as it represents the early stages of plant development when intervention is most effective.

**KPI check for subsystem - Statement in Grant Agreement:**

*Detection of the meristem positions of at least 80% of the weeds [with an] detection accuracy of  $\pm 3$  mm (Measurements based on picture analysis)*

According to the confusion matrix (Figure 3.7) the accuracy for meristem detection is 82% so the KPI is accomplished in this respect. The precision of the meristem localization is evaluated in the following section(s).

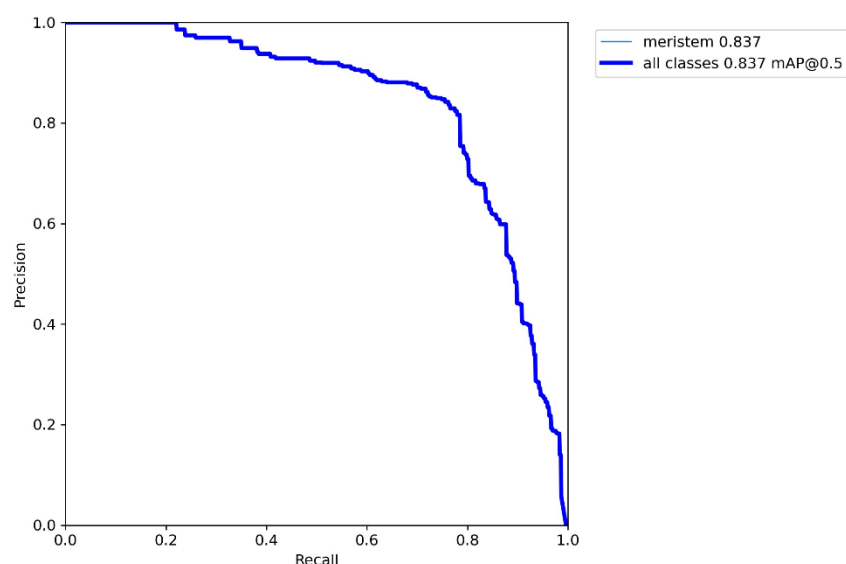


**Fig. 3.8. Precision-recall curve: The balance of precision and recall in AI's meristem detection.**

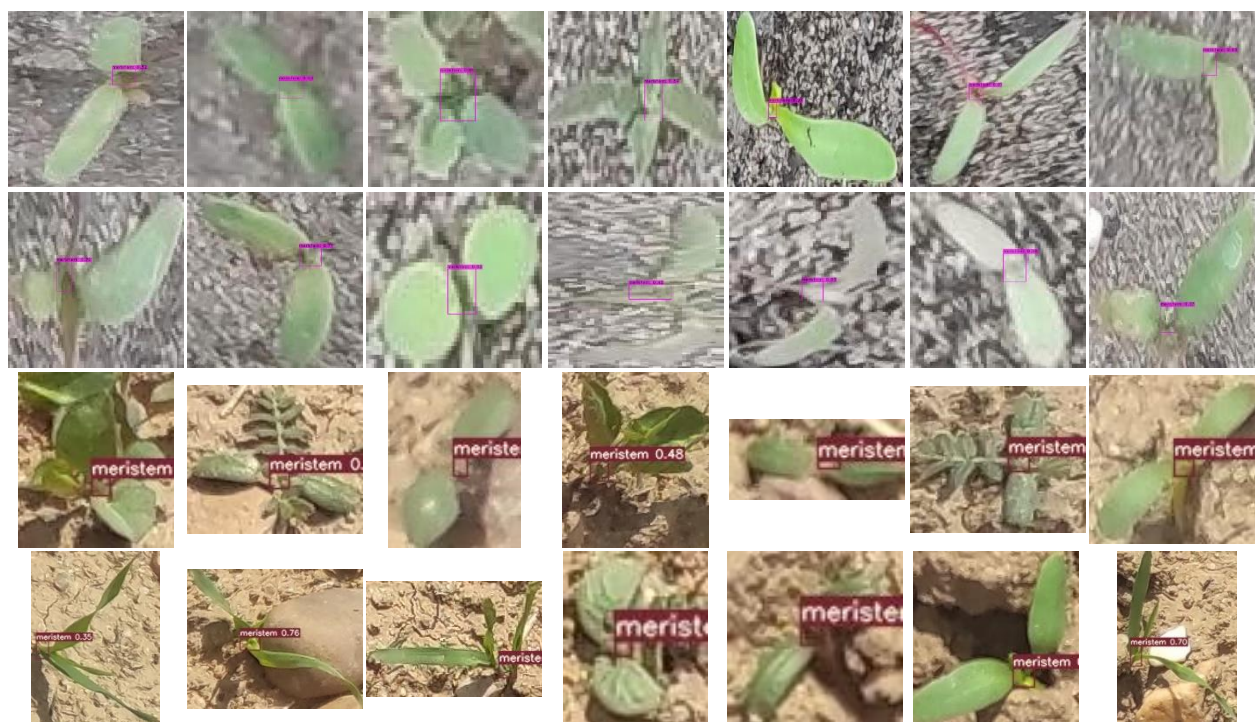


**Figure 3.9 Sample images: Demonstration of AI's meristem detection.**

### 3.2.3. Percentage of targeted meristems (KPI only, not SO)

Experimentally, it is difficult to provide valid visual evidence that and how well the meristems were targeted. The reason is that correct targeting and application of a (lethal) dose are basically inseparable in the weeding process. Furthermore, the performance in targeting depends mainly on the precision of the optical system and the accuracy of its calibration to real world coordinates. So, this assessment was broken down into measuring the accuracy of the laser targeting on image planes - allowing a well-defined assessment of the targeting performance in 3D - and the targeting performance for 3D objects (plants) in different regions of this 3D space. The latter is described in Section 3.2.4.

#### 3.2.3.1. *Measurement procedure (LZH test field only):*

- Create printouts of images from test areas.
- Run AI crop-weed discriminator and meristem localizer.
- Run the treatment process with a WeLASER scanner unit on the area with the treatment laser at exposure doses that burn the paper and image the targeted area. Repeat experiment in different distances from the laser scanner.
- Measure distances: Meristem position as determined manually versus positions that were hit by the laser.

#### 3.2.3.2. *Results*

The primary results are captured in Figs. 3.10 and 3.11. These images visualize the effectiveness of the laser targeting. They show the laser shots on the printouts, indicating how accurately the laser, guided by AI, hit the targeted meristems. The variations in laser impact at different heights offer a clear insight into the precision and adaptability of our targeting system.





**Fig. 3.10. Printout images with visible shots: Demonstrating the precision of AI-guided laser shots on meristems at a height of 800 mm.**



**Fig. 3.11. Printout images with visible shots: Demonstrating the precision of AI-guided laser shots on meristems at a height of 600 mm.**



Complementing these visual results is Table 3.2. This table provides a detailed quantitative analysis of the targeting accuracy. It outlines the distances between the intended growth centre, as identified manually, and the points actually hit by the laser. This data is crucial for quantifying the accuracy of the AI as well as the targeting system in guiding the laser to the correct targets.

**Table 3.2. Analysis of the distances between targeted and hit points on meristems at different heights.**

Experiment #	Distance to ground	Average distance from target	Standard deviation	Targeted plants (n)
1	800 mm	1.95 mm	1.62 mm	32
2	700 mm	1.81 mm	1.33 mm	32
3	600 mm	0.87 mm	0.95 mm	32

#### KPI check for subsystem - Statement in Grant Agreement:

*Targeted meristems have to be at least 90% of detected meristems.*

In the GA, this KPI is related to Specific Objective 5 (SO5).

Here, for subsystem evaluation, the assessment is connected with both the rate of hitting (targeting) a meristem that was previously detected by the AI and with the precision of the hitting (targeting) the meristems.

The WeLASER scanner targets each detected meristem (as long as the forward velocity of the robot fits the weed density). So, the precision is the main limiting factor here. In the WeLASER implement, the intended working distance to the ground is approximately 60 cm. According to Table 3.2, meristems are hit with an average error of 0.87 mm ( $\pm 0.95$  mm) at this height. Precision decreases with increasing working distance which may occur temporarily on uneven fields. Nevertheless, this KPI is accomplished including the precision parameters for (weed) meristem localization from the KPIs assessed in the previous section 3.2.2.

#### 3.2.4. Percentage of killed plants

Table 1.7 of the DoA states as the KPI for the WeLASER equipment:

Targeted meristems have to be at least 90% of the detected meristems → Detected meristems have to be at least 80% of the detected weeds → Detected weeds have to be at least 80% of the real weeds (Targeted meristems = 57,6% of the real weeds). Furthermore, SO1 states that the target is to thermally destroy at least 90% of the detected weeds when the laser beam falls on the weed meristems precisely. These KPIs and SO cover the complete weeding process. So, for the assessment of the weeding subsystem, the application of lethal doses was included in the assessment as well even though it was not demanded according to the Grant Agreement.



### 3.2.4.1. Measurement procedure, LZH test field only:

LZH developed an experimental setup to assess whether and how precise a plant is hit by laser radiation. The method is based on fluorescence imaging based on the well-known Kautsky kinetics of photosynthesis. So far, the method can only be applied in the laboratory and not during on-field laser weeding. This method was used to assess the precision of laser treatment for individual plants. If the precision of the laser application is not good enough under certain conditions, the treated area can be deliberately increased by moving the beam in small circles on the target area. In this way, imprecision can be compensated at the cost of efficiency. These relationships are evaluated as follows:

- Development of a dose-response relationship with manual beam alignment at the growth centre.
- Apply laser irradiation to plants
  - (a) in the centre under the laser scanner,
  - (b) at the sides of the scan field and
  - (c) at the corners of the scan field.
- Examine these areas using a chlorophyll fluorescence measuring device. Determine the mean deviation from the centre of growth.
- Develop a suitable beam trajectory to lethally damage the growth centre at the LD<sub>90</sub> established in the dose-response relationship.
- Repeat the chlorophyll fluorescence images in the two evaluation areas of the scanner, but with the additional beam movement.
- Verify the success of the treatment using sample plants.

#### 3.2.4.1. Results

In our study, documented in Section 3.2.4, we investigated the effectiveness of laser treatment for plant eradication, focusing on analysing and improving the precision of laser application.

Initially, *Amaranthus retroflexus* (AMARE) sample plants were assessed at the BBCH12 growth stage to determine the optimum condition for laser treatment. These initial images, shown in Fig. 3.12, served as a baseline for subsequent evaluations of changes induced by laser treatment.



**Fig. 3.12. Condition of AMARE before laser treatment at BBCH12.**

One week after the laser treatment, the plants were examined again to assess the immediate effects of the treatment. The results shown in Figure 3.13 were categorised into four groups to classify the immediate response to the treatment.

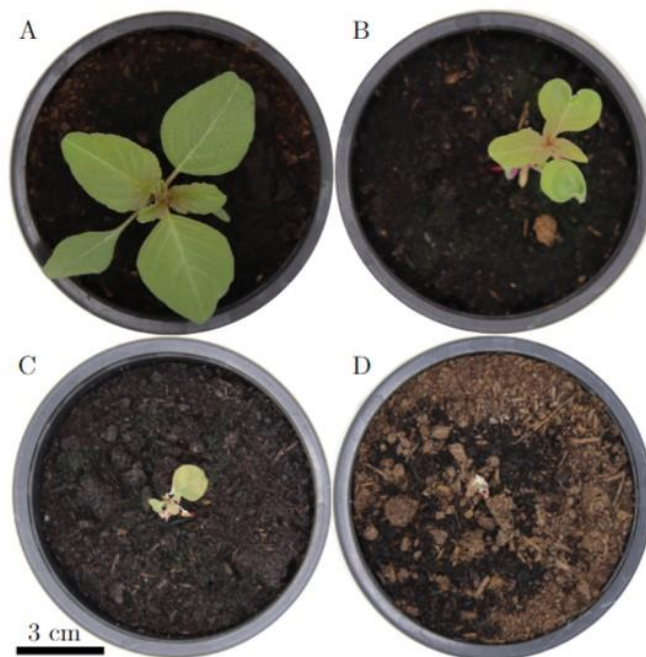


**Fig. 3.13. Condition of AMARE one week after different laser treatments. (A) untreated, (B) growth inhibited, (C) lethally damaged and (D) completely destroyed.**



**Fig. 3.14. Four-week long-term effect of the laser treatment, depending on the dose applied. Doses above 1.0 J/mm² are showing a favourable effect.**

Four weeks after the treatment, side views of the plants provided insight into the long-term, dose-dependent effects of the laser treatment. This long-term analysis, shown in Fig. 3.14 was crucial in determining an effective dosage strategy.

To provide a quantitative assessment of these experiments, the dry masses of the plants were determined after four weeks. This was used to determine the survival rate, which is shown in Fig. 3.15 as a function of received laser dose. Similar experiments were also carried out by UCPH using the same procedure and confirm the dose/effect relationships.

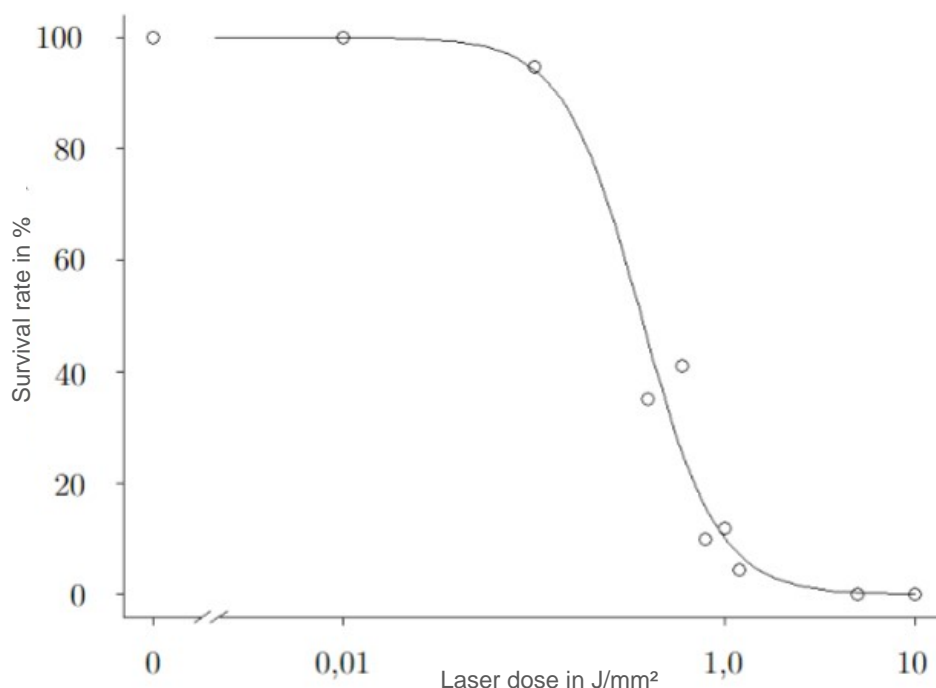


**Fig. 3.15. Graphical representation of the relationship between laser dose and plant response.**

An important aspect of the study was the use of chlorophyll fluorescence (CF) images alongside RGB images. The need for CF imaging arose from the fact that low laser doses could not be accurately detected in RGB images (see Fig. 3.16). Conversely, higher doses would prevent accurate localisation of the impact due to the destruction of plant material. CF imaging therefore provided a more effective method of visualising the accuracy of laser targeting and the treatment impact points. CF imaging was performed in three different areas under the scanner: directly under the scanner, on the sides and in the corners of the scan field. Fig. 3.16 and Fig. 3.17 each show a CF image with the corresponding RGB image for the areas directly under the scanner (Fig. 3.16) and in the corner of the scan field (Fig. 3.17)





**Fig. 3.16. Comparison of CF and RGB images to demonstrate the impact points of the laser treatment. The section shown is directly under the laser scanner.**

Table 3.3 with the measured deviations from the target point showed the areas where there was a lack of accuracy. This is particularly in the corners of the scanner's working area. This discovery led to the introduction of a high frequency beam movement to improve weeding performance.



**Fig. 3.17. Comparison of CF and RGB images to demonstrate the impact points of the laser treatment. The section shown is in the corners of the scan field.**

**Table 3.3. Deviations from the target point, highlighting the need for high frequency beam movement to increase the affected area.**

Experiment #	Investigated region of the scan field	Average distance from target	Standard deviation	Targeted plants (n)
1	Middle	2.02 mm	0.86 mm	17
2	Sides	2.16 mm	1.20 mm	11
3	Corners	3.09 mm	0.83 mm	10



After implementing the high-frequency beam movement, new CF images (see Fig. 3.18) confirm that better coverage of the target area has been achieved. To achieve a lethal dose of 90% ( $LD_{90}$ ), a minimum of  $1.0 \text{ J/mm}^2$  should be applied as shown in Fig. 3.16. The treatment time must be adjusted to ensure this. These results underline the improvement of the treatment process by adjusting the beam movement in the corners of the scan field.



**Fig. 3.18. CF images after the introduction of the high-frequency beam movement, confirming the effectiveness of the treatment adjustment for challenging areas of the scan field. The movement is achieved by a circular trajectory of 2 mm from the target point.**

The before and after images in Fig. 3.19 show the effectiveness of the modified laser treatment. They show 38 AMARE plants between sugar beets in optimal growing conditions. Additional experiments were carried out with 54, 63, 81 and 23 weed plants. They confirm that all the targeted weeds were successfully killed.



**Fig. 3.19. Before and after comparison to demonstrate successful laser treatment. This sample was treated with a 200 ms irradiation time, 100 W laser power and 5.1 mm average beam diameter.**



### 3.2.5. Testing the IoT devices

The devices have been tested in the laboratory and in the open air under operative conditions, in agreement with TRL7 statements - in particular:

#### RobotCamera

The set of cameras has been tested multiple times after installation, proving to be able to be correctly powered by the robot and to receive from the robot the messages triggering the snapshots. The Robot Cameras application system has also proved to be easy to install and remove so as not to alter or damage any inner or external part of the robot and the tools attached.

#### FieldCameras

The cameras have been stressed in the lab and outdoors, showing a critical point in the combination of the technologies used. In particular, the Passive Infra-Red (PIR) system is very sensitive to the presence of RF sources and the reflections of sun rays from vegetated surfaces, which may determine a number of false alerts; they, in turn, could determine an overload of controller and WiFi connection time, increasing the snapshot frequency, bringing to a significative depletion of Field Cameras battery lifetime. These aspects have been revealed from a debugging process that brought to the decision to limit the functionality of the cameras. As the cameras are also designed for time-lapse field-border images, they have been set to work in this modality. The mechanical solution adopted to apply them on the poles proved to be robust and easily replicable. The robustness of the poles and their setup show no issues over the period. In the field demo/days at Taastrup/Copenhagen, Denmark, and Reusel, The Netherlands, temporary poles have been adopted (see Fig. 3.20).



**Fig. 3.20. IoT devices at Taastrup demo field.**

## FieldBridge

As the field bridge node includes a WLAN access point allowing the connectivity of every WeLASER device, including field cameras, it suffered the same issues encountered by Filed Cameras. Though it has been designed with a wider PV cell and high-capacity battery, the controller (ESP32v2) and the protocol used (FTP) were not able to sustain a high frequency of false alerts. The troubles increased outside Arganda, Spain, i.e., (Taastrup, Denmark and Reusel, The Netherlands) where a low Digital Cellular Network coverage in some cases also compromised the time-lapse functionality.

## Weather Station and ETRometer

The WeatherStation and the ETRometer are two devices that introduce several innovations in the spirit of measurement, low cost, and ease of use. As the development focused on such aspects, they have been stressed for more than one year in a number of conditions (seasons, surfaces), proving their robustness and easy installation, while other features, including calibration protocol of adopted (commercial) sensors, are still under progress.

### 3.3. Performances of the final equipment

The system integration took until the first WeLASER Demo Days in summer 2023 leaving limited opportunity and time for the evaluation of the final integrated equipment due to a dense plan for demos and transportation between the demo sites. Furthermore, the assessment of the performance of the final system was hampered by technical (malfunction of laser source/chiller and further training of AI system) and agronomic issues during the limited on-field time (see also the following sections). Therefore, the performance of some subsystems (perception, targeting) could only be assessed qualitatively in the integrated equipment by comparing it to the performance of the standalone subsystem and an agronomic assessment of the on-field effectiveness of the WeLASER treatment has to be conducted on a larger scale in a follow-up research project (planned by UCPH, FUT, LZH). This section follows the indications for the whole system given in Table 1.7 of the DoA)

#### 3.3.1. Safety system

As described in the Grant Agreement (GA), a safety system was implemented that sought to ensure (i) safety to humans, (ii) safety to other vehicles or obstacles, and (iii) safety to the crop.

Regarding the first two points, the tests carried out to validate the safety system are presented below. Moreover, regarding crop safety, a guidance system was developed and the tests, which is presented in the following section.

To ensure the safety of humans, a system was implemented that connected the robot safety system with the weeding tool safety system. This connection was made following the schematic diagram presented in Fig. 3.21.

Individual validation tests were carried out in the final integration, executed in July 2023, ensuring the correct functioning of the implementation. Although no further tests could be carried out since a

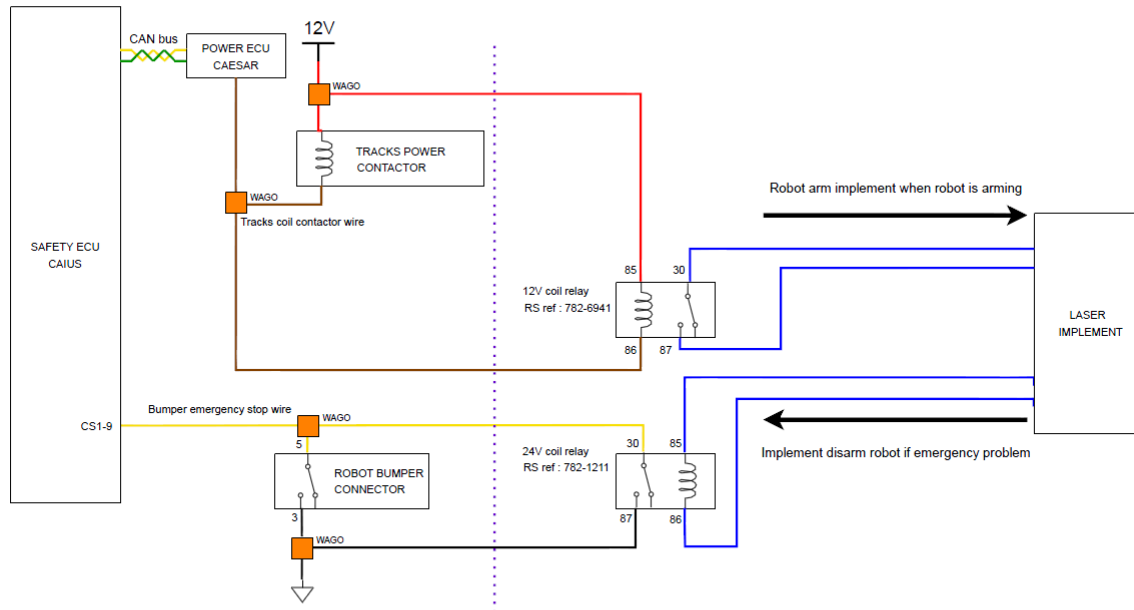


**Fig. 3.21. Schematic diagram of the implementation of the safety system between the mobile platform and the implement.**

set of problems with the logic of the implement's safety system were identified.

Regarding the safety of other vehicles and obstacles in general, including people, the GA stated that *“A safety system connected with the laser safety control and capable of reacting to static and dynamic obstacles in a circular area of 10-m radius around the vehicle (at 12 Km/h the vehicle will fully stop in 3.60 s)”* was expected as a Progress and innovation in Table 1.7 of the GA.

During the various project meetings, it was decided that the 10 m-circular area was not a viable solution for said implementation, given the following arguments:

1. The implementation of several sensors with a range of 10 m is only possible through the implementation of at least 3 LIDAR systems, such as the one provided by the mobile platform at the front (see Fig. 3.22), and given the morphology of the robot and the weeding tool, this solution was not feasible to implement. Moreover, under operating conditions, the 10-meter radius is a very large area where obstacles can always be found, such as weeds, trees, workers, etc.
2. The weeding tool already carries with it a safety system that consists of (i) curtains to protect against possible laser flashes and (ii) emergency buttons that disable the laser power.
3. The robot is only allowed to move forward and only allowed to move backward during the initialization process, which consists of aligning the IMU with the GPS. During this initialization process, the operator must be next to the robot since it is required to arm the robot (by pressing a button on the robot itself) and to enable automatic control (by pressing a switch on the remote control). During this process, the operator is responsible for the safety of the robot, the environment, and the people surrounding the robot.
4. The maximum operating speed for the execution of the treatment was defined as 2 km/h, i.e.,



0.55 m/s.



**Fig. 3.22. Image of the obstacle used for validation tests of the safety system.**

Given the previous arguments, it was decided to define a safety area in front of the robot as described in deliverable D4.1

Moreover, to evaluate this system, the GA stated that the system needs *“To detect 100% of 25 consecutive intrusion tests using a standard test obstacle based on the norm ISO 3411:2007”*.

The norm “ISO 3411:2007 - Earth-moving machinery - Physical dimensions of operators and minimum operator space envelope” provides the dimensions of operators of earth-moving machinery as defined in ISO 6165 and specifies the minimum normal operating space envelope within the operator. In this standard, a test obstacle is not described. But there is another standard, the ISO 18497:2018, that describes a test obstacle to ensure an adequate level of security of highly automated agricultural machines (HAAM). Therefore, an obstacle was prepared following the requirements of said standard, as shown in Fig. 3.22.

With the purpose of carrying out the evaluation of the safety system focused on the detection of objects, vehicles and people, a test was carried out in Section 2.3 (see Fig. 3.1) of the experimental fields at CSIC facilities, in Arganda del Rey, on September 19, 2023. As described in deliverable D4.1, the test consisted of the execution of a mission in a crop field, where the test obstacle was placed in 25 different locations, all blocking the robot's trajectory. Since there was only one test obstacle, 25 marks were made on the field, and the obstacle was moved to each mark once the robot had detected it. Each mark was acquired by the robot's mapping system (survey kit), and the locations of the marks were compared to the detections made by the robot. Figure 3.23 presents the trajectory executed by the robot in the safety test, in addition to the positions of the marks where the

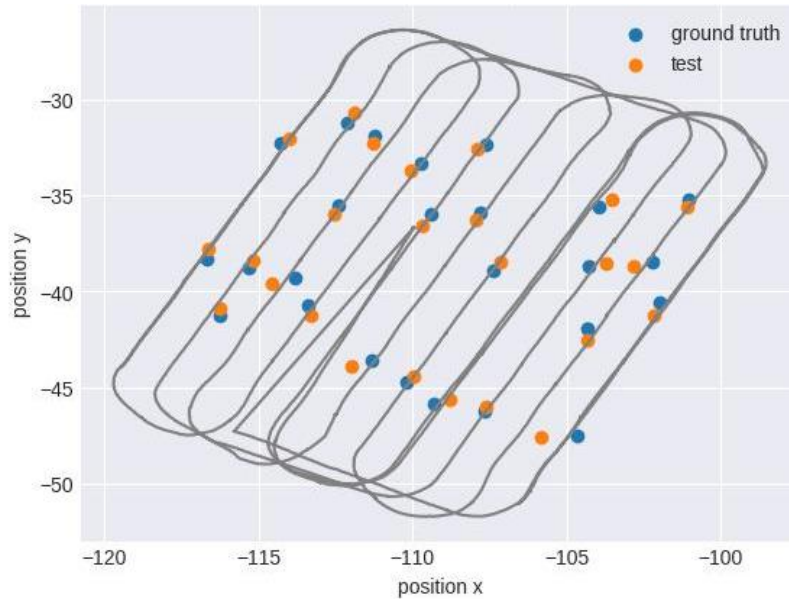


**Fig. 3.23.** Trajectory followed by the robot in the Section 2.3 (see Fig. 3.1.b) of the experimental fields at CSIC facilities, executing a treatment mission. In the blue locations, the test obstacle was placed following the standard ISO 18497:2018. The orange locations represent the estimated positions of the obstacle location according to the robot's safety system.

test obstacle was placed and the positions where the robot detected that the obstacle was found.

Table 3.4 presents the results of this test, where the positions of each mark (ground truth) and the obstacle positions detected by the robot are presented, together with the error in the detection.

**Table 3.4.** Performance of the object detection models. Coordinates in the local reference system of the mobile platform.

Obstacle	Mark location coordinates [m]	Obstacle detected coordinates [m]	Error [m]
1	[-104.67 -47.54]	[-105.83 -47.57]	1.15
2	[-101.97 -40.58]	[-102.15 -41.22]	0.66
3	[-101.04 -35.22]	[-101.09 -35.61]	0.39
4	[-102.20 -38.44]	[-102.84 -38.72]	0.69
5	[-104.32 -41.95]	[-104.33 -42.51]	0.55
6	[-107.65 -46.25]	[-107.59 -46.02]	0.23
7	[-104.25 -38.70]	[-103.72 -38.54]	0.55
8	[-103.94 -35.58]	[-103.53 -35.23]	0.53
9	[-109.31 -45.87]	[-108.77 -45.64]	0.58
10	[-110.21 -44.73]	[-109.95 -44.42]	0.39
11	[-107.36 -38.95]	[-107.12 -38.46]	0.54
12	[-107.82 -35.90]	[-107.94 -36.31]	0.41
13	[-111.32 -43.56]	[-111.97 -43.92]	0.73
14	[-109.38 -35.98]	[-109.65 -36.57]	0.64
15	[-107.62 -32.40]	[-107.91 -32.61]	0.36
16	[-109.73 -33.36]	[-110.03 -33.71]	0.45
17	[-113.37 -40.75]	[-113.27 -41.27]	0.53
18	[-113.82 -39.30]	[-114.53 -39.59]	0.76
19	[-112.40 -35.53]	[-112.51 -36.01]	0.48



20	[-111.22 -31.88]	[-111.27 -32.28]	0.40
21	[-112.09 -31.20]	[-111.86 -30.67]	0.57
22	[-115.32 -38.79]	[-115.14 -38.38]	0.45
23	[-116.23 -41.22]	[-116.25 -40.86]	0.36
24	[-116.69 -38.28]	[-116.64 -37.78]	0.50
25	[-114.27 -32.29]	[-113.97 -32.06]	0.37

Analysing the error of the 25 samples, the average distance between the planned location of the obstacle and the location detected by the robot is 0.54 meters with a standard deviation of 0.18. The minimum error is 0.23 m, with 25% of the samples having an error of less than 0.40 m. 75% of the samples have an error of less than 0.60 m, with a maximum of 0.76 m and an outlier near 1.20 m. Some particularities should be highlighted in this test:

1. The tests were conducted in a sugar beet field with a fairly advanced growth stage, much more than the target growth range for the laser system (see Fig. 3.22). It seemed relevant to carry out the safety test in this more complex scenario than usual to demonstrate the robot's capabilities in navigating complex environments.
2. The obstacle detection system mistook the obstacle's size and shape, identifying it as a straight line instead of a circle. This led to errors in pinpointing its exact location.
3. Given the crop growth stage, the presence of weeds, and that the trajectory of the robot was not consecutive to the crop lines (given the planning of the mission and the jumps), it was difficult, in some situations, to detect the mark, and the obstacle was placed where the mark was thought to be, hence obtaining some big errors.

Figure 3.24 presents the statistical analysis of the estimation error of the obstacle position, where it should be noted that the radius of the obstacle is 0.38 m.

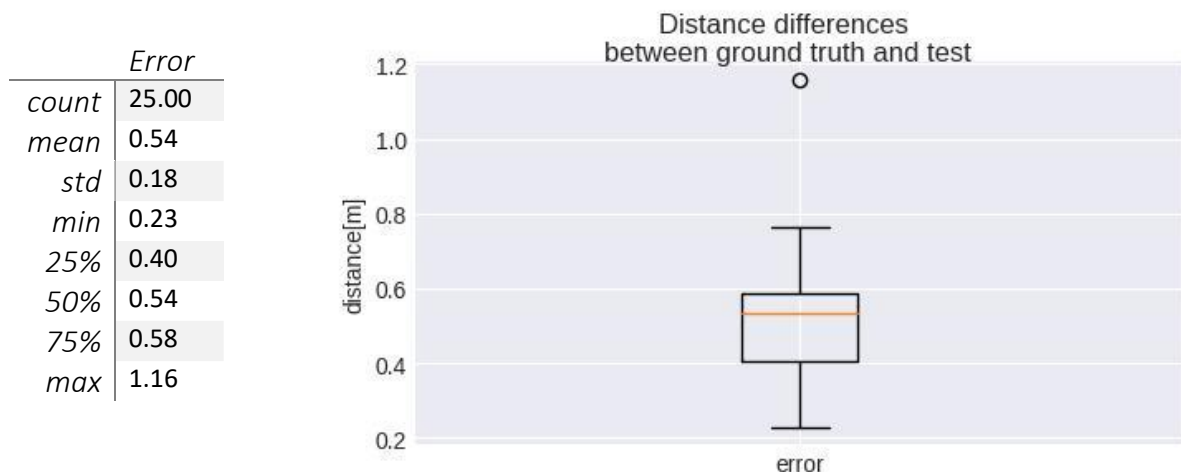


**Fig. 3.24. Statistical analysis of obstacle detection.**

Moreover, during the test, for every obstacle position, the following variables were recorded:

- Obstacle location (relative position to base antenna)
- Event time (mission time)
- Robot speed (m/s)

- Stop time (seconds)

Table 3.5 presents, for each obstacle, the reaction time of the robot to stop.

**Table 3.5. Results of reaction time when identifying an obstacle in the critical area.**

Obstacle	Event time [s]	Robot Speed [m/s]	Stop Time [s]
1	2023-07-19 10:17:12	-0.003	-
2	2023-07-19 10:19:26	0.427	0.6
3	2023-07-19 10:31:55	0.384	0.6
4	2023-07-19 10:34:01	0.356	0.36
5	2023-07-19 10:35:38	0.408	0.24
6	2023-07-19 10:35:59	0.377	0.6
7	2023-07-19 10:37:15	0.434	0.36
8	2023-07-19 10:37:45	0.381	0.6
9	2023-07-19 10:38:00	0.336	0.6
10	2023-07-19 10:39:28	0.398	0.48
11	2023-07-19 10:40:22	0.386	0.36
12	2023-07-19 10:41:53	0.366	0.24
13	2023-07-19 10:42:49	0.394	0.6
14	2023-07-19 10:44:26	0.399	0.24
15	2023-07-19 10:44:42	0.368	0.6
16	2023-07-19 10:44:57	0.377	0.24
17	2023-07-19 10:46:24	0.371	0.36
18	2023-07-19 10:46:48	0.364	0.36
19	2023-07-19 10:48:20	0.345	0.6
20	2023-07-19 10:48:38	0.375	0.36
21	2023-07-19 10:48:55	0.375	0.36
22	2023-07-19 10:52:45	-	-
23	2023-07-19 10:53:13	-	-
24	2023-07-19 10:54:36	-	-
25	2023-07-19 10:55:11	-	-

On average, the robot has a stop reaction capacity of 0.4 s at a nominal speed of 0.4 m/s, equivalent to a movement of 1 meter. Since the obstacle is detected 3 meters from the front of the robot, the reliability of the safety system is confirmed. It should also be noted that all obstacles were detected. Furthermore, during the field days and demonstrations, said safety system was active and functional and demonstrated its reliability since many of the attendees came to the field to see how the laser system worked, having the robot in automatic mode without the need to abort the mission nor the operator having to intervene.

### 3.3.2. Crop detection and row-follow tests

Throughout the entire development of the project and thanks to the preparation of the experimental fields at CSIC facilities, it was possible to generate a set of databases (described in “D6.7 - Data Management Plan (III)”) composed of images acquired by the frontal camera of the autonomous robot, in the 3 target crops: maize, sugar beet, and wheat. The acquisition of these images was crucial to implement a methodology described in “D4.1 - Autonomous vehicle: Design, integration and TRL assessment” to identify these crops in an early growth stage. In the first stage of the project,

the ability of this methodology to identify both wheat and maize was demonstrated, since they were the only two crops that could be planted out of season, between M13 – M14 (October - November 2021). Figure 3.25 presents two examples of the fields prepared during said period, both for maize (a) and wheat (b).

As indicated in deliverable D4.1, two different approaches were used to detect the crop: (i) segmentation for narrow-row crops, such as wheat, and (ii) object detection for wide-row crops, such as maize and sugar beet.

Regarding the segmentation approach, various segmentation models were evaluated (see Table 3.6) and it was decided to use the ResNet50-SegNet model since it demonstrated better results. Fig. 3.26 presents an example of the detection of wheat in conjunction with the training curve.



a



b

**Fig. 3.25. Example of (a) maize field, and (b) wheat field in the experimental fields at CSIC facilities at M13 (October 2021).**

**Table 3.6. Performance of the segmentation models**

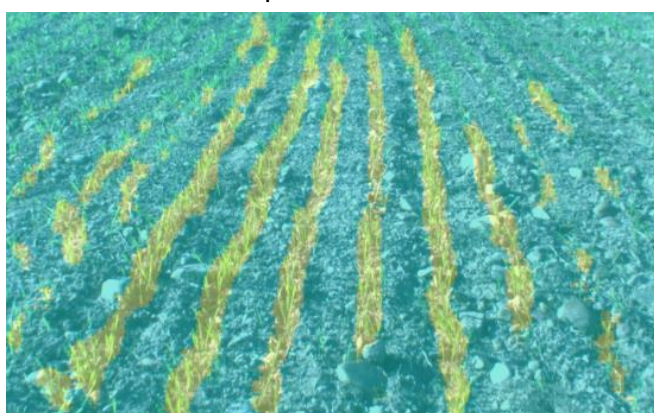
Model	IoU	Training time [s] per epoch
MobileNet SegNet	0.6815	124
MobileNet U-Net	0.7347	124
ResNet50 PSPNet	0.7370	180
ResNet50 SegNet	0.7578	164
ResNet50 U-Net	0.7406	183
VGG16 PSPNet	0.7343	227
VGG16 SegNet	0.7461	196
VGG16 U-Net	0.6982	208
CNN PSPNet	0.7321	171
CNN SegNet	0.7364	156
CNN U-Net	0.7339	155

Regarding the object detection approach, based on a bibliographic study, it was decided to use “You only look once” (Yolo) as an object detection architecture, given its easy implementation and short inference time compared to the rest of the options. At the beginning of the implementation, Yolo version 4 (Yolov4) was the most stable and compatible with ROS, so it was decided to use this version throughout the development of the project. However, in the last stages of the project, a more exhaustive study was carried out (see Table 3.7), where Yolo models were compared from version 4 to version 8, using 318 maize images, where 80% were used for training, 10% for testing, and 10% for validation. It was identified that version 5 had better performance than the implemented version, but it was decided to maintain version 4 throughout the entire development of the project, given the complexities of the migration of models during testing. In any case, although Yolov4 has a longer inference time than the rest, it was enough to demonstrate the guidance system.

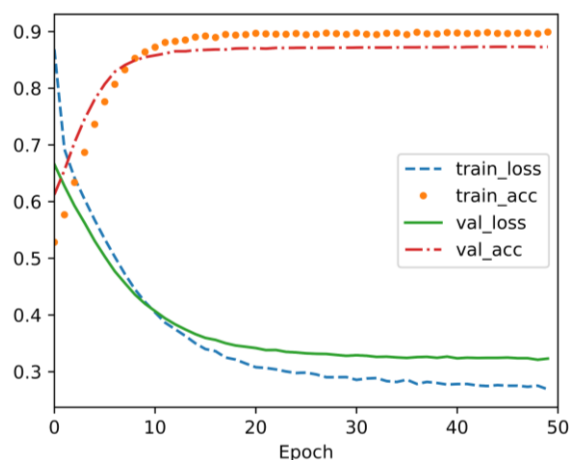
**Table 3.7. Performance of the object detection models.**

Model	Training Time (hours)	mAP	Inference Time (ms) <sup>1</sup>
Yolo v4	1.330	66.8%	673.1
Yolo v5	0.342	77.0%	15.9
Yolo v6	2.184	66.9%	8.2
Yolo v7	2.307	69.8%	22.0
Yolo v8	1.663	77.5%	16.6
<sup>1</sup> Machine characteristics: NVIDIA Tesla T4, 15 GB memory.			

Not only was a system implemented to detect the target crops of the WeLASER project, but also the said system was capable of identifying the growth status of each crop, focused particularly on maize and beets, given that throughout the development of the project, it was the two crops that were the focus of efforts. Table 3.8 presents the results of the detection of the different growth states for maize and sugar beet, following the BBCH phenological scale, and Fig. 3.27 presents an example of the detection of said crops.



**a**



**b**

**Fig. 3.26. Example of (a) output of the segmentation model for wheat, and (b) example of training curves (Y-axis normalized to compare loss curves and precision curves).**



**Table 3.8. Mean Average Precision (mAP) results for the detection of sugar beet and maize growth stages.**

Crop	Growth Stage	mAP
Sugar beet	12	57.2%
	14	76.6%
	16	86.3%
	18	89.7%
Maize	10	69.4%
	12	78.1%
	14	65.3%
	16	56.8%
	18	37.1%

With the models to detect the various crops, a set of tests were carried out to verify the correct operation of the row follower system. Since the main purpose of the guidance system is crop protection, the tests focused on wide-row target crops, such as maize and sugar beets, since if they



a



b

**Fig. 3.27. Detection (red) vs. ground truth (green) example. The model detections are highlighted in red, identifying the crop and confidence of the detection. The initial annotations for training are high-lighted in green. (a) Example of correct detections of sugar beet plants that were not initially labelled. (b) Example of a case of incorrect detection of weeds as sugar beet plants with a confidence of 0.26.**



were stepped on by the mobile platform they could be damaged and not grow again. This is in contrast to wheat, which is a narrow-row crop and if it is stepped on by the tracks it can regenerate again.

Within the period from July to September 2023, the information of the robot was recorded executing several missions in the maize and sugar beet fields at the experimental farm at CSIC facilities. This data includes images (both from the RGB and ToF cameras), position of the robot, state of the robot, among many others. These data have been used to validate the guidance system offline, given that during the different field tests the system that allowed estimating the orientation of the robot. i.e. the IMU, was not reliable. And the guidance system depends considerably on a stable and reliable IMU, since it is necessary to transform the detected crop positions to the robot's reference system.

In total, results from three records are presented, acquired on (i) June 21, 2023, in a sugar beet field with BBCH growth stage 14, August 1, 2023, in a maize field with BBCH growth stage 14, and on September 14, 2023, in a maize field with BBCH growth stage 12. Each record, in addition to containing the information generated by the autonomous robot executing a mission, also contains the positions of the centre line of the crop rows that the robot had to follow, this being the ground truth. These positions were acquired by the AGREENCULTURE survey kit with a precision of  $\pm 0.015$  m.

Table 3.9 presents a summary of the general results obtained when analysing the crop guiding system for the three scenarios proposed. This table presents, for each record, the growth stage of the crop, the number of passes (Total Lines) that the robot makes through the field, and the lateral error of the robot in following the line. Each pass or line corresponds to two crop rows, given that both maize and sugar beets were planted at 75 cm. Moreover, this table also presents the overall results obtained by the guidance system for each record.

**Table 3.9. Crop guidance results.**

Date	Crop	Ground Truth		Crop-Row Follower	
		Total Lines	Robot's Mean Lateral Error [m]	Lines followed	Mean Lateral Error
Sep-14-10-36-34	Maize12	6	0.046	5	0.147
Aug-01-11-39-39	Maize14	11	0.01	8	0.103
Jun-21-11-51-29	SugarBeet14	10	0.1	8	0.083

If the guidance system is analysed in overall terms, the results are not the desired ones, given that it was not possible to follow all the lines adequately, and the errors obtained in the detection of the crop lines are greater than expected. For this reason, a detailed analysis of each record is carried out to better estimate the performance of the guidance system.

In this sense, Table 3.10 presents, for each record, the average detection errors for each crop line followed, whose tracking had a length greater than 5 meters. In this case, an analysis is carried out separating the crop-row tracking into two main parts: (1) the first consists of the initial 20% of the line,

i.e. when the robot finishes turning and faces the crop lines and advances 20% of the trajectory, and (2) the remaining 80% of the trajectory. This separation is due to the fact that at the beginning of the line the robot rotates based on the spiral controller, which focuses on aligning the robot rather than positioning it in the correct place. And this generates an inclusion of noise added to the drift of the IMU measurements.

As previously indicated, to carry out a more objective evaluation of the crop-row guidance system, each record must be analysed individually. Therefore, the statistical results and detection examples for each of the records described in Table 3.10 are presented below.

**Table 3.10. Crop guidance results.**

Date	Crop	Line id	Mean lateral error [m]		
			Total per line	First 20%	Last 80%
Sep-14-2023	Maize12	1	0.068	0.046	0.028
		2	1.648	2.963	1.321
		3	0.087	0.066	0.037
		4	0.140	0.093	0.064
		5	0.221	0.083	0.113
		<b>Mean</b>	<b>0.129</b>	<b>0.072</b>	<b>0.061</b>
Aug-01-2023	Maize14	1	0.139	0.188	0.081
		2	0.121	0.175	0.109
		3	0.055	0.051	0.031
		4	0.047	0.074	0.035
		5	0.109	0.110	0.088
		6	0.151	0.135	0.131
		7	0.154	0.172	0.122
		8	0.038	0.035	0.028
		<b>Mean</b>	<b>0.115</b>	<b>0.123</b>	<b>0.085</b>
Jun-21-2023	Sugar beet 14	1	0.054	0.117	0.039
		2	0.140	0.107	0.034
		3	0.075	0.169	0.045
		4	0.075	0.035	0.017
		5	0.080	0.044	0.049
		6	0.093	0.035	0.097
		7	0.189	0.045	0.049
		8	0.050	0.073	0.026
		<b>Mean</b>	<b>0.084</b>	<b>0.060</b>	<b>0.042</b>

#### 3.3.2.1. Row follower for maize12

By observing the mean average errors of each line separately in Table 3.10, and especially those corresponding to 80% of the line, more encouraging results can be observed. These are errors corresponding between 2 and 6 centimetres, taking into consideration that they are based on the GPS localization system, whose sensitivity is  $\pm 1.5$  centimetres, and are affected by the unwanted variations in the IMU.

From the observed data, an outlier can be detected, which corresponds to line 2 of the Maize12 record. To appreciate in detail what happened, Fig. 3.28 presents the trajectory followed by the robot

in the maize field when executing the mission on September 14, 2023. Furthermore, this figure

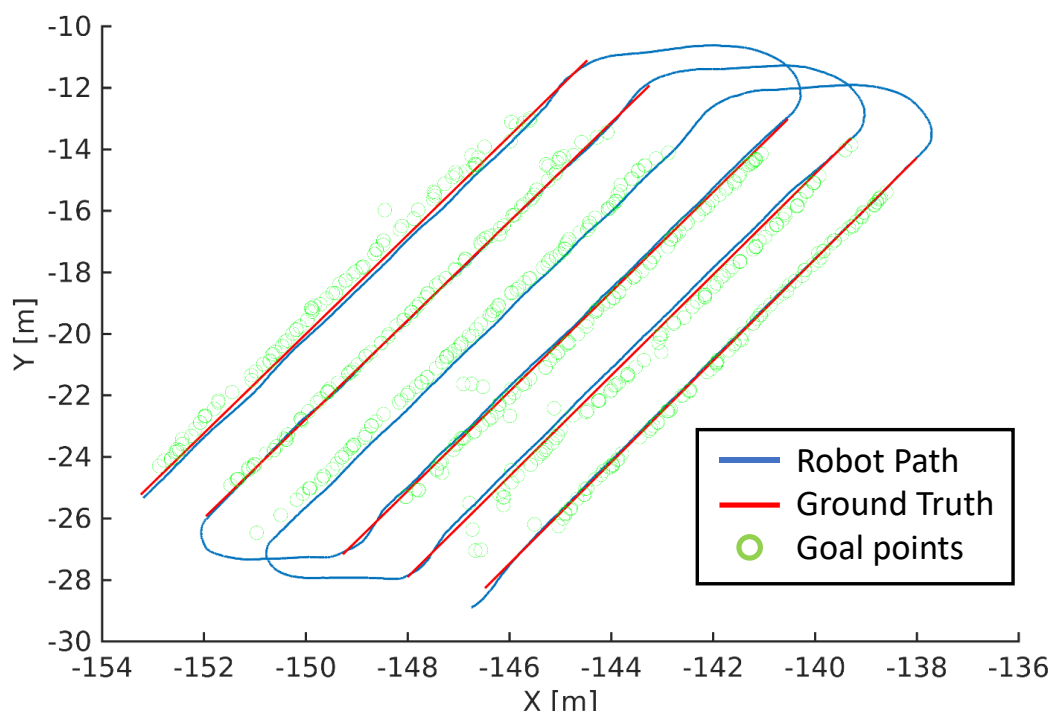


**Fig. 3.28. Mission executed by the robot in the maize field with BBCH growth stage of 12, which includes: (i) Robot trajectory (blue), ground truth (red), target points generated by the guidance system (green).**

presents the lines that the robot had to follow (ground truth), which represent the centroid between two consecutive crop lines, and the goal points generated by the crop guidance system.

The first thing that stands out about this figure is that the ground truth cannot be observed in the central line, and hence the errors in line 2 for maize 12 in Table 3.10 are very large. To have a greater explanation of what happened, Fig. 3.29 presents the estimation of states of the guidance system, where it identifies when the robot enters a line (Lane) and when it leaves, i.e. when it reaches the headlands.

The guidance system depends not only on the identification of the crop lines, but also on the identification at their entry and exit. To do this, it uses a strategy based on probability to estimate the probability of being either in the lane or in the headlands. And this probability strategy in conjunction with the metric estimation builds the guiding strategy. In this particular test, an error occurred (see red box in Fig. 3.29) which did not allow the state estimator to properly estimate that the robot had left the line it was following, line 2, and continued generating objective points on line 3 but maintained the ground truth of line 2, hence the large errors in line 2 and the lack of a line in Table 3.10.

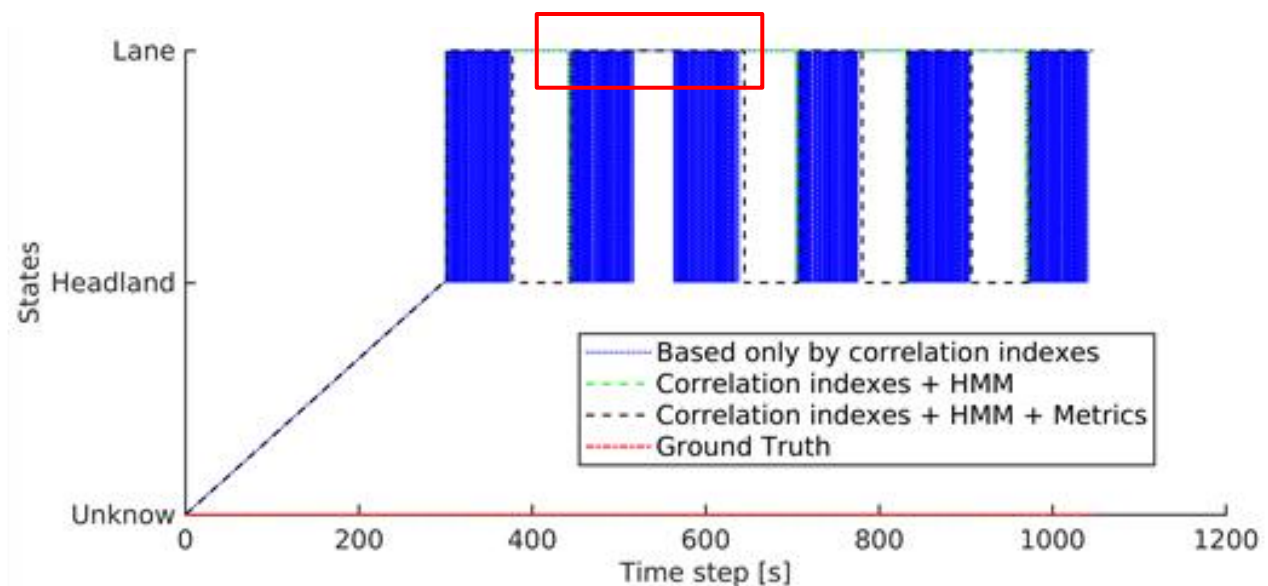


**Fig. 3.29. Estimation of states of the robot's localization in the field, while executing a mission in the maize field with BBCH growth stage of 12.**

Performing a deeper statistical analysis, and eliminating outliers due to an error in the appropriate selection of the ground truth, Fig. 3.30 presents a histogram that compares the average error values of the robot lateral error with respect to the crop guidance system. This statistical analysis indicates that the crop guidance system presents a smaller lateral error than the robot guidance, particularly in 80% of the trajectory.

Regarding the identified problems of the IMU, Fig. 3.31 presents a histogram of the angular error of the robot in tracking the trajectory. It can be seen that a considerable error is perceived, which, as previously indicated, affects both the guidance of the robot and the detection of crop lines.

And as a graphic result, Fig. 3.32 presents an example of the detection of the crop for this record and an example of the detection of the crop lines and the estimation of the objective points for monitoring them. To detect the crop rows, a clustering of the points that represent the crop positions is carried out, and in the figure this clustering is seen with the red and green points. Furthermore, the goal points are represented with yellow and grey vectors, and define the trajectory that the robot should follow to adjust to the crop lines.



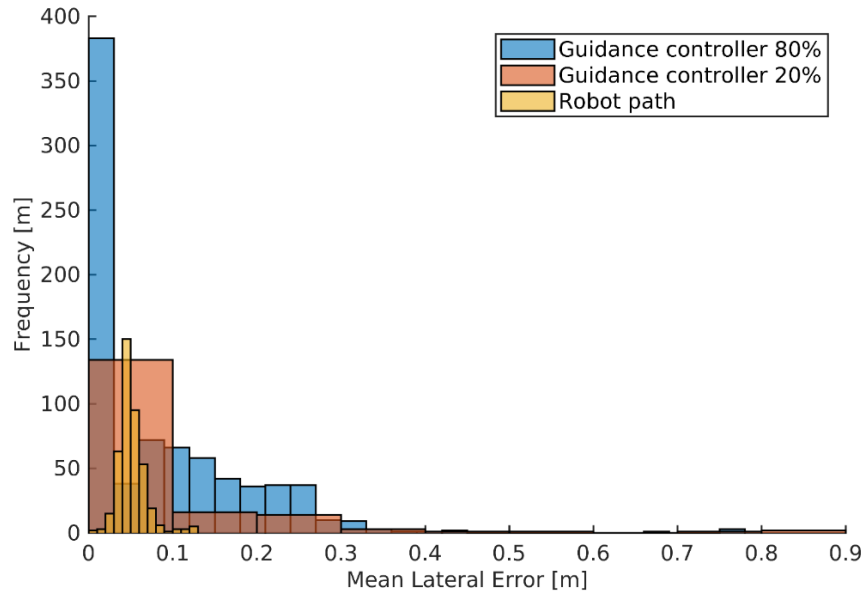


**Fig. 3.30. Histogram of the mean lateral error of the row guidance system compared with the robot error in following the path. The row guidance systems histogram is divided in the first 20% of the trajectory, and the 80% remaining.**

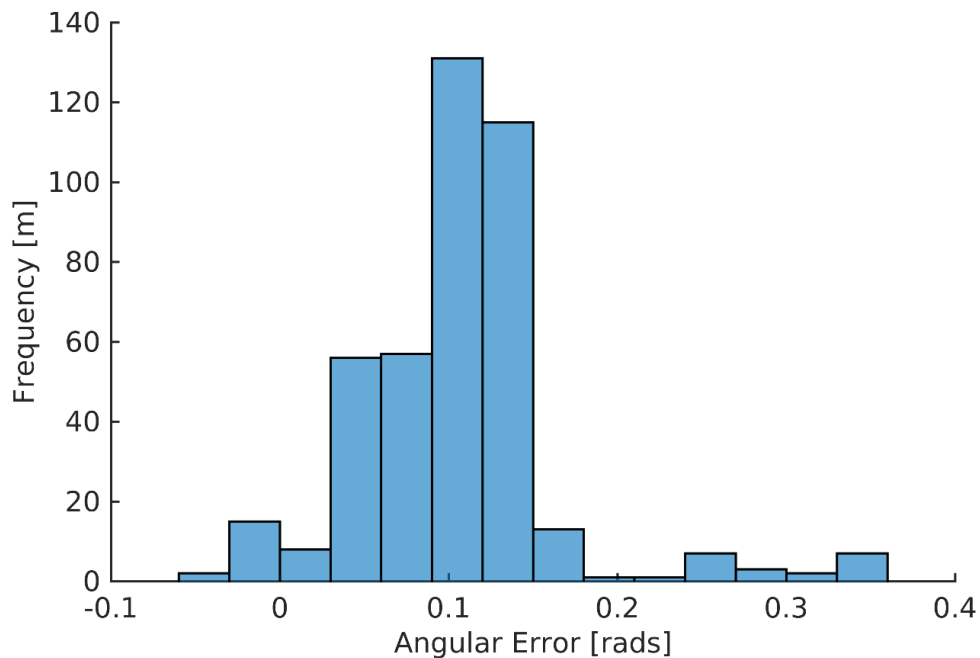
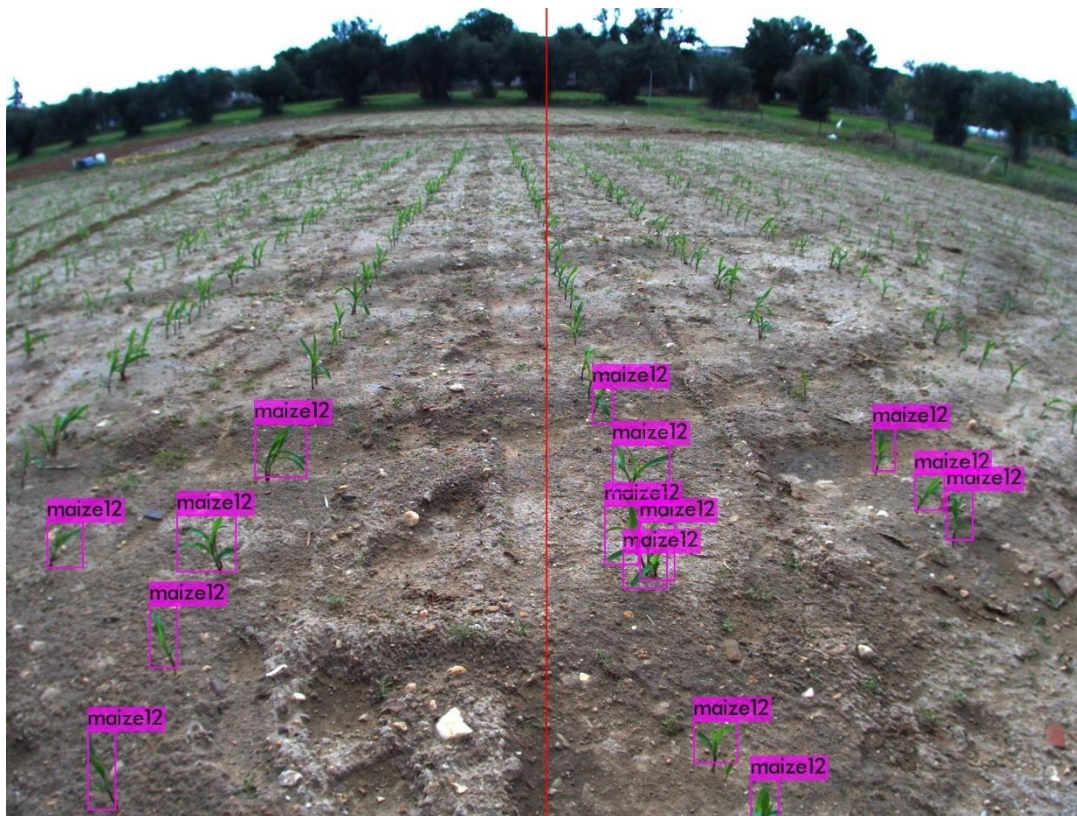
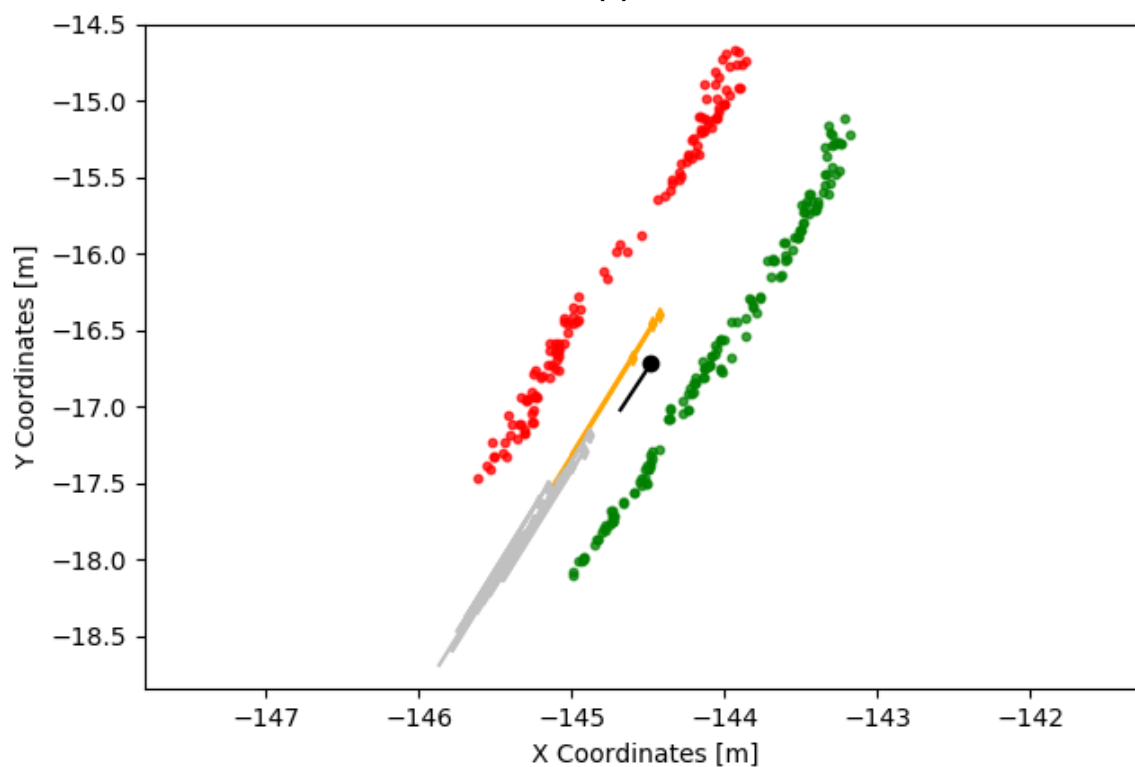


**Fig. 3.31. Histogram of the mean angular error of the robot in following the straight path of the mission in the maize field with BBCH growth stage of 12.**



(a)



(b)

**Fig. 3.32.** Example of: (a) crop detection, and (b) crop row following for the mission in the maize field with BBCH growth stage of 12. The red and green dots represent the identification of the crop rows, and yellow and grey vectors the goal points.

### 3.3.2.1. Row follower for maize14

For the record obtained on August 01, 2023, no significant outliers are observed, although some errors in the estimation of the goal points are greater than desired (see Table 3.10). To better appreciate what has happened in this record, Fig. 3.33 presents the trajectory followed by the robot in the maize field when executing the mission on August 01.

In this record it can be observed that the robot has satisfactorily followed the majority of the crop lines, with 3 remaining to be identified. Regarding these lines that were not identified, this has occurred because many maize plants were missing. This is mainly due to the time when the maize was planted, which did not correspond to the preferred dates for this type of crop. Fig. 3.34 presents a deeper insight into the detection of state change.

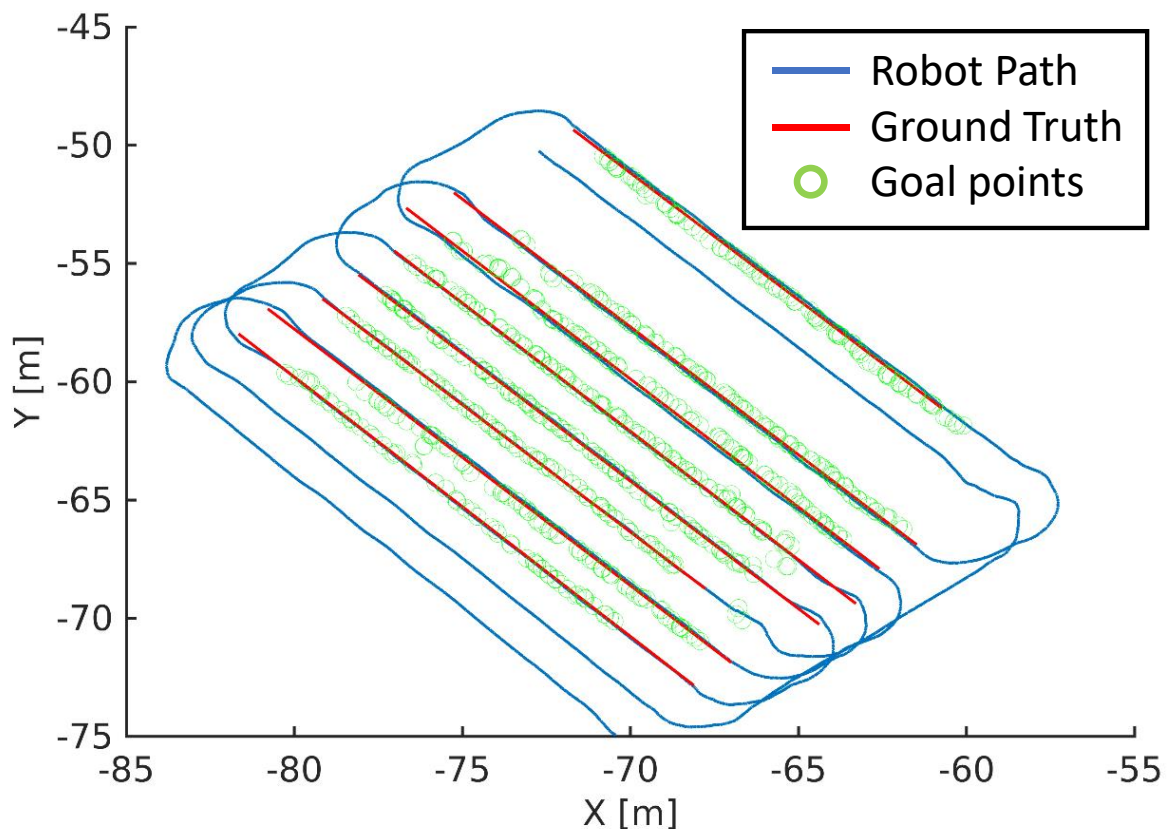


**Fig. 3.33. Mission executed by the robot in the maize field with BBCH growth stage of 14, which includes: (i) Robot trajectory (blue), ground truth (red), target points generated by the guidance system (green).**

It can be observed in Fig. 3.34 that in lines 9 and 11 the system detects a change of state, from the Headland to the Lane. But shortly after, there is no longer a detection, i.e. no more estimation (see blue lines). This is due to the lack of information coming from the vision system. The same situation happens at the beginning of the mission, where the system is in an unknown state, also due to the lack of information.

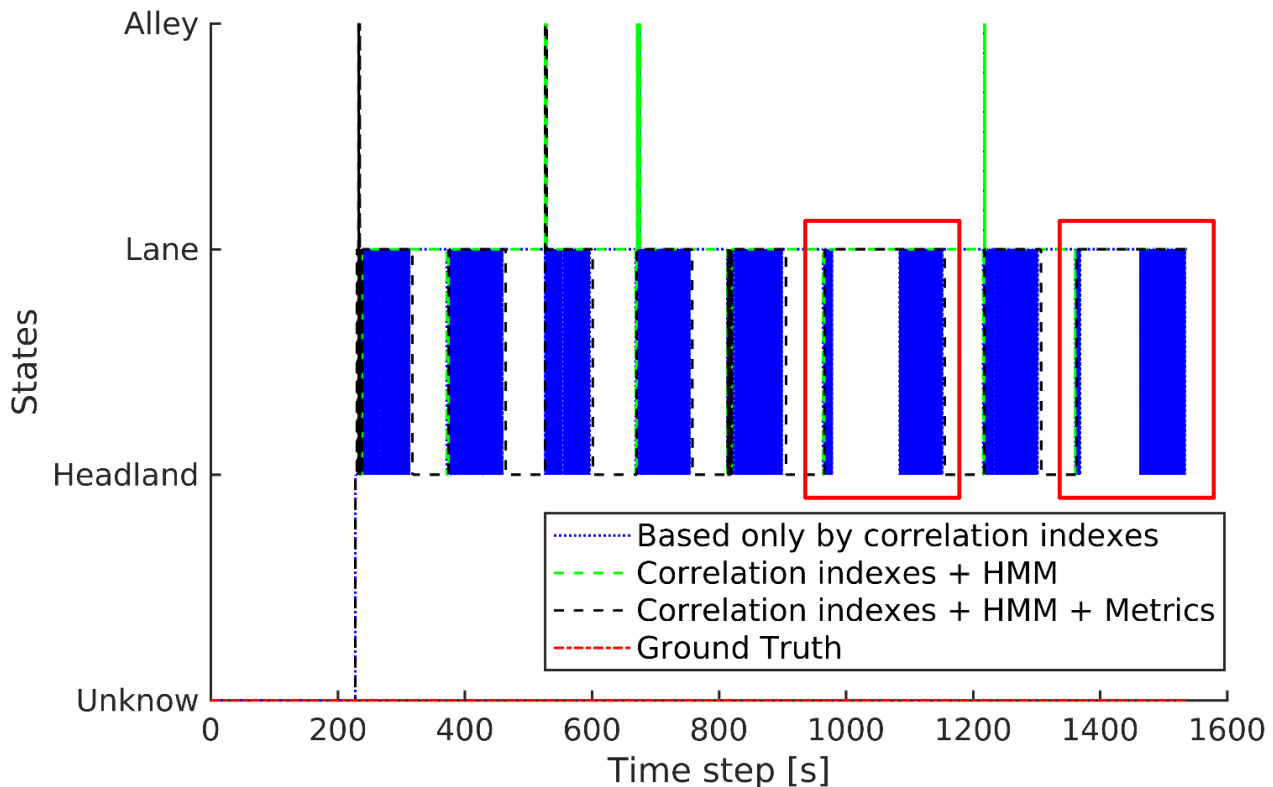


**Fig. 3.34. Estimation of states of the robot's localization in the field, while executing a mission in the maize field with BBCH growth stage of 14.**

By conducting an in-depth statistical examination, Fig. 3.35 illustrates a histogram contrasting the average error values between the robot's lateral error and the crop guidance system. The analysis reveals that, for 80% of the trajectory, both the crop guidance system and the robot guidance exhibit the same smaller lateral error. This is because, for this particular test, the phase shift generated by the IMU was not significant (see the angular error of the robot guidance in the Fig. 3.36), so the error of the robot following the trajectories was not large. This confirms the precision of the crop guidance system



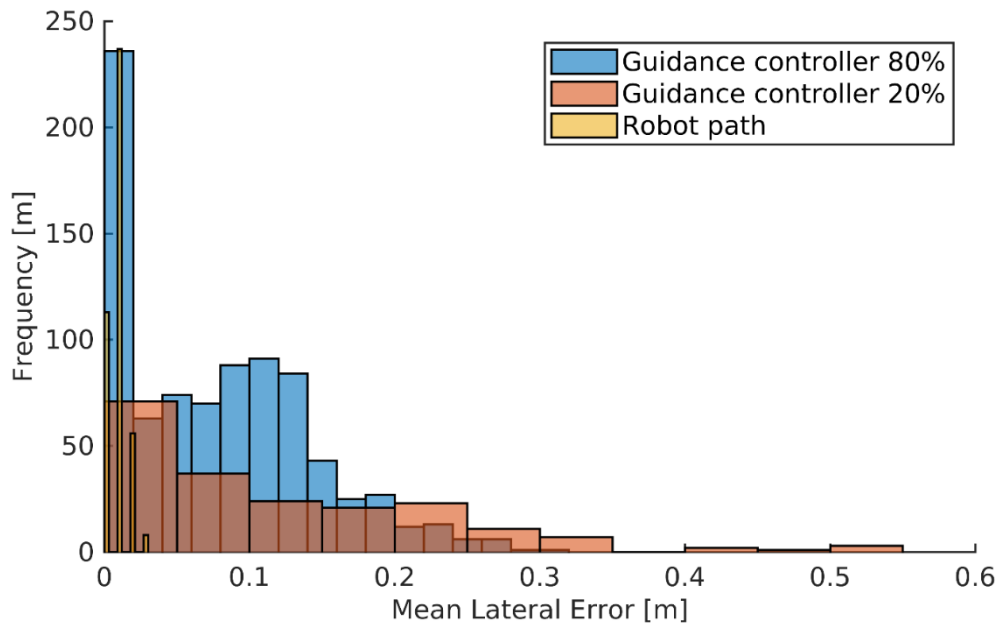


**Fig. 3.35. Histogram of the mean lateral error of the row guidance system compared with the robot error in following the path. The row guidance systems histogram is divided in the first 20% of the trajectory, and the 80% remaining.**

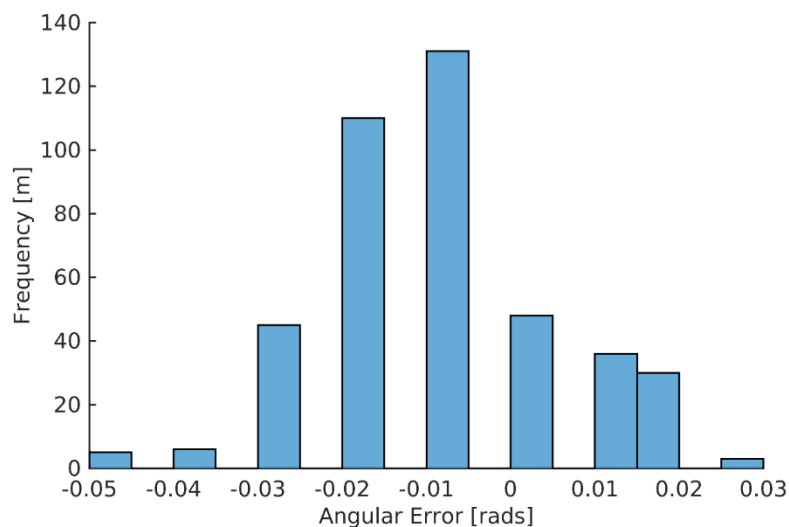
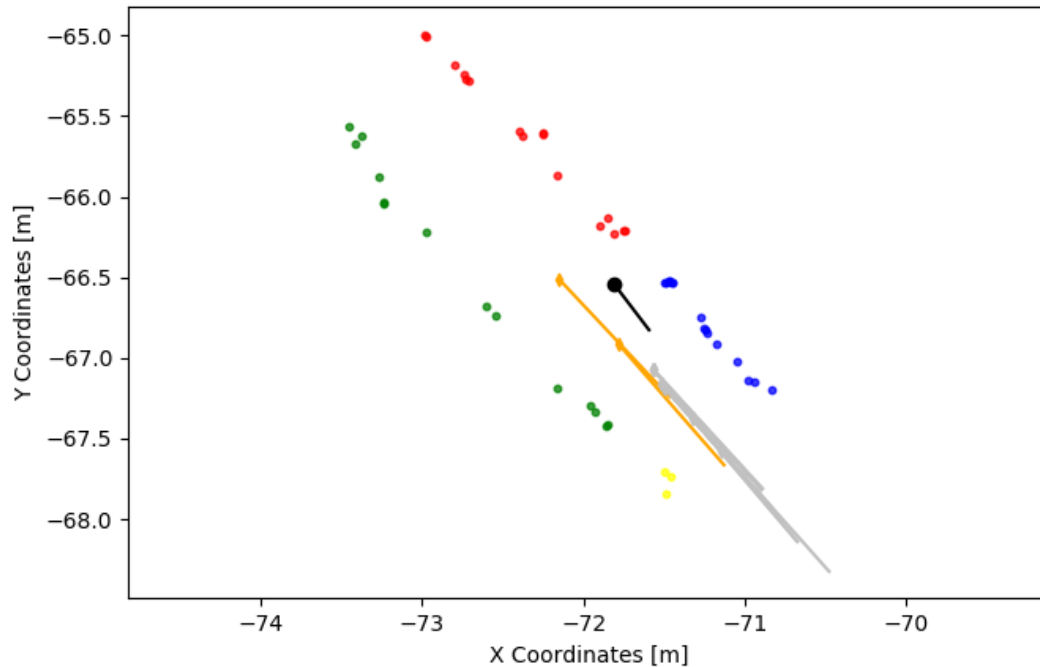


**Fig. 3.36. Histogram of the mean angular error of the robot in following the straight path of the mission in the maize field with BBCH growth stage of 14.**

Figure 3.37 visually demonstrates the identification of the crop in this record and showcases the process of detecting crop lines and estimating goal points for their monitoring. The crop rows are detected through a clustering method applied to the points indicating crop positions, visible in the figure as red and green clusters. Additionally, the yellow and grey vectors represent the goal points, outlining the trajectory adjustments necessary for the robot to align with the crop rows.



(a)



### 3.3.2.1. Row follower for sugarbeet14

Regarding the record obtained on June 21, 2023, also no significant outliers are observed, and although also in this case the guidance system failed to detect two lines (see Table 3.10), the results present satisfactory values. Figure 3.38 presents the trajectory followed by the robot in the sugar beet field when executing the mission on June 21, 2023.

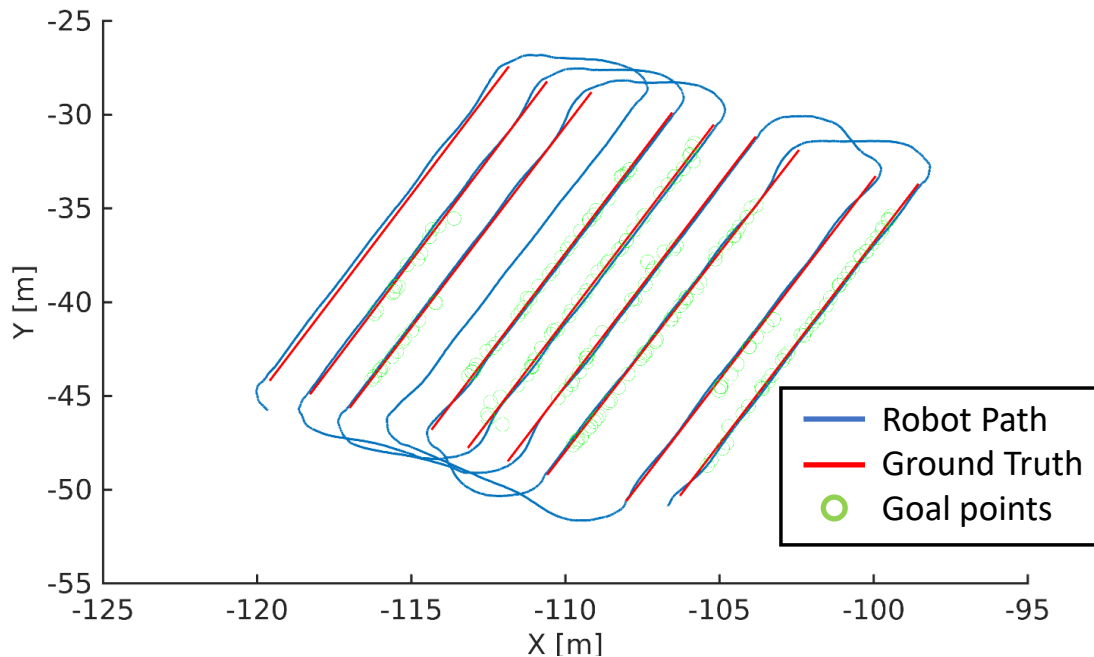


**Fig. 3.38. Mission executed by the robot in the sugar beet field with BBCH growth stage of 14, which includes: (i) Robot trajectory (blue), ground truth (red), target points generated by the guidance system (green).**

This record shows the robot's successful tracking of most crop lines, with only two remaining unidentified. This situation is similar to the one presented above, primarily caused by missing sugar beet plants due to the planting timing not aligning with the optimal schedule for this crop type. Moreover, Fig. 3.39 provides a more detailed examination of the state change detection.

It can be observed in Fig. 3.39 that there is a systematic failure to adequately detect changes in state (see red boxes in Fig. 3.39), or a change from Lane to Headland is detected but it returns to the Lane again. This is a failure in the guidance system estimation of the chase of the goal points, and requires further development to mitigate these failures. Moreover, it is also possible to observed that in several cases an alley detection is carried out (especially in yellow box in Fig. 3.39). This is because only one of the crop rows is detected, or there is only the presence of crops in one of them.

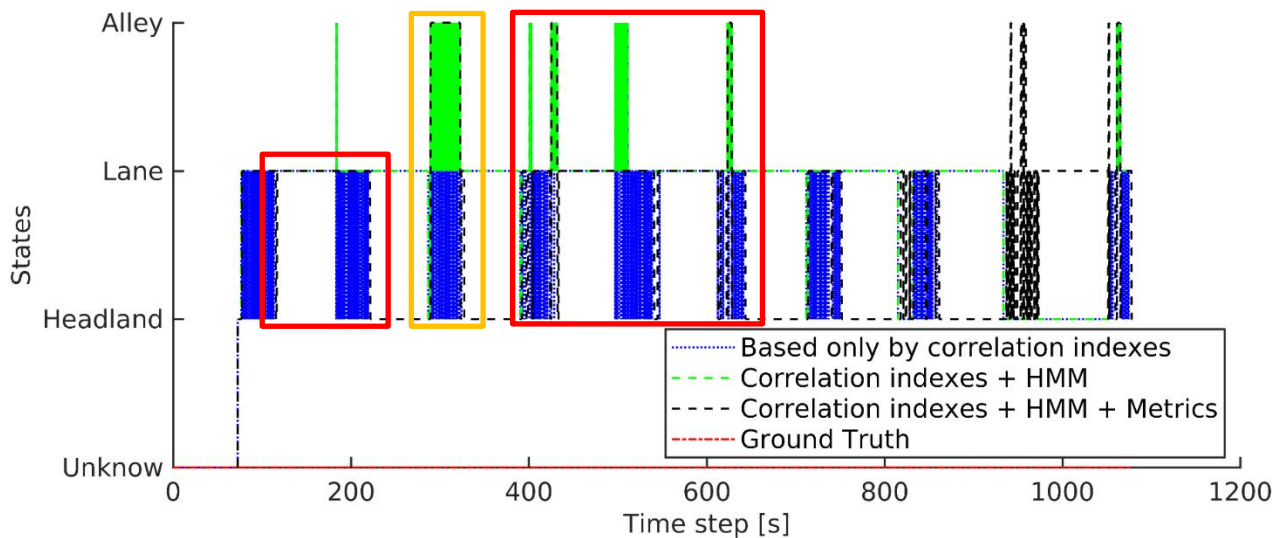


**Fig. 3.39. Estimation of states of the robot's localization in the field, while executing a mission in the sugar beet field with BBCH growth stage of 14.**

Regarding the in-depth statistical examination, Fig. 3.40 presents a histogram contrasting the average error values between the robot's lateral error and the crop guidance system. The analysis reveals that, for 80% of the trajectory, the crop guidance system presents a smaller lateral error than the robot guidance, confirming the value of the crop guidance system on improving robot guidance in crops. Greater advances are required to be able to develop a more robust crop guidance system, which adapts to the real conditions of the field, where in many cases the crops are missing or are occluded by weeds.

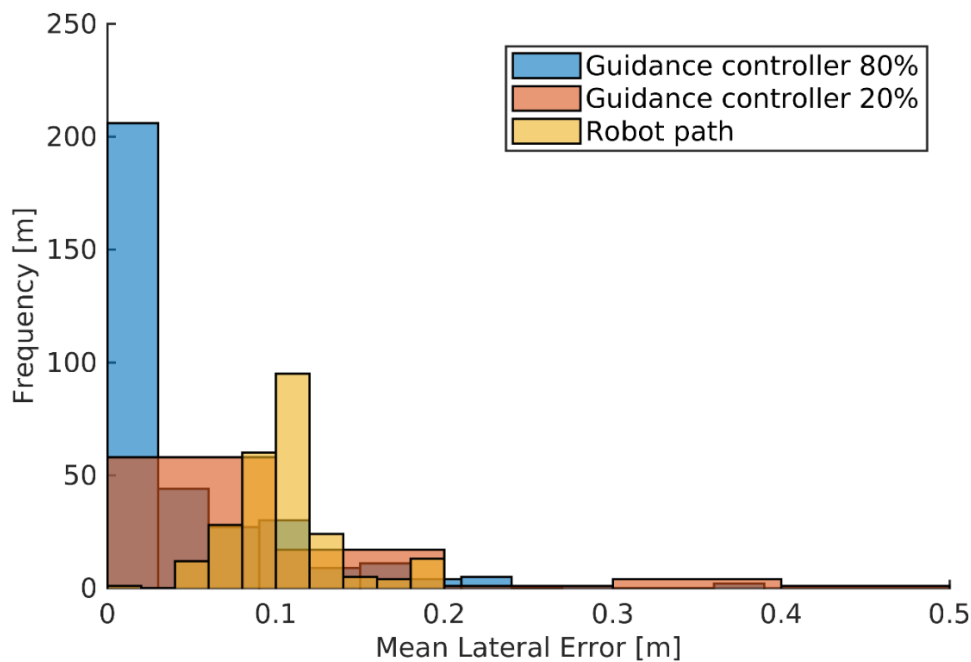
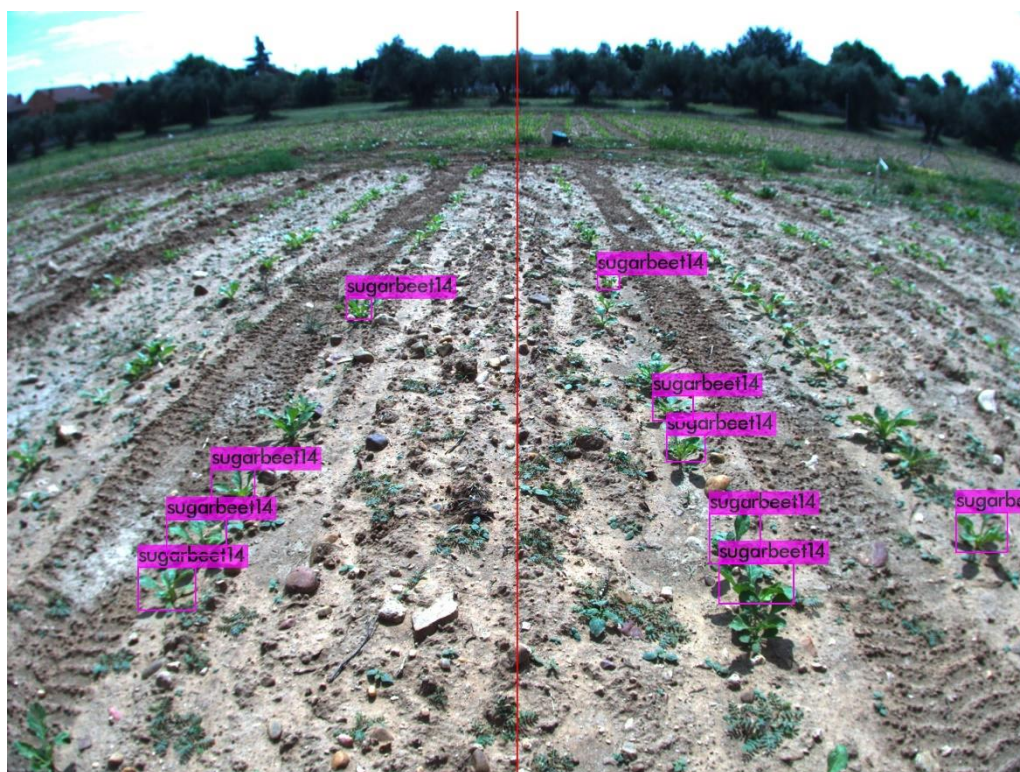


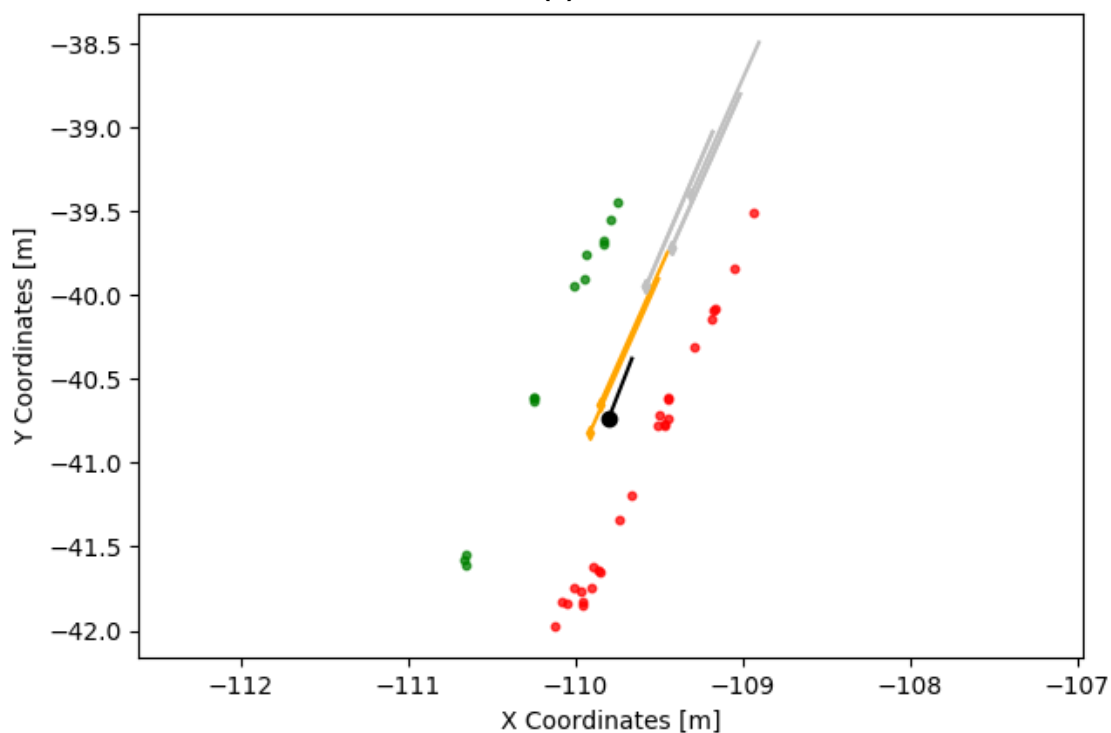
**Fig. 3.40. Histogram of the mean lateral error of the row guidance system compared with the robot error in following the path. The row guidance systems histogram is divided in the first 20% of the trajectory, and the 80% remaining.**



To conclude, Fig. 3.41 presents the identification of the crop within this record and highlights the procedure for detecting crop lines and estimating goal points for their guidance.



(a)



(b)

**Fig. 3.41. Example of: (a) crop detection, and (b) crop row following for the mission in the sugar beet field with BBCH growth stage of 14. The red and green dots represent the identification of the crop rows, and yellow and grey vectors the goal points.**

### 3.3.3. Planner

To evaluate the mission planner and to comply with the statements presented in the Grant Agreement (*Sensitivity analysis by slightly modifying the planner trajectories and checking if performances become worse*), some tests were carried out in the CSIC experimental fields in September 2023. In these tests, the performance of the autonomous robot in the execution of missions in the field was evaluated by changing the main configuration parameter of the missions, which is the number of jumps between crop lines (see Annex 2 of “D4.1 - Autonomous vehicle: Design, integration and TRL assessment”). Given the characteristics of the mobile platform, the distance between tracks (1.48 m), and the operating width of the laser system (1 m), in conjunction with the characteristics of the target crop fields (maize and sugar beets, seeded between 0.5 m and 0.75 m), the optimal jump parameter for the execution of treatment emissions was identified as 3. This allowed

1. the robot always moves forward, avoiding manoeuvres that required backward movements since there were no safety sensors available for these manoeuvres,
2. that the preferred turning radius is 1.5 m, a little larger than the width of the tracks, allowing in most situations both tracks to move forward and avoid further damage to the soil, and
3. the minimum number of jumps based on the two previous requirements that entails the shortest possible path.

To evaluate the performance of the mission, not only the total distance travelled or the execution time of the mission were calculated, but the energy consumption related to the mobility of the mobile platform was measured. To do this, the voltage (V) and current (I) sensors of each inverter were used to calculate the instantaneous power at each instant of time (kW). Therefore, the total energy consumption (kWh) was calculated by taking the current and voltage of the left and right inverters required to execute the mission. Following these measurements and the duration of the mission, the energy consumption was estimated as follows:

$$Left\_inverter\_power = inverter\_current\_left * inverter\_voltage\_left$$

$$Right\_inverter\_power = inverter\_current\_right * inverter\_voltage\_right$$

$$Total\_consumption = ((Left\_inverter\_power + Right\_inverter\_power) * duration) / 1000$$

For this study, 3 missions were carried out in the same field, with different jump parameters: 3, 6 and 8. It should be noted that given the characteristics of the field and that the planner is a system that seeks the optimal trajectories in terms of distance travelled, the robot does not execute the desired jumps in all situations. Table 3.11 presents the results of the tests carried out, making it clear that the optimal configuration of 3 jumps prevails as the most appropriate option for this robot.

**Table 3.11. Results of the sensitivity tests carried out on the mission planner**

Jumps	Treatment distance (m)	Treatment time (s)	Total consumption (kW)	Jumps sequence
8	381.6	1618.8	2029.4	8/7/8/7/8/7/8/6/7/6/1/3/8
6	381.5	1758	1761.3	7/6/7/6/7/6/7/6/7/6/6/6
3	325.4	1411.8	1517.4	3/3/4/3/3/3/4/3/3/9/2/3/3

Figure 3.42 presents the trajectories executed by the robot in the crop field for each of the 3 test missions.

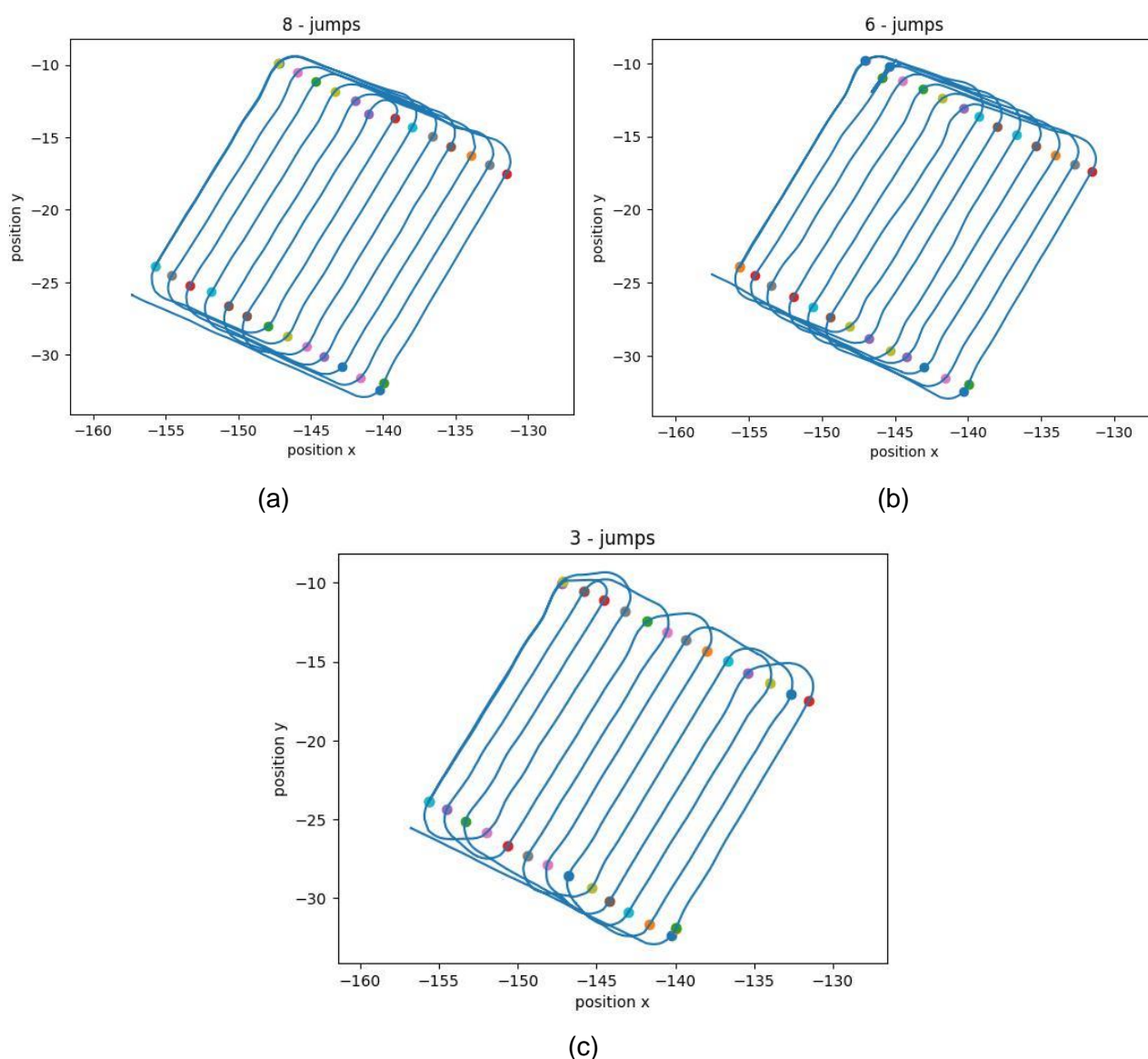


**Fig. 3.42. Trajectories performed by the autonomous robot in Section 2.1 (see Fig. 3.1.b) of the experimental fields at CSIC facilities, executing a treatment mission with different configuration parameters: (a) 8 jumps; (b) 6 jumps; and (c) 3 jumps.**

### 3.3.4. Supervisor

To evaluate the Mission Supervisor and to comply with the statements presented in the Grant Agreement (*Simulation of 25 consecutive malfunctions. 100% have to be detected and diagnosed*), a set of tests were carried out in the CSIC experimental fields between July and September 2023, which corresponds to the period of the field days and demonstrations.

A list of malfunctions was identified and described in deliverable “D4.1 - Autonomous vehicle: Design, integration and TRL assessment”, although some of them were very complicated to simulate manually, and others could affect the performance of other tests that were conducted in parallel. Therefore, it was decided to make a record of the malfunctions identified by the robot during tests and demonstrations executed in the period indicated above, whose information was stored in the cloud to carry out an analysis later for the supervisor's validation.

The malfunctions were divided into two types: errors and warnings. The errors represented critical malfunctions, which caused either the robot to be unable to carry out a mission, or the robot to abort a mission autonomously. The warnings were unwanted situations, and it was the operator who had to decide if, in this situation, the mission should be aborted or not.

Therefore, a total of 34 days of malfunction messages were analysed, between 6 July and 28 September, 2023. During this period, a total of 40 different warnings and 17 errors malfunctions were detected. Table 3.12 presents the list of warning and error malfunctions recorded.

**Table 3.12. List of malfunctions tested.**

Malfunction Messages	Identifier
Vision System RGB not active	0
Cameras Supervisor: No ToF. No RGB.	1
Robot Management: Robot Status: Standby in task: Running. Waiting for user to go to automode.	2
Cameras Supervisor: No RGB.	3
Robot Management: Timeout in task: Enable	4
Vision System Yolo not active	5
Robot Supervisor: Pan-and-tilt to Safe position	6
Robot in Standby mode	7
Check Robot: Robot Status: Waiting for user to go to automode	8
Robot Management: Motion NOT autorised. Waiting for user to arm the robot	9
Response: No Comm. Service: SpiralCo. Waiting for Controller to be active ...	10
Supervisor Local. GoToGoal status but disable. Finishing Controller	11
Supervisor Local. RowFollw status but disable. Finishing Controller	12
Robot Supervisor: CPU Temperature Critical	13
Robot Management: Timeout in task: Running	14
Class name not in list	15
Critical situation. CollisionCritical activated.	16
Robot paused. Collision Critical. Waiting for collision situation to be solved	17
Vision System Segmentation not active	18



Low connection	19
Low battery	20
Bumpy field	21
Robot in Manual mode	22
Critical situation. Controller is status Stopping. Stopped	23
Timeout in Initializing Yolo	24
Warning situation. Robot in RowFollw mode and Controller RowFollw in status Reached. Stopped	25
Warning situation. Robot in RowFollw mode and Controller RowFollw in status Stopping. Stopped	26
Error in YawInit. No GPS signal	27
Supervisor Local: Program terminated. Ros Master offline	28
Warning situation. Robot in RowFollw mode and Controller RowFollw in status Continue. Stopped	29
Starting Field Localization	30
Critical situation. Controller is status Continue. Stopped	31
Timeout in Initializing FieldLoc	32
Critical situation. Controller is status Reached. Stopped	33
FieldLoc not Initialized because Timeout in Initializing Yolo	34
Supervisor Local. Resume received but no in Pause. Continue	35
Nav Controllers: Shutdown. Error in closing controller.	36
Implement warning, is already active: False	37
GoToGoal status Replan received. Replan activated.	38
GoToGoal status NotReachable received. Replan activated. Radius:0.75	39
Error in Robot Management Robot Enable	40
Robot not moving. It is possible that a stone blocked the wheel or error with an inverter. Please switch to manual mode and move the robot.	41
Error in GoToGoal activation. CommCode: No Comm	42
Error in checkRobot. No controller active	43
Error in Robot Management	44
Error in GoToGoal activation. CommCode: Reset_ack	45
Yaw initialization: Aborted	46
GPS antenna disconnected	47
Obstacle detected	48
Error in Critical. No controller active	49
Error in None activation. CommCode: No Comm	50
Supervisor Local. Resume received but no controller. Finishing Task	51
RosMaster not active	52
Cameras Supervisor: No ToF.	53
Robot Supervisor: No RTK.	54
Supervisor Local. Task Stop received from Remote but SupState is not Task Stop	55
Robot Supervisor: No GPS. No RTK.	56

Figure 3.43 presents the distribution of the different malfunctions in the period of time under study.

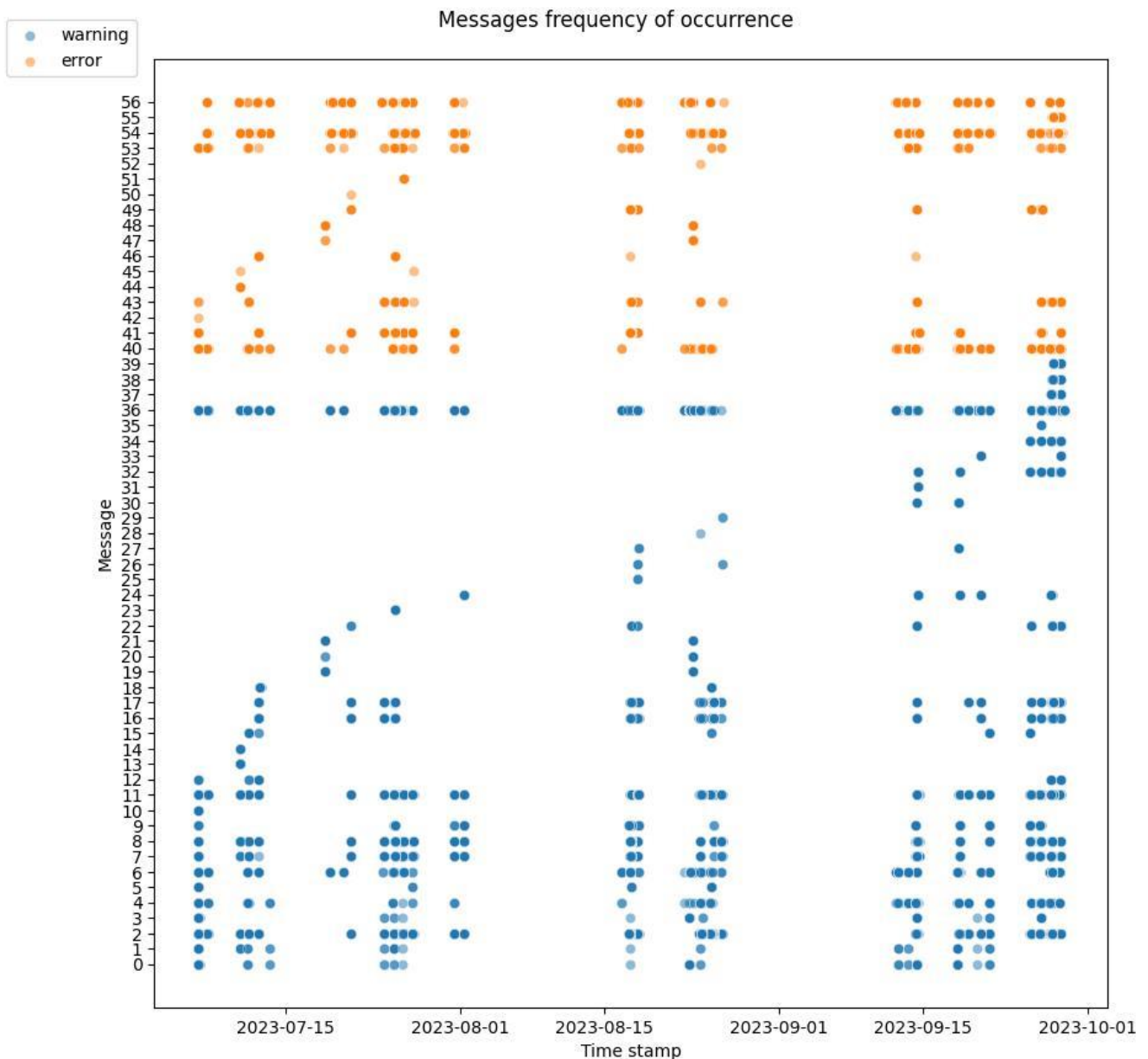


**Fig. 3.43. Distribution of the different malfunctions in the period of time under study, where each malfunction is represented by its identifier presented in the Table 3.12.**

Moreover, Table 3.13 presents the percentages of occurrence of each malfunction. In this case, the malfunctions are classified into warning type and the error type.

**Table 3.13. Count and percentage of occurrence of malfunctions during the testing period.**

Warnings	Count	% of occurrence
Check Robot: Robot Status: Waiting for user to go to automode	21377	39.25%
Vision System Segmentation not active	8093	14.86%
Robot Management: Robot Status: Standby in task: Running. Waiting for user to go to automode.	7156	13.14%
Robot paused. Collision Critical. Waiting for collision situation to be solved	6299	11.57%

Supervisor Local. GoToGoal status but disable. Finishing Controller	2886	5.30%
Nav Controllers: Shutdown. Error in closing controller.	2724	5%
Robot Supervisor: CPU Temperature Critical	1149	2.11%
Cameras Supervisor: No RGB.	892	1.64%
Vision System RGB not active	743	1.36%
Critical situation. CollisionCritical activated.	721	1.32%
Robot in Standby mode	420	0.77%
Robot Management: Motion NOT authorized. Waiting for user to arm the robot	415	0.76%
Robot Supervisor: Pantilt to Safe position	356	0.65%
Robot Management: Timeout in task: Enable	287	0.53%
Vision System Yolo not active	126	0.23%
Timeout in Initializing FieldLoc	109	0.20%
FieldLoc not Initialized because Timeout in Initializing Yolo	88	0.16%
Robot in Manual mode	67	0.12%
Timeout in Initializing Yolo	66	0.12%
Class name not in list	65	0.12%
Implement warning, is already active: False	58	0.11%
Cameras Supervisor: No ToF. No RGB.	57	0.10%
Low connection	54	0.10%
Starting Field Localization	40	0.07%
GoToGoal status Replan received. Replan activated.	40	0.07%
Supervisor Local. RowFollw status but disable. Finishing Controller	30	0.06%
GoToGoal status NotReachable received. Replan activated. Radius:0.75	26	0,05%
Critical situation. Controller is status Reached. Stopped	20	0.04%
Bumpy field	18	0.03%
Response: No Comm. Service: SpiralCo. Waiting For Controller to be active ...	18	0.03%
Error in YawInit. No GPS signal	13	0.02%
Low battery	12	0.02%
Critical situation. Controller is status Continue. Stopped	9	0.02%
Critical situation. Controller is status Stopping. Stopped	8	0.01%
Warning situation. Robot in RowFollw mode and Controller RowFollw in status Stopping. Stopped	5	0.01%
Robot Management: Timeout in task: Running	5	0.01%
Supervisor Local. Resume received but no in Pause. Continue	4	0.01%
Warning situation. Robot in RowFollw mode and Controller RowFollw in status Reached. Stopped	3	0.01%
Warning situation. Robot in RowFollw mode and Controller RowFollw in status Continue. Stopped	2	0.001%
Supervisor Local: Program terminated. Ros Master offline	1	0.001%
<b>Errors</b>	<b>Count</b>	<b>% of occurrence</b>
Robot Supervisor: No RTK.	126218	72.18%
Robot Supervisor: No GPS. No RTK.	45770	26.18%
Robot not moving. It is possible that a stone blocked the wheel or error with an inverter. Please switch to manual mode and move the robot.	2.049	1.17%
Error in Robot Management Robot Enable	393	0.22%
Cameras Supervisor: No ToF.	121	0.07%
Error in checkRobot. No controller active	92	0.05%
Error in Critical. No controller active	80	0.05%
Supervisor Local. Task Stop received from Remote but SupState is not Task Stop	60	0.03%
Obstacle detected	33	0.02%

Yaw initialization: Aborted	14	0.01%
GPS antenna disconnected	12	0.01%
Error in Robot Management	5	0.001%
Supervisor Local. Resume received but no controller. Finishing Task	5	0.001%
Error in GoToGoal activation. CommCode: Reset_ack	2	0.001%
Error in None activation. CommCode: No Comm	1	0.001%
RosMaster not active	1	0.001%
Error in GoToGoal activation. CommCode: No Comm	1	0.001%

When analysing the frequency of occurrence, the difference between the malfunctions is notorious. Eighty per cent (80%) of the occurrences of warning messages are concentrated in just 4 messages, as follows: **(i)** *“Waiting for user to go to automode”*, **(ii)** *“Vision System Segmentation not active”*, **(iii)** *“Robot Management: Robot Status: Standby in task: Running”*, and **(iv)** *“Waiting for user to go to automode”*, considering all time stamp subscriptions. These 4 malfunctions are directly related to the interaction with the operator, where the robot requests the operator to intervene to solve a situation.

On the other hand, if the error messages are analysed, the result is more shocking, as only 2 messages account for 98% of the occurrences, as follows: **(i)** *“Robot Supervisor: No RTK”* and **(ii)** *“Robot Supervisor: No GPS. No RTK”*. These are two separate messages since the first indicates that there is GPS, but there is no RTK, while the second indicates that there is no GPS, and obviously no RTK.

By analysing the time stamps and looking at individual occurrences by day, there are some malfunctions that may not appear too often during the same mission but appear repeatedly on different days. This is the case of the *“Error in Robot Management Robot Enable”* malfunction, which is related to communications between the central controller and the mobile platform. This malfunction occurred when the mobile platform was turned on or reset because another malfunction caused it, such as the GPS or RTK error.

To analyse the occurrence of malfunctions per day, Table 3.14 presents the percentages of occurrence of each malfunction for both the warning type and the error type per day.

**Table 3.14. Amount of days and percentage of time of malfunctions occurrence.**

Warnings	Days	% of time
Nav Controllers: Shutdown. Error in closing controller.	33	97%
Supervisor Local. GoToGoal status but disable. Finishing Controller	26	76%
Robot Management: Robot Status: Standby in task: Running. Waiting for user to go to automode.	26	76%
Robot Supervisor: Pantilt to Safe position	26	76%
Robot Management: Timeout in task: Enable	23	68%
Check Robot: Robot Status: Waiting for user to go to automode	23	68%
Robot in Standby mode	22	65%
Robot paused. Collision Critical. Waiting for collision situation to be solved	16	47%
Critical situation. Collision Critical activated.	15	44%



Vision System RGB not active	15	44%
Cameras Supervisor: No ToF. No RGB.	14	41%
Robot Management: Motion NOT authorized. Waiting for user to arm the robot	12	35%
Cameras Supervisor: No RGB.	11	32%
Robot in Manual mode	7	21%
Timeout in Initializing FieldLoc	6	18%
Supervisor Local. RowFollw status but disable. Finishing Controller	5	15%
Timeout in Initializing Yolo	5	15%
Class name not in list	5	15%
FieldLoc not Initialized because Timeout in Initializing Yolo	4	12%
Vision System Yolo not active	4	12%
Starting Field Localization	2	6%
Vision System Segmentation not active	2	6%
Bumpy field	2	6%
Warning situation. Robot in RowFollw mode and Controller RowFollw in status Stopping. Stopped	2	6%
Critical situation. Controller is status Reached. Stopped	2	6%
Low connection	2	6%
Low battery	2	6%
Implement warning, is already active: False	2	6%
GoToGoal status Replan received. Replan activated.	2	6%
GoToGoal status NotReachable received. Replan activated. Radius:0.75	2	6%
Error in YawInit. No GPS signal	2	6%
Warning situation. Robot in RowFollw mode and Controller RowFollw in status Reached. Stopped	1	3%
Warning situation. Robot in RowFollw mode and Controller RowFollw in status Continue. Stopped	1	3%
Critical situation. Controller is status Continue. Stopped	1	3%
Robot Supervisor: CPU Temperature Critical	1	3%
Critical situation. Controller is status Stopping. Stopped	1	3%
Robot Management: Timeout in task: Running	1	3%
Supervisor Local. Resume received but no in Pause. Continue	1	3%
Response: No Comm. Service: SpiralCo. Waiting For Controller to be active ...	1	3%
Supervisor Local: Program terminated. Ros Master offline	1	3%
<b>Errors</b>	<b>Days</b>	<b>% of time</b>
Robot Supervisor: No GPS. No RTK.	31	91%
Robot Supervisor: No RTK.	30	88%
Error in Robot Management Robot Enable	27	79%
Cameras Supervisor: No ToF.	24	71%
Error in checkRobot. No controller active	14	41%
Robot not moving. It is possible that a stone blocked the wheel or error with an inverter. Please switch to manual mode and move the robot.	14	41%
Error in Critical. No controller active	6	18%
Yaw initialization: Aborted	4	12%
Obstacle detected	2	6%
Error in GoToGoal activation. CommCode: Reset_ack	2	6%
Supervisor Local. Task Stop received from Remote but SupState is not Task Stop	2	6%
GPS antenna disconnected	2	6%
Error in Robot Management	1	3%

Error in None activation. CommCode: No Comm	1	3%
Error in GoToGoal activation. CommCode: No Comm	1	3%
RosMaster not active	1	3%
Supervisor Local. Resume received but no controller. Finishing Task	1	3%

To carry out the analysis of the identification of the detection of 25 consecutive malfunctions, the messages were grouped by day (see Fig. 3.44). And within the total window time it was identified that September 14 was the day with the most malfunctions detected, with a total of 25. Table 3.15 presents the list of malfunctions for that test day.

**Table 3.15. List of the 25 consecutive different malfunctions detected during the test on September 14 2023**

Id	Malfunction message
1	Error in Robot Management Robot Enable
2	Yaw initialization: Aborted
3	Robot not moving. It is possible that a stone blocked the wheel or error with an inverter. Please switch to manual mode and move the robot.
4	Error in checkRobot. No controller active
5	Error in Critical. No controller active
6	Robot Supervisor: No GPS. No RTK.
7	Robot Supervisor: No RTK.
8	Cameras Supervisor: No ToF.
9	Robot Management: Robot Status: Standby in task: Running. Waiting for user to go to automode.
10	Robot Management: Motion NOT autorized. Waiting for user to arm the robot
11	Robot Management: Timeout in task:Enable
12	Robot in Standby mode
13	Check Robot: Robot Status: Waiting for user to go to automode
14	Supervisor Local. GoToGoal status but disable. Finishing Controller
15	Critical situation. CollisionCritical activated.
16	Robot paused. Collision Critical. Waiting for collision situation to be solved
17	Starting Field Localization
18	Cameras Supervisor: No RGB.
19	Robot Supervisor: Pantilt to Safe position
20	Vision System RGB not active
21	Robot in Manual mode
22	Timeout in Initializing Yolo
23	Critical situation. Controller is status Continue. Stopped
24	Timeout in Initializing FieldLoc
25	Nav Controllers: Shutdown. Error in closing controller.

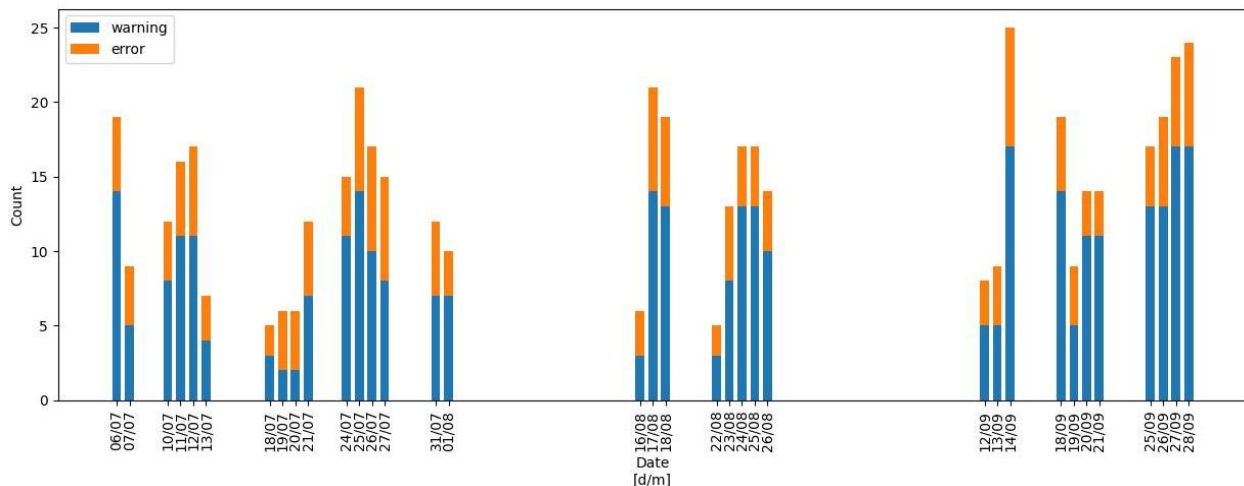


**Fig. 3.44. Distribution of unique malfunctions detected per day**

### 3.3.5. Motion controller

As described in the Grant Agreement (GA), the Motion controller coordinates the sensors and systems and performs the vehicle guidance while the agricultural tools work independently. To evaluate the motion controller, the GA stated that *“The performances of both the perception system and the laser scanner are kept when carried by the mobile platform”*. Unfortunately, this performance study was not accomplished. In any case, a set of tests were carried out the days prior to the field days to evaluate the performance of the implemented controllers.

The tests were conducted between July 7 and September 28, 2023, in the different test fields described in Section 3.1. During this period of time, 40 missions were analysed, which were missions that made at least 4 passes through the field and cultivation. Many more missions were executed during this period, but given that they were periods of testing different components and demonstrations, not all missions managed to reach an adequate time and length for the analysis of results. The general information of the data analysed to validate the Motion Controller is as follows:

- Total missions: 44
- Total operational time: 13.11 h
- Mean mission time = 1180 seconds (~20 min)
- Total missions travelled distances: 6.2 km
- Row\_follower travelled a distance of 4.8 km
- Total hectares travelled in row follower (performing treatment): 0.7 ha
- GoTo travelled a distance of 1.4 km.

As described in deliverable “D4.1 - Autonomous vehicle: Design, integration and TRL assessment”, the guidance system is mainly composed of three controllers: **(i)** lateral controller, **(ii)** spiral controller, and **(iii)** linear speed controller. To evaluate the performance of each controller, three fundamental

measurements were carried out: **(1)** reach error, which is the error (Euclidean distance in meters) in reaching a target point and which does not depend exclusively on the linear speed controller but also on the other two controllers; **(2)** mean lateral error, which corresponds to the average error (orthogonal distance in meters) in following a trajectory segment, which can be curved or straight; and **(3)** mean angular error (in radians), which represents the error in the alignment of the orientation of the trajectory with the orientation of the robot, also for both straight and curved trajectories.

To evaluate the performance of the controllers, and given that both lateral controller and spiral controller depend on the linear speed controller, an analysis was carried out depending on what type of planning the robot executed, whether is GoToGoal or LineFollowing. Details of these planners are given in deliverable D4.1.

### 3.3.5.1. LineFollowing results

In total, 265 situations were analysed, i.e. the number of times the robot follows a straight line with a length greater than 5 meters. Figure 3.45 presents the histogram of the average reach error to the target point for all these situations analysed.

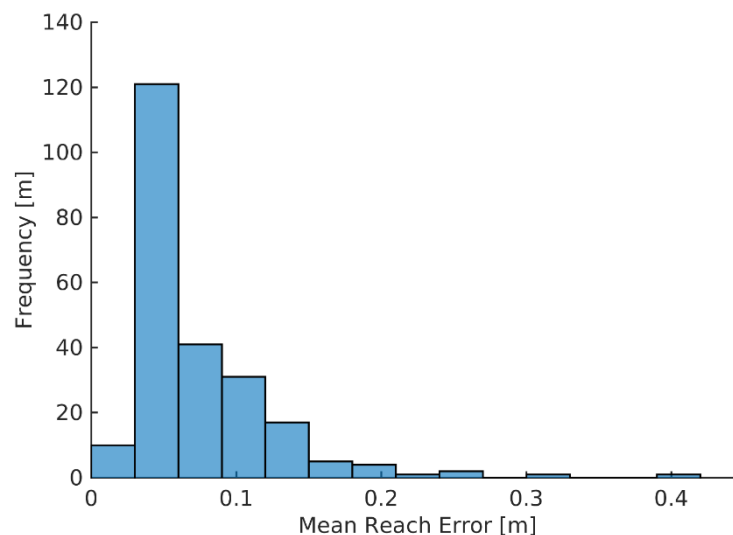


**Fig. 3.45. Histogram of the reach error of the lateral controller**

In 11.7 % of situations analysed, the absolute error was greater than 0.5 m, and this is because in the tests carried out in some situations the robot stopped either because it was necessary for an operator to approach the robot or because the mission was aborted. By eliminating those situations where the controller did not finish the following task (41.45 % of the situations), the absolute error was less than 0.05 m. Moreover, in 80.77 % of the situations analysed, the absolute error was less than 0.1 m. It should be noted that this corresponds to the linear error and that if the robot stops a few centimetres before or after the end of the crop line, it does not considerably affect the execution of the mission and the treatment. It should also be noted that these measurements were made while many other tests were being performed on the robot, including tests to evaluate the laser. During these tests, a mean reach error of approximately 0.07 m ( $\pm 0.015$  m) was achieved.

On the other hand, Fig. 3.46 presents the histogram of the average value of the lateral error each



time a row following task was executed. It is the mean value taking into consideration each time the controller performed a control action, and it was configured at 10 Hz. In this case, in only 0.8 % of the situations, the absolute error was greater than 0.5 m. This outlier is also because of external factors of the mission, and it has occurred to a lesser extent, given that although the mission has been aborted, the robot remained on the trajectory.

By eliminating those situations where the controller did not finish the following task (81 % of the situations analysed), the absolute error was less than 0.06 m. Moreover, in 91.6 % of the situations, the absolute error was less than 0.09 m. It should be noted that this corresponds to the absolute lateral error, and the situations where the error is greater is when the robot performs the manoeuvre to enter the crop lines, as can be seen in Fig. 3.46, where after the beginning of the row following (after 20% of the line) 54.4 % of the absolute error is less than 0.03 m, while only 25% of times the lateral error was below 0.03 m at the beginning of the row following. During these tests, a mean lateral error of approximately 0.04 m ( $\pm 0.015$  m) was achieved.

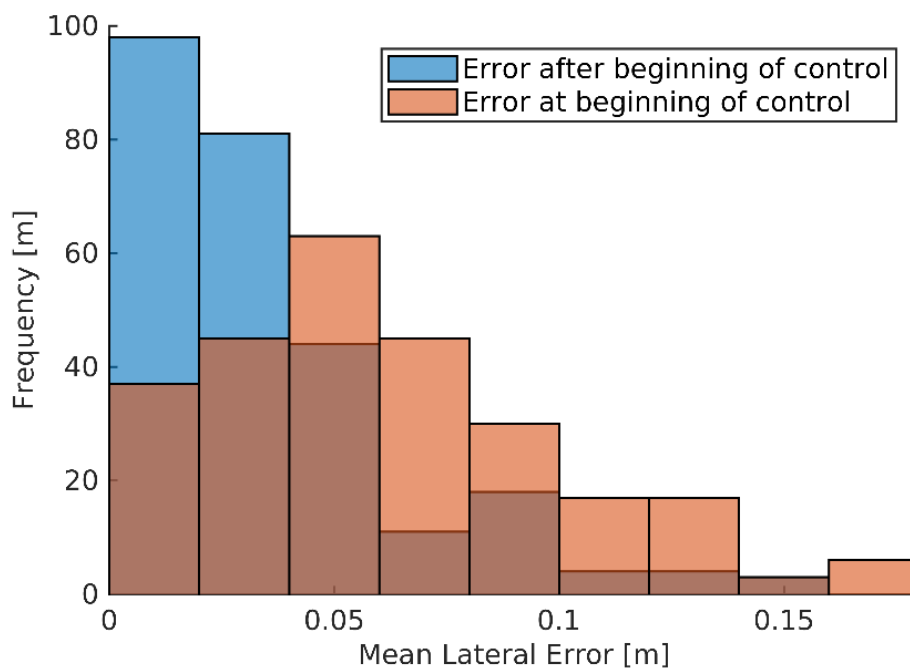


**Fig. 3.46. Histogram of the lateral error of the lateral controller**

Furthermore, Fig. 3.47 presents the histogram of the absolute value of the angular error of the lateral controller. In 58 % of the situations the mean angular error remained below 0.05 radians, which

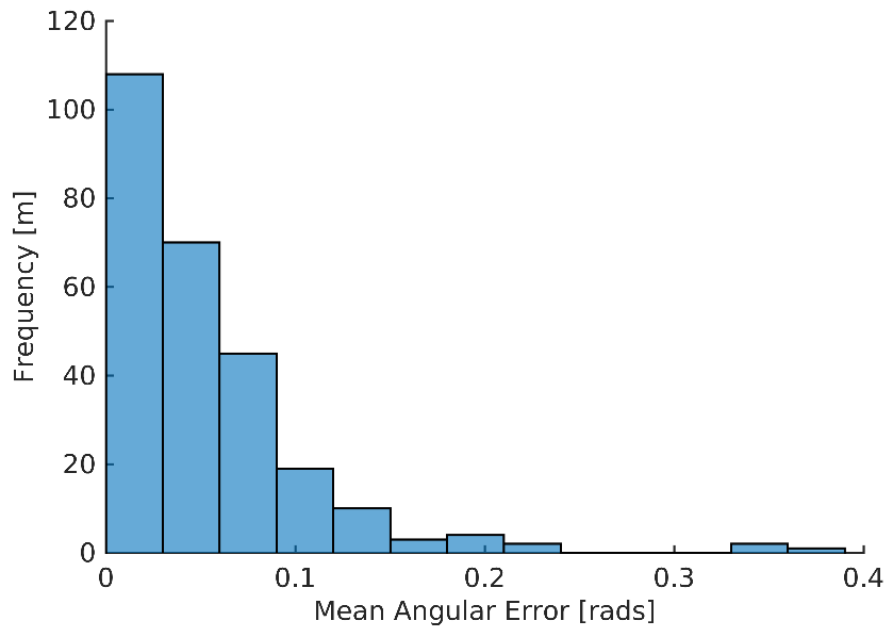


**Fig. 3.47. Histogram of the angular error of the lateral controller**

corresponds approximately to an angular error of about 3 degrees. Moreover, during these tests, a mean angular error of approximately 0.05 rad was achieved, with a standard deviation of approximately 0.0028 rad ( $\pm 0.01$  rad).

### 3.3.5.1. GoToGoal results

For this planner, 186 situations were analysed, given that in the missions, the change of crop lines was executed by this planner. Therefore, Fig. 3.48 presents the histogram of the average reach error to the target point for all situations where the spiral controller was involved.

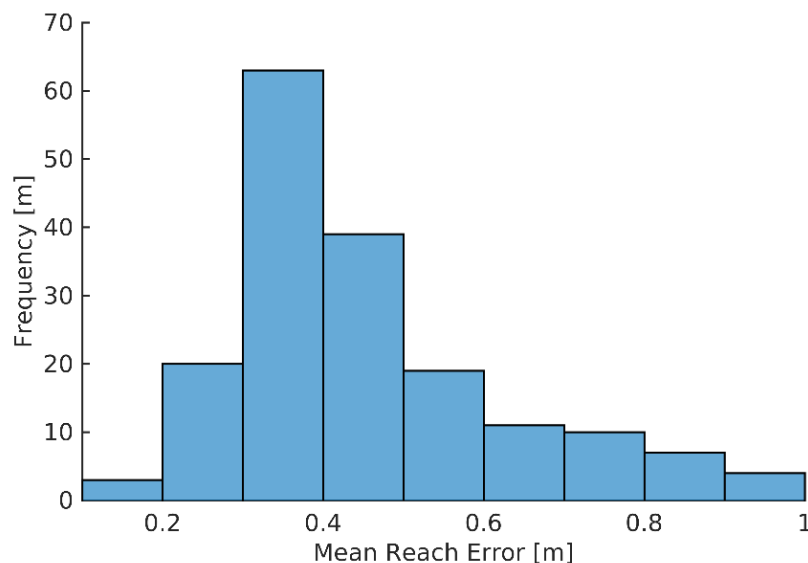


**Fig. 3.48. Histogram of the reach error of the spiral controller**

In 5.4 % of the situations, the absolute error was greater than 1 m. This situation is similar to the one presented with the error in the row follower controller: in some situations, the robot stopped either because it was necessary for an operator to approach the robot or because the mission was aborted. Moreover, 29% of the time the controller stopped the robot at a distance between 0.5 and 1 m from the target. These situations were common since the controller not only sought to reach the target position, but also sought to reach the target orientation. The controller was defined so that it takes higher priority to arrive at the desired orientation even if the robot is far from the target. This means that the robot manages to reach the target at an error distance of less than 0.5 m 71% of the time. For this controller, this is a splendid result, taking into consideration the dimensions of the robot. During these tests, a mean reach error of approximately  $0.45 \text{ m} \pm 0.015 \text{ m}$  was achieved. This result contrasts considerably with respect to the row follower controller, given that the execution of turns using a tracked robot in complex terrain conditions (presence of stones, loose or wet earth, etc.), and without taking into consideration the dynamic model of the robot, can generate this discrepancy. In any case, these results were more than sufficient for the purpose of the navigation capabilities that the robot was intended to obtain.

On the other hand, Fig. 3.49 presents the histogram of the average value of the lateral error each time a GoToGoal task was executed. It is the mean value taking into consideration each time the controller performed a control action, and it was configured at 10 Hz. In this case, all error measurements were kept below 0.5 m, so it is not considered that there were outliers. Moreover, given that this planner involves two controllers, both the lateral and spiral controllers, and that one affects the other in the path following, an analysis is carried out together. A mean total lateral error in following curve paths was approximately  $0.21 \text{ m} \pm 0.015 \text{ m}$ , compared with the mean total lateral error in following the straight lines, where  $0.073 \text{ m} \pm 0.015 \text{ m}$  was obtained. It is to be expected that following curves has a greater lateral error than following straight lines, and as indicated above, the spiral controller was configured to give priority to maintaining the robot's orientation, even if it moved

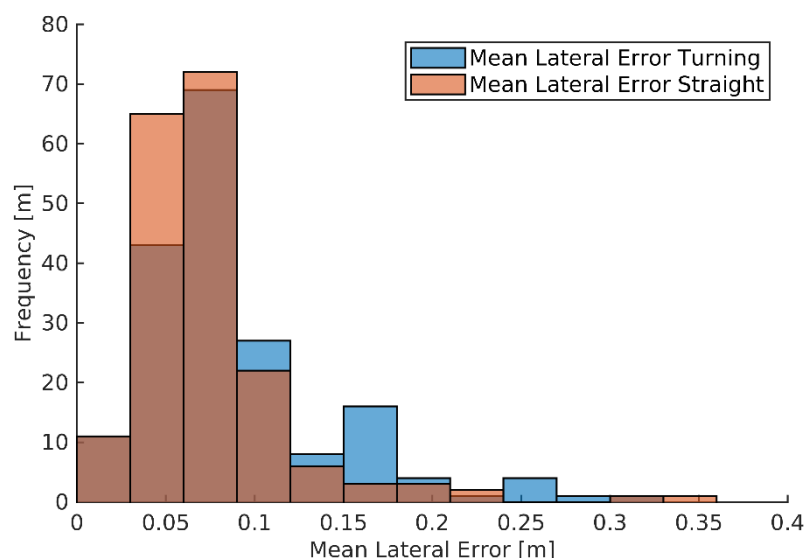


**Fig. 3.49. Histogram of the lateral error executing a GoToGoal trajectory**

a little out of the way.

To confirm these claims, Fig. 3.50 presents the histogram of the absolute value of the angular error of the spiral controller. In 98.9 % of the situations, the mean angular error remained below 0.05 radians, which corresponds approximately to an angular error of about 3 degrees. Moreover, during these tests, a mean angular error of approximately 0.011 rad was achieved, with a standard deviation of approximately  $0.0023 \text{ rad} \pm 0.01 \text{ rad}$ , demonstrating that the spiral controller was capable of following the shape of the curvature at the expense of maintaining the position on it. This is positive, given that the robot in this type of situation has the manoeuvring capacity to adjust to the trajectory in the straight sector.

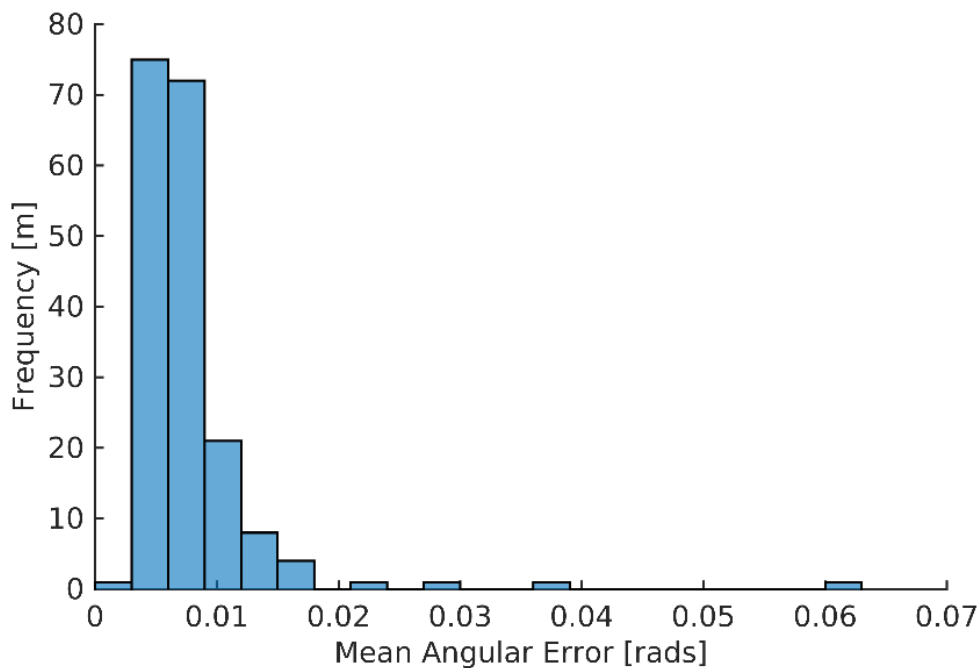


**Fig. 3.50. Histogram of the angular error of the spiral controller**

### 3.3.6. Laser source

To achieve the targeted output power of 500 W in continuous operation, Futonics realised a laser source with six high-power pump diodes. Each laser diode had an output power of about 200 W and with a 6+1→1 combiner a combined power of 1250 W is available. With this configuration, a maximum continuous output power of 507 W was achieved. The output power was measured at Futonics with a calibrated power meter from MKS-Ophir (Ophir Power Meter FL400A-BB-50 and Ophir Starlite Display). In Fig. 3.51, the input – output curve of the laser for analogue power control is shown. At maximum output power, about 50 W of pump power are transmitted and over 95 % are absorbed.



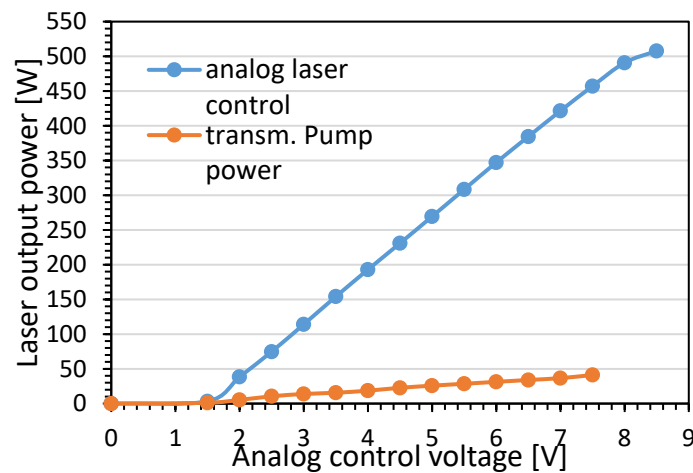


**Fig. 3.51. Output curve of the 500 W laser system using analogue control.**

The optical-to-optical efficiency of this laser is 44 % with respect to the diode power and 48 % with respect to the absorbed pump power. The emission spectra at different output powers of the laser are shown in Fig. 3.52. The centre wavelength is 1998 nm and the bandwidth is 0.8 nm. The wavelength shift from minimum to maximum power is about 0.5 nm.

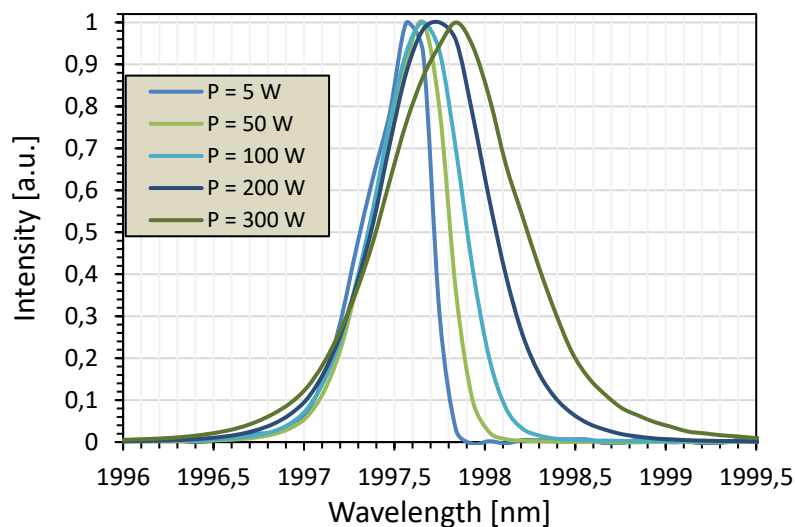


**Fig. 3.52. Emission spectra of the 500 W laser system at different output powers.**

With the laser system, different long-term tests were carried out at Futonics in the laboratory. The maximum power was tested for continuous and pulsed operation. With sufficient cooling the long-term power stability is about 1 % at laser power above 50 W. The long-term tests showed that about 3 kW cooling capacity is needed, when the laser is operated at maximum power under room temperature conditions (22 °C). The tests also showed that the heat and cooling distribution is not optimal for high-power operation. For future stable operation, the construction of the laser will be changed, but the outer housing will be kept.

As the available cooling capacity of the chillers was limited to 1.2 kW for each chiller, the maximum power of the laser was reduced, and a second laser was added. For the field tests on the autonomous

vehicle, two laser sources, each cooled by one chiller, were integrated. The maximum output power of operation of each laser in the field was limited to 250 W by software control. With this limitation, both lasers could operate simultaneously with maximum power. All parameters of the two laser systems are listed in Table 3.16.

**Table 3.16. Parameters of the two lasers used in the field tests.**

Type of Specifications for each laser	
<b>Optical Specifications</b>	
Max. output power	$P_{\max} = 250 \text{ W}$
Fibre laser wavelength	$\lambda = 1998 \text{ nm}$
Beam quality	$M^2 < 1.1$ , single-mode
Operation mode	cw, modulated up to 1 kHz
Fibre connector	Futonics standard
Fibre length	$l = 10 \text{ m}$
<b>Electrical specifications</b>	
Supply voltage 1	$U = 24 \text{ VDC}$
Supply voltage 2	$U = 45 \text{ VDC}$
Power input	$P \leq 3400 \text{ W}$
<b>Dimensions</b>	
Proportion (width x height x depth)	483 mm x 177 mm x 705 mm (19'', 4 RU)
Weight	35 kg

During the field tests at Copenhagen, Reusel and Madrid, different problems with the laser systems and the chillers occurred. However, one operative system was always available, as two chillers and laser systems were integrated. On a laser system, once the connector from the application fibre, which is connected to the scanner optic, was overheated and the fibre inside burned. This laser had to be repaired at Futonics and was sent back then for integration. To overcome this problem, fans were integrated into the scanner to cool the fibre connector. With these fans, no further overheating was observed. During the final test in Madrid, one laser failed due to a fibre crack. This could result from shocks during the operations on the field. Futonics is further optimising the fibre protection and analysing the behaviour of the laser under different operation conditions.

During the tests in Madrid the chiller systems a few times shut down due to overheating. After replacing some internal electronics, one chiller worked fine, but the other one still did not operate

continuously at higher surrounding temperatures. Futonics will analyse these problems further after the returning of the systems.

### 3.3.7. AI-perception system

Statement in Grant Agreement:

1. Identification of at least 80% of the weeds with a detection accuracy of  $\pm 3$  mm (Measurements based on picture analysis).
2. Detection of the meristem positions of at least 80% of the weeds with an detection accuracy of  $\pm 3$  mm (Measurements based on picture analysis)

In comparison to the subsystem assessment, a ground truth measurement is more challenging for on site assessment of the full system. Identification of weeds requires on-site assessment and possibly follow-up of very young plants until they can surely be classified to a certain species, so plot trials have to be set out on the experimental field and possibly be followed for some days for verified classification. Due to the condensed time schedule of the demo and field days, such experiments could not be conducted (see below for site-specific reasons). So, ground truth could only be obtained on image data. Quantitative results have been covered above in Sections 3.2.1 and 3.2.2.

Qualitative assessment of the AI-perception system was conducted during field tests and demos near Copenhagen, Reusel and Madrid. Some site-specific results of the assessment are described in the following paragraphs, followed by a more general assessment.

In Copenhagen, the performance in plant detection and identification was similar to that presented in Section 3.2.1. This is in accordance with the fact that a comparatively large amount of data for AI training originated from Denmark and Germany, and consequently, there was a high overlap between the weed (and crop) spectrum at this site and the trained data.

At Reusel, the layout and seeding of the test fields for the Precision Days could only be done a little more than one week before the event. This led to crop plants at a very early growth stage (maize only) and a very unusual weed spectrum at the time of the event. The weeds were volunteer grain (barley) from the just harvested crop, with only a few exceptions. So, the weeds to be identified for weeding by the perception system were almost exclusively former crop plants and belonged to the class of grass weeds (monocot plants). As outlined in Section 3.2.1, grass weeds are more difficult to identify for the perception system. Moreover, the grass weeds in Reusel were very straight upright reducing the imaged area per plant in the camera view of the perception system and further hindering their correct recognition. Thirdly, training for maize crop recognition was still ongoing at that point of time. In summary, this situation was highly challenging for the perception system and consequently performance was not satisfactory. The WeLASER team rated the small visible area of the weeds as the main fundamental reason for the poor performance. Better identification of grass weeds or other plants that have little area exposed to top view cameras is expected by implementing further camera

systems for side view of these plants. As noted before, this weed situation is highly unusual for agricultural fields, usually dicot weeds outnumber monocot weeds.

The test site near Madrid was used for tests and demos several times in 2023. Performance of the perception system was noticeably weaker here compared to the subsystem assessment. In contrast to the central and northern European sites, the south of Europe shows a different and more variant weed spectrum. This had quite strong effects on the performance of the perception system. The amount of data available for training of the AI was comparably low given the wide variability of plants possibly occurring on the field. This was aggravated by the fact that training data for seasonal variances of weed plants could only be done successively over time, so the AI competence in having seen a plant already – usually during the same season the year before – was lagging behind and stayed more incomplete than for the northern European sites. A fast procedure for onsite labelling and training could have minimized this effect but was not feasible within the limitations of the WeLASER project.

In general, it is a well-known issue that the performance of AI plant identification is weaker for new agricultural plots than for well-known (and trained) fields. A commercial realization of the WeLASER device needs a strategy for site specific retraining of the AI during the first year of usage on a specific farm.

In addition to these agronomic factors, assessment showed some technical factors lowering the system performance in the integrated device compared to the subsystem assessment. At high ambient temperatures like noon and afternoon in Madrid during summertime, the onboard AI computer for the vision system automatically reduced performance to prevent overheating. Consequently, the maximal framerate for AI perception was reduced limiting in turn the maximal forward velocity for laser weeding. Since each plant that is to be treated needs to appear in several frames (default setting: 5 frames) for analysis to track them. If the frame rate that can be computed by the AI is too low relative to the ground speed of the vehicle, strips between the captured frames will even be missed completely. Besides, movement of the robot may lead to image blur at too high velocity. For the current setup, this maximal ground speed is approximately 2,5 km/h. This was an issue at the first field trials so the camera system was changed in favour of a device with lower exposure/shutter time.

Another limiting factor was the low ground resolution of the installed 3D camera. During the course of the project, the ZED X Mini was identified as the best possible option. However, even with this choice, which was otherwise well suited to the application, it was not possible to achieve better ground resolution than 1.5 px/mm. This meant that reliable detection of plants at the cotyledon stage was not always possible. Nevertheless, this work paved the way for the use of the newer version of the same camera, which has just become available. This has a lower Field of View (FOV), allowing sufficient ground clearance with a ground resolution of 2.5 px/mm, which is a significant improvement.





### 3.3.8. Targeting system

**Statement in Grant Agreement<sup>1</sup>: Targeted meristems have to be at least 90% of the detected meristems.**

There is no reliable on-field procedure for quantitative assessment of the targeting system discriminating the effect of successful targeting and energy application. As described in Section 3.2.3 and Section 3.2.4, LZH developed a method for lab assessment of the hitting accuracy based on plant fluorescence. This approach cannot (yet) be used for on-field assessment. As a less valid alternative, laser treatment was to be performed at high laser power to introduce burn marks on plants and/or soil and evaluate their position with respect to the targeted meristem. However, this approach could not be conducted successfully during the field days. At Copenhagen, there was an error in the targeting system while at Reusel and Madrid, laser power was not sufficient to cause clear burn marks or targeted and hit plants could not be assigned unambiguously.

Generally, the optomechanics in the galvo scanners are always fast enough to point the laser beam to a target position within its working range for the intended ground speed of the WeLASER device. Full angular movement of the mirrors takes in the order of 6 ms.

Limitations of the targeting are caused by imprecision or inaccuracy in perception-targeting coordination. Inaccuracies result from errors in the registration of the involved coordinate systems: real world, camera, scanner. Imprecision is mainly due to the lower precision of the camera point cloud in its peripheral field of view as compared to the centre and a hardly sufficient precision in z-measurement that is connected with a fairly high uncertainty of the measurement in this height dimension. Most of these factors do not change between lab and on-field environment. The main additional source of error for on-field conditions is unexpected movements of the implement with respect to the ground. The computing time necessary for the xyz-localization algorithm for the plants and signalling path to the scanner controller and to the optomechanics of the scanner causes a significant latency between image acquisition and setting of the expected mirror positions in the scanner. Thus, unexpected movement cannot be compensated in real-time by the process control. Field demos showed that the intended forward movement of the robot can be compensated well (see Fig. 3.53). Good velocity compensation leads to the round hit marks that can be seen on the image. If the ground speed is not matched well, the round laser beam profile creates elongated hit marks or even lines on the plants or soil. The image also shows the effect of errors in latency compensation. Such basic quality checks are very useful for setting up the machine on the field.

---

<sup>1</sup> According to the amendment

Qualitative assessment of the targeting system was conducted during field tests and demos in Copenhagen, Reusel and Madrid. During the first field trials at Copenhagen the ground speed compensation was not yet operative. In Reusel, the targeting system worked as expected (compare Figure 1), but a valid assessment was not possible due to the reported agronomic issues hindering good target recognition by the vision system. In Madrid, targeting assessment was strongly limited again because of the issues in weed recognition reported in the previous section. For normal operation, the AI identifies each plant and remembers whether they were targeted already or not. If a plant was targeted already, it is deleted from the target list to avoid a plant being hit several times which would be a waste of energy. Furthermore, a plant must be identified positively on several frames to be rated a valid target. In response to the recognition issues in Madrid, multi-hit was allowed in the software to have more targeted plants leading to several hit-marks on and around some of the recognized plants. Figure 3.54 shows such an example from the Madrid demo to roughly estimate the targeting accuracy during field tests. Obviously, not all hit marks are on the plant. This is probably due to up and down movement of the implement leading to changes in the height of the scanner output above the ground, which cannot be compensated in real time by the AI imaging pipeline as reported above.



**Fig. 5.53. Hit marks of laser treatment (light blue arrows) on maize crops. This image was taken during the latency assessment of the system in Reusel to check and correctly set the latency between image acquisition and laser shot for compensation of forward movement. At this checking run, latency compensation was set too high, so all laser hits were shifted in the movement direction of the robot (dark blue arrow). Crop plants (maize) were hit deliberately to have a better check of the hit position in comparison to the narrow barley grass leaves.**

The overall effectiveness of the treatment with the WeLASER weeding implement on farms is one of the most relevant performance indicators for the end-user. On-field assessment of the weeding



effectiveness was not possible during the project duration because of time constraints and seasonal boundary conditions.



**Fig. 3.54. Multi-hit marks on and near to weed plants on the test site in Arganda del Rey showing the targeting accuracy under field conditions.**

### 3.3.9. IoT sensor network

The development of devices underwent a classic development cycle: concept- design-making-assembly-test. At every occurrence of a problem the debug-restart analysing every step and apply proper changes, starting from the concept, for every each of the technology components: mechanical, electronic and logic (software, for every devices), which also carried to the production of progressively different versions:

- Cameras (all): 3 versions, tried with 4 different RF modules, 2 different PIRs, 2 different focus approaches
- Robot cameras - 2 different robot communication, 4 python modules for retransmission of images to the server
- Field Bridge - 2 different versions due to the change of AP (connectivity non-stable) and of powering system (bigger PV panel and battery).

As Robot Cameras, Field Cameras and Field Bridge share the same technology, every change due

to the change of a technological block, requires applying the changes to each of the components - e.g., it occurred when we decided to apply the OTA technology allowing to update firmware on line.

The Weather Station and the ETrometer also underwent the development of 3 version each - despite the apparent simplicity of the devices they have been progressively refined in terms of duration of battery charge and connectivity procedure so as to reach the reliability required for TRL7, which can now be considered to be reached up for every device.

Table 3.16 reports the malfunction that occurred with a comment related to the probability of their occurrence at the current state of the art.

**Table 3.16. List of malfunctions.**

Device	Issue	Observation
Robot Camera	Lots of messages and images	Lack of synchronisation between robot activities - should be amended
Field Camera	Reception of messages and images	High frequency of alert from PIR - the camera is now working in time lapse
	High response time	The choice of FTP determines a considerable delay in image availability on the cloud - a newer controller issued in the last year could allow the use of fast communication libraries
	Low-quality images	The quality is due to a version of the controller available at the beginning of the project - newer issues allow the development of further node versions with enhanced image quality
Field Bridge	Self-shut down	An overload of activity (too many alerts, high time-lapse rates) could put the device in shut down - a logics for self-awake has not been implemented yet.
Weather Station	-	The last development steps evidenced the need for a user-friendly calibration protocol (see comments below)
ETrometer	-	The last development steps evidenced the need for a user-friendly calibration protocol (see comments below)
Every node	Loss of connection	It occurred (and still may do) when AP or Field Bridge or cloud services (MQTT) were down.

Due to the level of reliability reached by the devices, they have been presented (also during the Field Days) to vendors and possible business partners, revealing how the TRL7 is still a point far from a commercial level (TRL9), concluding that the ‘present prototypes’ need nonnegligible investments aimed at industrial design aspects, professional cloud hosting, dashboard development, user-friendly calibration protocol and market investigation.



### 3.3.10. Cloud computing

During the WeLASER projects and the four field days, the cloud computing architecture collected 1,689,590 entity updates out of 230 entities (for a storage amount of 2GB). Some of these updates also refer to images. Overall, we have collected 487,545 images (for a storage amount of 102 GB). Figure 3.55 shows detailed statistics for Field Days 1 and 4; the behaviour has been consistent in Field Days 2 and 3, as well. Given a 10-second granularity, we show (on the left) the messages that have been collected and the average message delay (on the right). As to the delay, we distinguished the “Collection” delay (i.e., the time it takes for a message to be transferred through the internet; this is out of the platform control) and the “Internal” delay (i.e., the delay necessary to process and visualise the data within the platform). Overall, the internal platform delay is negligible with respect to the collection delay.

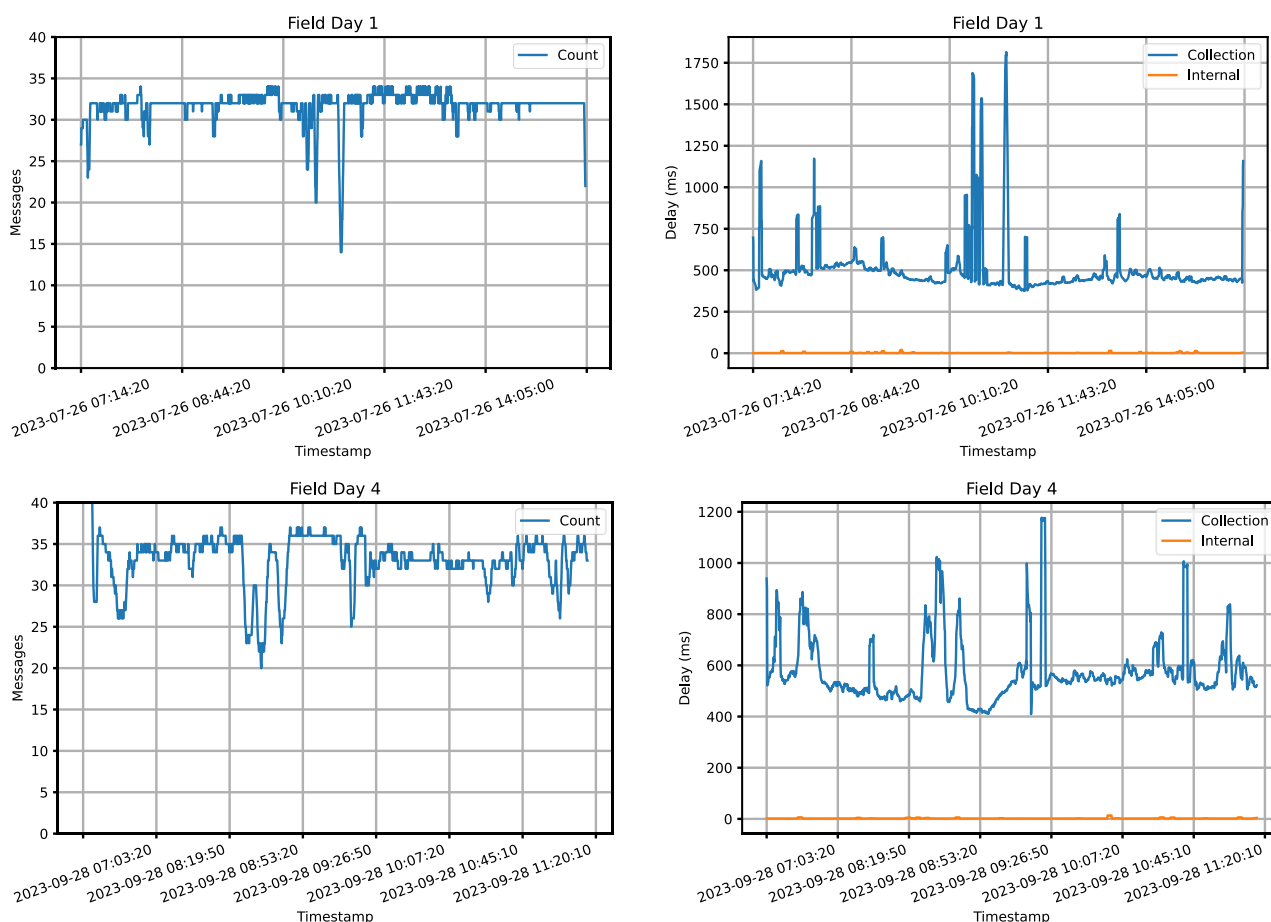


**Fig. 3.55. Message collection (left) and average delay (right) during Field Days 1 and 4; collection delay accounts for data transfer between Madrid and Bologna.**

**Table 3.17 summarises some statistics for the four field days.**

Event	Sum of messages	Average messages	Average collection delay (ms)	Average internal delay (ms)
Field Day 1	79214	31.76	506.0	1.94
Field Day 2	28654	25.09	772.39	2.66
Field Day 3	134384	21.88	1178.5	4.24
Field Day 4	45769	33.21	577.79	1.9

The performance is compliant with the correct functioning of the overall system. In particular, no interaction errors have been encountered when controlling the robot with the GUI hosted on the cloud platform.

### 3.4. Stakeholder's Evaluation

The WeLASER Field Days were organized to share the project results and gather feedback from stakeholders. In addition to the direct information provided by stakeholders, the consortium collected valuable written information through questionnaires. The questionnaires were divided into two sections that recorded:

- a) General questions on high-tech agriculture machinery, and
- b) Specific questions on the WeLASER weeding tool.

The questionnaire forms are included in Annex 2. The number in every cell is the total number of ticks recorded from the individual questionnaires. All the questionnaires are collected in an internal report available on the member's area of the WeLASER website.

Some attendees to Field Day 1 (Madrid, Spain, July 26, 2023) and Field Day 2 (Taastrup, Denmark, August 18, 2023) freely answered these anonymous questionnaires. The structure of Field Days 3 (Reusel, The Netherlands, August 24-26, 2023) was part of a trade fair and did not allow the distribution of the questionnaires. During Field Day 4 (Madrid, Spain, September 28, 2023), the system exhibition lasted longer than planned, and stakeholders had no time to answer the questionnaires.

Stakeholder's answers can be summarised as:

#### **General questions on high-tech agriculture machinery**

- How important are the following characteristics of a high-tech system for you?

Three answers were ticked similarly: Access to information and education (21), compatibility and integration (20), and adaptability and scalability (20).

- What features or functionalities do you consider essential for an agricultural tool to be useful to you?

For this question, most participants indicated that cost-effectiveness is essential (20).

- What kind of user interface do you prefer?

A touch path seems to be the preferred interface (27).

- Do you have any preferences regarding the power source for the tool?

Hybrid systems (Fuel and battery) are primarily in the minds of the stakeholders (20).

- Are there any specific safety considerations you would like the tool to address?

Safety regarding transportation and storage (15) is the most preferred by users, followed by ergonomics (10), guarding and shielding (10) and regular maintenance and inspections (10).

- What kind of support would you need to effectively use a hi-tech tool?

Most of the participants considered that training sessions (26) are valuable for using high-tech tools.

### **Specific questions on the WeLASER weeding tool**

- Have you used the WeLASER user interface during the demo?

Only four stakeholders had the opportunity to handle the system, and eight more expressed their opinions on the system, rating its interface as fair to good [Very Poor, Poor, Fair, Good, Excellent].

- Are there any WeLASER-specific features or functionalities that are difficult to understand or use?

The functionalities of the Autonomous robot, Laser implement, Map builder, Mission planner, Mission launch, and Mission supervisor were mostly rated Easy to Normal [Very easy, Easy, Normal, Difficult, Very difficult].

- Does the WeLASER system provide an efficient workflow for its main task? (Click one).

Moderately Inefficient (10) was the most selected answer [Highly Inefficient, Inefficient, Moderately Inefficient, Efficient, Highly Efficient].

- How responsive is the system in terms of speed and performance? (Click one)

Most participants agreed the system is Slow [Very slow, Slow, Moderately Responsive, Responsive, Highly Responsive].

- On a scale of 1 to 10, how would you assess the overall WeLASER System?

The average number of participants answering this question (26) was 6.40.

- On a scale from 1 to 10, how would you rate the friendliness of the WeLASER human-machine interface?

The average number of participants answering this question (26) was 6.65.

– How would you assess the following WeLASER characteristics?

○ It is an autonomous robot.

Most participants rated Positively (14) to Very positively (8). One participant rated it as Negatively.

○ It is a tracked vehicle.

Most participants rated Normal (9) to Positively (12). Four participants rated it as Negatively.

○ It exhibits Internet connectivity.

This is considered a Positively (13) characteristic, but four participants view it as a Negative characteristic.

○ The graphical user interface is web-based

This was rated as Normal (9) to Positively (10).

○ It has a friendly graphic user interface

The graphic interface is considered Normal to Very positive (26), with two participants considering that having an interface is a Negative system characteristic.

○ It allows the user to observe the mission development in real-time.

This feature is appreciated by the participants who scored mainly Positively (14) and Very positively (11).

## 4. SYSTEM IMPACT ON CROPS AND SOIL

The relevance of the WeLASER project stays in the fact that the control of weeds is a fundamental task in crop management, which is largely based on the use of chemicals. The effects of use of herbicides on the environment and human health have been studied for a number of years, producing a huge amount of bibliography (a Googles Scholar search about “effects of use of herbicides on the environment and human health” produces more than 500 K pages of results). A general belief emerging from a broad analysis is that, though herbicides are normally considered of low toxicity with respect to other pesticides (fungicides, insecticides), their active principles and metabolites tend to persist in the environment and bio-accumulate within organisms and/or enter the (soil) ecosystem and human food chains (including groundwater). This is the reason why, in the framework of the current European policy, ‘Pesticide-Free Agriculture’ has become a mandatory objective, and alternative solutions are strongly encouraged.

WeLASER weeding solution is based on the adoption of two technologies, autonomous vehicles and laser-based weeding, combining the physical weeding approach to another critical issue of ongoing agriculture, the lack of labour, claiming for hand-free solutions. WeLASER had the task of proving that such an approach is feasible and working.



However, such new technology has to be analysed to discover the eventually hidden effects of WeLASER on crops and soil. This is the reason why, in this section, the effects of the two mentioned technologies (autonomous vehicles and laser) have been discussed separately and in combination. In Fig. 4.1, the laser weeding characterisation is depicted in a general drawing, including most field operations.

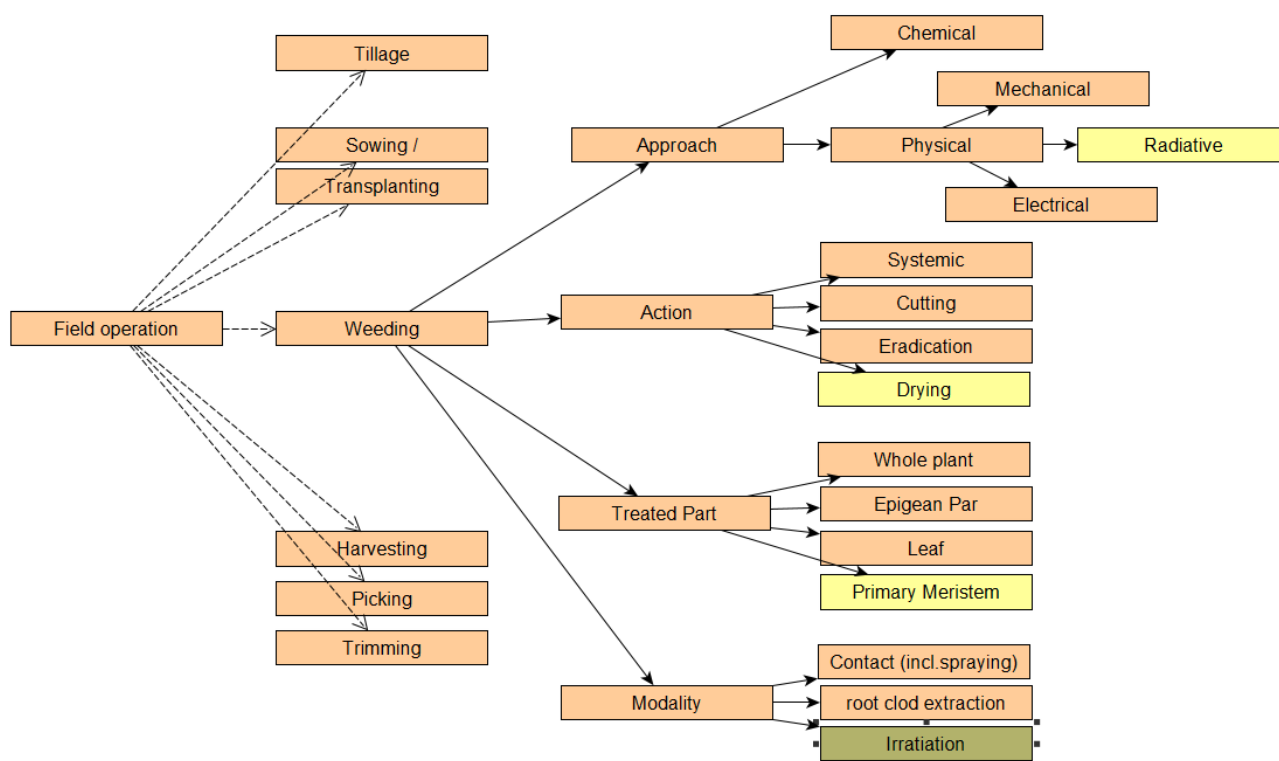


**Fig. 4.1. Most relevant crop operation with details on weeding technique putting in evidence the specification of WeLASER approach.**

## 4.1. System impact on crops

### 4.1.1. Effect of Autonomous vehicles

Autonomous vehicles can directly harm the crop by accidental wrong driving and steering capacity, bringing the vehicle on the wrong path. Such a possibility should, however, be regarded as a minor risk and related to anomalous conditions, including soil non-well levelled, imperfect sowing rows, etc.

### 4.1.2. Effect of Laser

The laser is a coherent radio-electromagnetic (EM) energy source, quite different from the Sun's thermal radiation, but its effect on minerals and living tissues is proved to be that of a huge point-wise heating source. Because of the high Heat Capacity of water and the high water content of most living tissues, a high amount of energy is required to dry (kill) an organism or part of it. A soil with a major mineral component, especially when well-watered, acts like a shield preventing the laser beam from going beyond a few millimetres down the surface while limiting its effect to the skin of a living

body (as WeLASER is addressed to hit the more sensitive part of the epigeal part of the plant: the primary meristem), it can hardly affect the rooting system. If the laser beam is accidentally addressing a crop tissue, what we are likely to observe are just surface burn spots, negligible sufficient to be concerned about some yield loss or reduction of produce quality. Further details are given in deliverable “D2.3 - Impact of laser doses on living organisms and the environment”. On the contrary, most of the consequences of laser on the crop are represented by the dropping of most of the well-known negative effects of the standard (chemical) approach, e.g., assimilation and biological accumulation of chemicals and its metabolites on the crop, non-target plant, u- and mesofauna, mobility process in water bodies, accumulation and persistence in the whole food chain (Waring et al., 2023<sup>2</sup>).

#### 4.1.3. Combined effect

A comparison of the combined effect of the toolset used for chemical weeding and WeLASER put in evidence a major difference in the effects of the weeding tool, which in the first case is often represented by a large wheeled spray-bar, while in WeLASER, the tool is mechanically supported by the autonomous vehicle itself. The bar solution reduces the number of required passages; therefore, the WeLASER weeder (in its current configuration) increases the risk of accidental damage to the crop due to the passage of tracks on sown rows (see Fig. 4.1).

### 4.2. System impact on soil

In Fig. 4.2, the most relevant crop categories are shown to evidence those WeLASER has been addressed to.

#### 4.2.1. Effect of the Autonomous Robot

A well-defined and precise geometry is fundamental to define the mission, and we have to avoid the tracks to compact the soil surface where not strictly required. About the effect of passages, the adopted vehicle is lighter than other commercial track-based tractors, and expected to have a lower impact on soil surface. The number of passages (discussed below) could, however make a difference.

---

<sup>2</sup> Rosemary H. Waring, Stephen C. Mitchell, Ian Brown, Chapter 3 - Agrochemicals in the Food Chain, Editor(s): Michael E. Knowles, Lucia E. Anelich, Alan R. Boobis, Bert Popping, Present Knowledge in Food Safety, Academic Press, 2023, Pages 44-61, ISBN 9780128194706, <https://doi.org/10.1016/B978-0-12-819470-6.00006-8>.

### 4.2.2. Effect of laser

The effect of the laser tool on crops is described in depth in other WeLASER documentation (“D2.3- Impact of laser doses on living organisms and the environment”) together with possible adverse effects on soil and its hosted fauna, proving that most issues can be easily considered negligible. Although the laser beam heats the spot it hits, the exposure time is short (less than a second)<sup>3</sup>, and

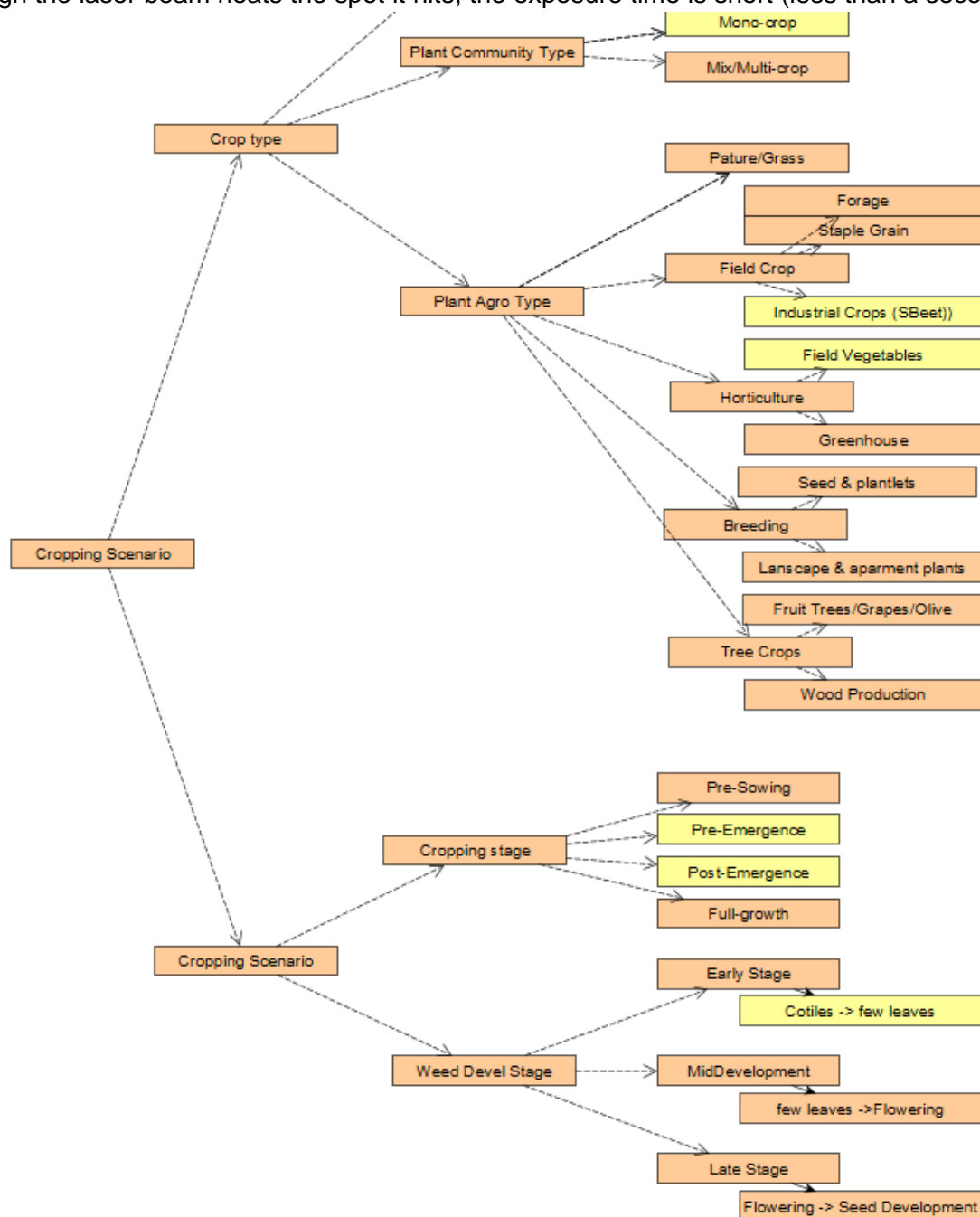


**Fig. 4.2 - Main types of crops with evidenced in yellow those WeLASER has been addressed to.**

<sup>3</sup> Christian Andreasen, Karsten Scholle and Mahin Saberi, Laser Weeding with Small Autonomous Vehicles: Friends or Foes?, Frontiers in Agronomy, 07 March 2022, <https://doi.org/10.3389/fagro.2022.841086>.

the temperature increase around the place is limited. Therefore, the temperature increase may only affect the surrounding environment insignificantly. On the other hand, the positive effects have already been mentioned (about on crop) on the previous section and correspond to the removal of most of the negative effects of chemicals on soil when meant as a hydrological and ecological system.

#### 4.2.3. Combined effect

When comparing WeLASER and the ‘conventional chemical spraying’ approach, some important differences arise. In fact, the number of passages and the surface density of tracks can be considerably different due to the fact that the spray-based approach is based on a (relatively light) wheel-based large wing bringing a number of sprayers.

The passage of wheels and tracks can be expressed in terms of pressure, frequency and distribution combined with the state of the soil surface. They could determine compaction, and more specifically, a deterioration of soil structure, affecting the physical fertility of the soil, including

- Crop water availability.
- Root pore availability.
- Reduced aeration and consequent depletion of biological activity.
- Reduced infiltration capacity, inducing the occurrence of phenomena such as water-logging.
- Leading to reduced crop growth and productivity (see Fig. 4.3).

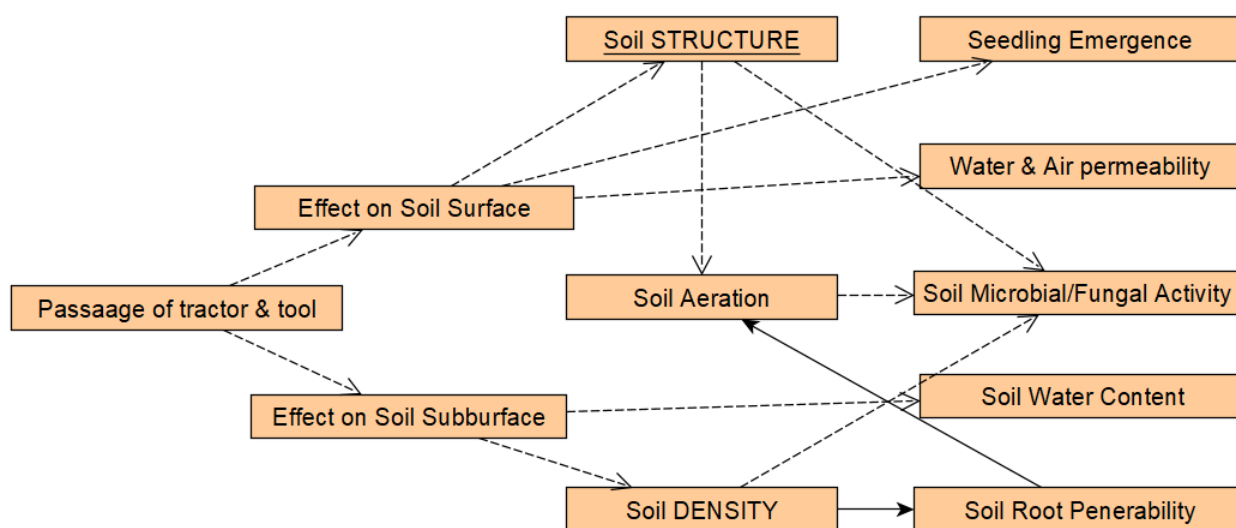


**Fig. 4.3. Major effects of passage of tools on soil.**

The bibliography has already analysed most of such aspects<sup>4</sup>. However, because of the similarity to

<sup>4</sup> Kokieva G.E., S A Voinash, V A Sokolova, V A Gorbachev and A A Fedyaev, 2020, IOP Conf. Ser.: Earth Environ. Sci. 548 062036



other contexts, many variables can be neglected.

- The assets of machinery, such as wheel and track geometry and pressure exerted on soil, is similar to other commercial machinery.
- The frequency of passages depends on the weather (need for repeating the treatment) as well as on the efficiency of the treatment itself and the availability of precise prescription information.
- Soil state. The decision of performing a weeding treatment is given by a trade-off between the urgency of weeding and the soil status. An application during the wrong period could deeply deteriorate the surface of the soil structure, affecting the structure of the soil.

In sum, it emerges that the most relevant parameter affecting the impact of machinery on the surface is the ratio of the width of a spraying wing/bar to one of WeLASER weeding tools, which could be estimated in the range [3 to 10] corresponding to the increase of the surface which is subject to passages in the WeLASER tool.

Such an aspect should, however, be taken into consideration together with the possibility to adopt the laser weeding tool as a separate tool (with a normal tractor) - also, the laser weeder is a modular system, and the tool width can be considerably increased.

### 4.3. Conclusions

From the analysis, it emerges that the effects of WeLASER on crops and soil have been almost recognised in terms of benefits as they drop every one of the deleterious effects of herbicides. The analysis allows us to reach such conclusions without a need for further experimental assessments on the base of the analysis of the most recent literature.

In the cropping context, WeLASER has been designed for a geometrically (homogeneous) distributed field crop, including field vegetables or industrial crops (sugar beet), together with a weeding scenario represented by the former development stage of a crop and of weeds (pre- or post-emergence, as pointed out in Fig. 4.2). Therefore, it is important to evidence the limits of such technology with respect to conventional chemical weeding.

## 5. ANNEX 1 STATUS OF THE FINAL SYSTEM INTEGRATION

**Table A.1. Status of completion of the subsystems at month 39**

Subsystem	Component	Leader	Status of design/ Implementation (%)			Comments
			M12	M24	M39	
Laser-based weeding system	Laser source	FUT	40	70	90	Design: 100 % Implementation: 100 % Validation: 70 %
	Diode Power supply	FUT	60	80	100	Design: 100 % Implementation: 100 % Validation: 100 %
	Chiller	FUT	40	80	90	Design: 100 % Implementation: 100 % Validation: 70 %
	Targeting system	LZH	40	65	95	Design: 100 % Implementation: 95 % Validation: 85 % The system is almost fully developed. Validation has not been fully completed. Any changes that may result from full validation will result in additional work in implementation, resulting in a 5% shortfall.
	Tests on crops and living organisms	UCPH	25	50	90	UCPH could only do some of what it expected to do because the weeding tool did not work during its stay in Denmark and Spain. In any case, UCPH did some unexpected tasks in providing annotated pictures to LZH to train the perception system and provided more PA and publications than scheduled so that UCPH used all the allocated costs.
	Laser safety	LZH	30	60	90	Design: 100 % Implementation: 90 % Validation: 70 % A thorough evaluation of all the safety components could not be carried out due to staff shortages and delays in delivery. As a result, not all of the ambitious safety objectives could be fully achieved. In order to ensure the suitability of the system for demo use, the systems


						directly affecting this were implemented and validated first.
Weed-meristem perception system	Weed-meristem perception device (Hardware)	LZH	100	100	100	According to plan
	Crop/weed discrimination algorithms	LZH	32	66	95	Design: 100 % Implementation: 95 % Validation: 85 %
	Impact-point AI-vision system and weeding control system	LZH	20	56	95	Design: 100 % Implementation: 95 % Validation: 85 % Technical difficulties and a lack of time due to a shortage of specialised personnel during the demo days prevented a thorough validation of the detection systems. These validation steps were carried out in subsequent trials, but validation of the complete system is still desirable.
Autonomous vehicle for laser weeding	Mobile platform	AGC	60	80	100	The robotic platform is complete and safe.
	Smart navigation manager	CSIC	30	60	100	The Smart navigation manager consists of (see D5.1) the central controller; the Agri-decision support system (Agri-DSS), whose name was changed to Smart Operation Manager SoM (see D4.1); the planner and the supervisor; the IoT sensor network; and the cloud computing structure. All subsystems were adequately developed and integrated within the autonomous vehicle.
	IoT system	UNIBO	40	65	95	Design: 100 % Implementation: 100 % Validation: 85 %
	Cloud computing	UNIBO	40	65	100	According to the plan
System integration	Mass distribution	CSIC	15	75	100	In the final integration, the platform's stability was verified, confirming the correct distribution of masses.
	Mechanical integration	CSIC	--	90	100	All subsystems were properly integrated mechanically in the final integration.

	Electrical integration	CSIC	--	90	100	All subsystems were properly integrated electrically in the final integration.
	Communication integration	CSIC	--	70	100	All communication protocols between the different subsystems were properly implemented.





## 6. ANNEX 2. QUESTIONNAIRE FORMS AND RESULTS



**Sustainable Weed Management in Agriculture  
with Laser-Based Autonomous Tools**

**Stakeholder Event  
Questionnaire**

**GENERAL QUESTIONS ON HIGH-TECH AGRICULTURE MACHINERY**

1. How frequently do you interact with high-tech systems? (Click one)
 

Daily	Weekly	Monthly	Yearly	Never
9	5	7	4	8
  
2. How important are the following characteristics of a high-tech system for you?  
Please tick ☒ a level for every input.
 

	Trivial	Low	Medium	High	Critical
Cost		1	9	19	3
Access to information and education		1	7	21	4
Connectivity and Internet access			12	12	7
Data management and privacy		7	8	14	1
Compatibility and integration			5	20	6
Adaptability and scalability			8	20	3
Maintenance and support		2	6	14	10
Legal Regulation	5	4	10	8	3
  
3. What features or functionalities do you consider essential for an agricultural tool to be useful to you? (Please tick ☒ a level for every input)
 

	No essential	Slightly essential	Moderately essential	Very essential	Absolutely essential
Durability and reliability			3	16	14
Ease of use			6	21	5
Accuracy and precision			6	19	8
Adaptability to work with different crops		1	7	14	11
Real-time monitoring and alerts		3	13	12	6
Cost-effectiveness			4	20	9
Connectivity and data sharing	1	1	14	10	6
Compatibility with farming practices		2	4	16	10
Energy efficiency	1	8	9	12	3
Support and training		2	9	11	10
  
4. What kind of user interface do you prefer?
 

Keys	Buttons	Touch path (smartphone, tablet)	Mouse
	8	27	1
  
5. Do you have any preferences regarding the power source for the tool?
 

Manual	
Fossil fuel	2
Battery-powered (Fully electric),	14
Hybrid (Fuel and battery)	20
Solar	9
  
6. Are there any specific safety considerations you would like the tool to address?
 

Design for safety and ergonomics	10
Guarding and shields ( <i>safety shields, protective covers, and physical barriers to minimize the risk</i> )	10
Visibility and signalling ( <i>such as reflective surfaces or warning signs</i> )	3
Safety interlocks and controls ( <i>a two-step start mechanism or use of both hands to operate</i> )	8
Operator training and instructions ( <i>against electrical hazards, fire, protective equipment, etc.</i> )	7
Regular maintenance and inspections	10
Low noise and vibration	9
Power sources and fuel handling	6
Transportation and storage	15
  
7. What kind of support would you need to effectively use a hi-tech tool?
 

	Trivial	Low	Medium	High	Critical
Instructional materials		2	14	13	3
Training sessions		1	1	26	5
Safety guidelines		2	18	17	2
Technical support			5	14	12
Ongoing updates and maintenance		1	5	19	8



**Sustainable Weed Management in Agriculture  
with Laser-Based Autonomous Tools**

## Stakeholder Event Questionnaire

### WeLASER SPECIFIC QUESTIONNAIRE

1. Have you used the WeLASER user interface during the demo?

Yes	No
4	29

If yes:

How would you rate the overall user interface of the WeLASER system in terms of usability and intuitiveness? (Click one)

Very Poor	Poor	Fair	Good	Excellent
		5	6	1

2. Are there any WeLASER-specific features or functionalities that are difficult to understand or use?

	Very easy	Easy	Normal	Difficult	Very difficult
Autonomous robot (mobile platform)	5	18	9	1	
Laser implement		2	13	4	
Map builder		5	11	3	1
Mission planner		9	7	4	
Mission launch	2	9	7	2	
Mission supervisor	2	7	7	1	2

3. Does the WeLASER system provide an efficient workflow for its main task? (Click one)

Highly Inefficient	Inefficient	Moderately Inefficient	Efficient	Highly Efficient
	7	10	7	2

4. How responsive is the system in terms of speed and performance? (Click one)

Very Slow	Slow	Moderately Responsive	Responsive	Highly Responsive
2	13	6	1	2

5. Does WeLASER system support the following aspects required for your work? (Click in supported aspects)

	<input checked="" type="checkbox"/>
File formats	6
Protocols	5
Hardware	9
Software	8
Standards	6

6. On a scale of 1 to 10, how would you assess the overall WeLASER System?

7. On a scale from 1 to 10, how would you rate the friendliness of the WeLASER human-machine interface?

8. How would you assess the following WeLASER characteristics?

	Very negatively	Negatively	Normal	Positively	Very positively
It is an autonomous robot		1	6	14	8
It is a tracked vehicle		4	9	12	3
It exhibits Internet connectivity	1	3	6	13	5
The graphical user interface is web-based	1		9	10	7
It has a friendly graphic user interface	1	1	8	12	6
It allows the user to observe the mission development in real-time			3	14	11